NATIONAL CENTER FOR EARTHQUAKE ENGINEERING RESEARCH

State University of New York at Buffalo

LINEARIZED IDENTIFICATION OF BUILDINGS WITH CORES FOR SEISMIC VULNERABILITY ASSESSMENT

by

I-K. Ho and A. E. Aktan
Department of Civil and Environmental Engineering
University of Cincinnati
Cincinnati, OH 45221-0071

Technical Report NCEER-89-0041

November 1, 1989

This research was conducted at the University of Cincinnati and was partially supported by the National Science Foundation under Grant No. ECE 86-07591.

NOTICE

i, ii

50272-101

REPORT DOCUMENTATION PAGE	1. REPORT NO. NCEER-89-0041	2.	3. Recipient's Accession No. PB90-251943

4. Title and Subtitle
Linearized Identification of Buildings with Cores for Seismic Vulnerability Assessment

5. Report Date
November 1, 1989

6.

7. Author(s)
I-K. Ho and A.E. Aktan

8. Performing Organization Rept. No.

9. Performing Organization Name and Address

10. Project/Task/Work Unit No.

11. Contract(C) or Grant(G) No.
(C) 88-1015
(G) ECE 86-07591

12. Sponsoring Organization Name and Address
National Center for Earthquake Engineering Research
State University of New York at Buffalo
Red Jacket Quadrangle
Buffalo, New York 14261

13. Type of Report & Period Covered
Technical Report

14.

15. Supplementary Notes
This research was conducted at the University of Cincinnati and was partially supported by the National Science Foundation under Grant No. ECE 86-07591.

16. Abstract (Limit: 200 words)
This report presents a study of three dimensional analytical modeling of buildings based on the computer program SUPER-ETABS. A 27-story RC building with unsymmetric cores was simulated. First, a predictive analytical model was developed based on the engineering theory for member analysis of the cores. A series of forced-excitation dynamic tests were then conducted of the real building in the context of modal testing. Its global dynamic responses were measured to validate, improve, and identify the parameters of the predictive analytical model. The first nine frequencies and the corresponding 3D normalized mode shapes were measured by modal testing. After correlating the measured results with those from the predictive ETABS model, this had to be revised. An improved model termed "simulative ETABS model" was hence developed. The frequencies, mode shapes, and flexibilities of predictive, measured, and simulative analytical models were compared, revealing an excellent correlation between the ETABS simulative model and measured responses. This was accomplished without a rigorous adjustment of its parameters. The predictive model, however, was shown to have poor correlation with experiments, without any numerical adjustment of its parameters. This indicated the importance of experimental identification in evaluating existing buildings with unusual attributes.

17. Document Analysis a. Descriptors

b. Identifiers/Open-Ended Terms

SYSTEM RESPONSE INVESTIGATIONS
SEISMIC RISK ASSESSMENT
ANALYTICAL MODELING
EARTHQUAKE ENGINEERING
EARTHQUAKE ENGINEERING
SEPER-ETABS
STRUCTURAL DYNAMICS
TALL BUILDINGS

c. COSATI Field/Group

18. Availability Statement	19. Security Class (This Report)	21. No. of Pages
Release Unlimited	Unclassified	132
	20. Security Class (This Page)	22. Price

LINEARIZED IDENTIFICATION OF BUILDINGS WITH CORES FOR SEISMIC VULNERABILITY ASSESSMENT

by

I-K. Ho[1] and A.E. Aktan[2]

November 1, 1989

Technical Report NCEER-89-0041

NCEER Contract Number 88-1015

NSF Master Contract Number ECE 86-07591

1 Graduate Student, Department of Civil and Environmental Engineering, University of Cincinnati
2 Associate Professor, Department of Civil and Environmental Engineering, University of Cincinnati

NATIONAL CENTER FOR EARTHQUAKE ENGINEERING RESEARCH
State University of New York at Buffalo
Red Jacket Quadrangle, Buffalo, NY 14261

PREFACE

The National Center for Earthquake Engineering Research (NCEER) is devoted to the expansion and dissemination of knowledge about earthquakes, the improvement of earthquake-resistant design, and the implementation of seismic hazard mitigation procedures to minimize loss of lives and property. The emphasis is on structures and lifelines that are found in zones of moderate to high seismicity throughout the United States.

NCEER's research is being carried out in an integrated and coordinated manner following a structured program. The current research program comprises four main areas:

- Existing and New Structures
- Secondary and Protective Systems
- Lifeline Systems
- Disaster Research and Planning

This technical report pertains to Program 1, Existing and New Structures, and more specifically to system response investigations.

The long term goal of research in Existing and New Structures is to develop seismic hazard mitigation procedures through rational probabilistic risk assessment for damage or collapse of structures, mainly existing buildings, in regions of moderate to high seismicity. The work relies on improved definitions of seismicity and site response, experimental and analytical evaluations of systems response, and more accurate assessment of risk factors. This technology will be incorporated in expert systems tools and improved code formats for existing and new structures. Methods of retrofit will also be developed. When this work is completed, it should be possible to characterize and quantify societal impact of seismic risk in various geographical regions and large municipalities. Toward this goal, the program has been divided into five components, as shown in the figure below:

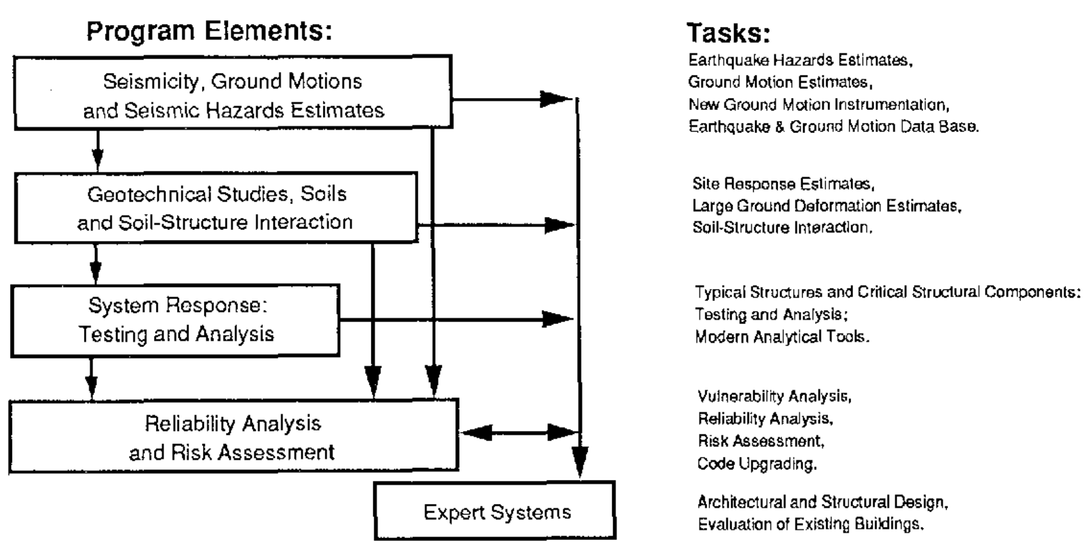

System response investigations constitute one of the important areas of research in Existing and New Structures. Current research activities include the following:

1. Testing and analysis of lightly reinforced concrete structures, and other structural components common in the eastern United States such as semi-rigid connections and flexible diaphragms.
2. Development of modern, dynamic analysis tools.
3. Investigation of innovative computing techniques that include the use of interactive computer graphics, advanced engineering workstations and supercomputing.

The ultimate goal of projects in this area is to provide an estimate of the seismic hazard of existing buildings which were not designed for earthquakes and to provide information on typical weak structural systems, such as lightly reinforced concrete elements and steel frames with semi-rigid connections. An additional goal of these projects is the development of modern analytical tools for the nonlinear dynamic analysis of complex structures.

The analysis of buildings relies on good estimates of the properties of the structure. The stiffness of a building may be influenced by walls, cracking of reinforced concrete, floor flexibility, foundation effects, and complex geometries. This report describes a test program and associated analytical developments on a 27-story building, and provides conclusions and guidelines for improved analytical simulation of buildings. Such experimental/analytical investigations on realistic structures are essential in order to check and enhance analytical prediction and risk assessment capabilities.

ABSTRACT

This report presents a study of three dimensional analytical modeling of buildings based on the computer program SUPER-ETABS. A 27-story RC building with unsymmetric cores was simulated. First, a predictive analytical model was developed based on the engineering theory for member analysis of the cores.

A series of forced-excitation dynamic tests were then conducted of the real building in the context of modal testing. Its global dynamic responses were measured to validate, improve, and identify the parameters of the predictive analytical model. The first nine frequencies and the corresponding 3D normalized mode shapes were measured by modal testing.

After correlating the measured results with those from the predictive ETABS model, this had to be revised. An improved model termed "simulative ETABS model" was hence developed. The frequencies, mode shapes, and flexibilities of predictive, measured, and simulative analytical models were compared, revealing an excellent correlation between the ETABS simulative model and measured responses. This was accomplished without a rigorous adjustment of its parameters. The predictive model, however, was shown to have poor correlation with experiments, without any numerical adjustment of its parameters. This indicated the importance of experimental identification in evaluating existing buildings with unusual attributes.

ACKNOWLEDGMENTS

The research described in this report was sponsored by the National Science Foundation through the National Center for Earthquake Engineering Research, Buffalo, N.Y., Project No : NCEER 88105.

Drs. Michael Baseheart and Bahram Shahrooz of the CEE Department were faculty associates in this research as well as members of Mr. Ho's MS thesis committee. Their participation in the research and their ideas and help in improving this report are gratefully acknowledged. In addition, Dr. Baseheart directly participated in all of the experimental components of this research.

Drs. R. Allemagne and D. Brown of the Structural Dynamics Research Laboratory at the university were also faculty associates in the research. Their collaboration as well as the participation of Dr. Havard Vold of the Structural Dynamics Research Corporation of Cincinnati are gratefully acknowledged.

ZONIC Corporation and Structural Dynamics Research Corporation of Cincinnati provided valuable help through equipment and personnel loans. Their contributions are acknowledged.

The planning of the test, data acquisition during the modal test and subsequent data reduction were proficiently carried out by Mr. Stu Shelley, graduate student at the Structural Dynamics Research Laboratory of the university. His help throughout the research project has been invaluable and the writers express their deep appreciation to Mr. Shelley. Contributions of Messers K.L. Lee, Madwesh Raghavendrachar and Michael S. Lenett during the modal test are also acknowledged.

The senior writer would like to express special appreciation to Dr. P. L. Bishop, Head of the CEE Department and Dr. C. N. Papadakis, Dean of College of Engineering for their extraordinary support and confidence which permitted to initiate and conduct the reported research.

TABLE OF CONTENTS

LIST OF FIGURES

SECTION 1

INTRODUCTION

1.1 General Comments

In evaluating seismic vulnerability of unusual, complex, aged, or damaged constructed facilities and for their reliable upgrades, accurate analyses are necessary [2]. Recent developments in high-speed micro-computers permit the analysis of refined 3D analytical models of buildings, and number-crunching is no longer a problem for structural engineers for routine problems. But how to establish an analytical model to accurately simulate a real structure remains a problem, especially for complex or irregular structures such as buildings with thin-walled core systems or wall elements. Such elements cannot be simulated accurately by 1D analytical elements [5], and developing their macro-element representations by a combination of several analytical elements is recommended. For example, in ETABS, a shear wall may be represented by an analytical assembly using panel, column, and beam elements. In such cases, how to assign parameters such as moment of inertia, shear area, torsional inertia, etc. to each analytical element to correctly simulate the flexibility of the real structure becomes a major problem. In this report, application of the structural identification concept to improve analytical modeling of buildings with core systems is described. The concept of structural identification has been advocated by many researchers [1,7,14,16], and has been applied to solve different types of civil-structural problems [17]. Using structural identification as a means of detecting damage is gaining importance, evidenced by recent research in Europe [12,19].

1.2 Literature Survey

Structural identification is defined as correlating the measured responses of a structure with those of an analytical model in order to improve, validate, and quantify the parameters of the model [15]. Recently, several engineers and scientists have approached identification of buildings and bridges using general purpose structural analysis programs such as SAP or ETABS. For example, a multistory steel framed structure was idealized in order to conform to the 3-D building response model incorporated in ETABS [6], and the dynamic properties of a 30-story R.C. tower building were measured and correlated with the results from an ETABS analytical model [22]. In these reports, ambient and/or forced-excitation tests were performed. The dynamic responses measured in these tests and the results from an ETABS analytical model were compared. The tested buildings were regular and they did not possess any undesirable attributes or thin-walled core systems.

1.3 Objectives and Scope

Two distinct objectives were defined in this current study of building structural modeling and identification :

(1) A documented effort to model buildings with open or closed thin-walled core systems by utilizing ETABS does not exist to the knowledge of the writer. On the other hand, many RC medium-rise to tall buildings or composite structures are typically designed with RC core systems. Availability of ETABS and other building analysis software for the PC is leading to their increased use by practicing engineers. Analysis provisions of 1988 UBC for the seismic design of "irregular" buildings and the provisions of ATC-14 for the seismic vulnerability evaluation of buildings require 3D modeling and analysis of complete building-foundation systems. These documents further motivate the use of software such as ETABS for design and evaluation of irregular buildings. Therefore, exploring manners of using ETABS to accurately model buildings with undesirable attributes and RC core systems was considered a worthwhile effort which may have immediate significance for practicing engineers.

(2) While forced-excitation testing of buildings have been carried out, these were not conducted with the currently developed hardware and software used by modal test specialists. Exploring the use of recently developed modal test tools for building identification comprises the second objective of the study.

Organization of the report is as follows :

The second chapter describes the test building, its structural system, and lists the undesirable attributes of the building.

The third chapter introduces SUPER-ETABS briefly and describes the procedure followed to generate an ETABS analytical model. Rules followed in modeling the closed thin-walled core system are presented.

The fourth chapter describes modal testing of the building, discusses the equipment used, instrumentation and test procedures, and compares the measured responses with the results from the predictive analytical model given in chapter 3.

The fifth chapter discusses how the predictive model was revised. A new ETABS model termed "simulative model" is described. The frequencies, mode shapes, and flexibilities from the predictive and simulative ETABS models and those measured by the modal test are correlated.

The final chapter includes a summary, conclusions and recommendations for further study.

SECTION 2

DESCRIPTION OF THE BUILDING

2.1 Test Building and Existing Documentation

Photographs of the test building are shown in Fig. 2-1. The building was designed and constructed in 1968 as a residence hall at the University of Cincinnati campus, and was closed in 1981 due to issues related to fire safety. In addition to the design drawings, extensive documentation was available regarding the site geotechnical characteristics, as-built dimensions, reinforcement detailing and variation in the concrete properties obtained by sonic tests. Core samples were taken from the slab concrete at various floors in 1982, revealing a measure of the attained concrete strength and its variation within the building.

2.2 Conceptualizing the Soil-Foundation-Structure

The data was studied and the building was visited several times in an effort to understand the site, relation of the building to other structures on the site, the structure-foundation system, and possible interactions between structural and non-structural components. The photographs in Fig. 2-1 indicate an elevation difference which is approximately 15 ft. between the grade at E and W faces. A three-story building adjacent to the north side is separated by a construction joint.

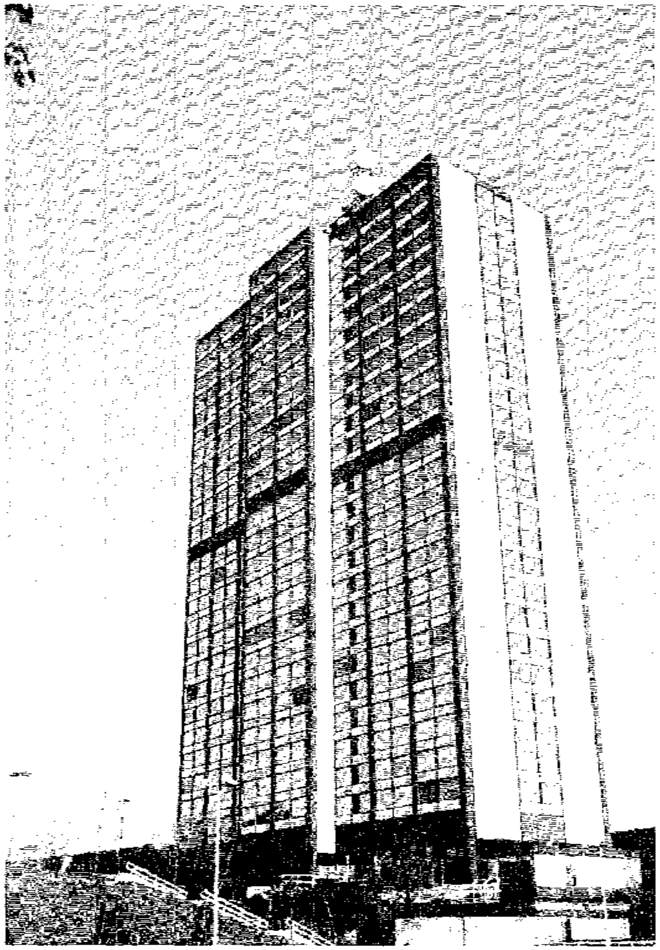

(a). View from S(Long Facade)–E(Short Facade)

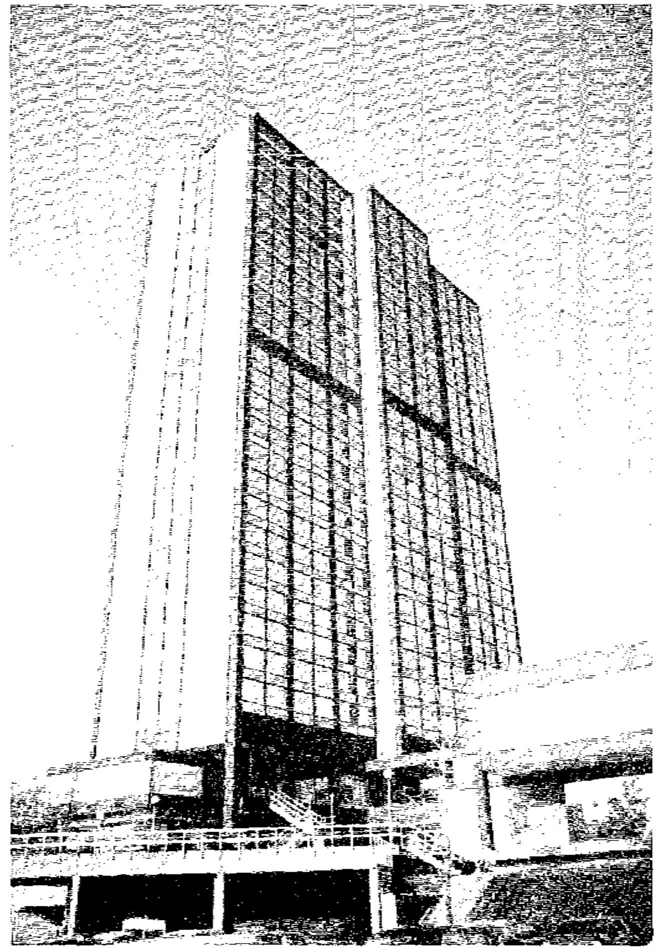

(b). View from N(Long Facade)–W(Short Facade)

Fig. 2-1 Photographs of the Test Building

-- Continued

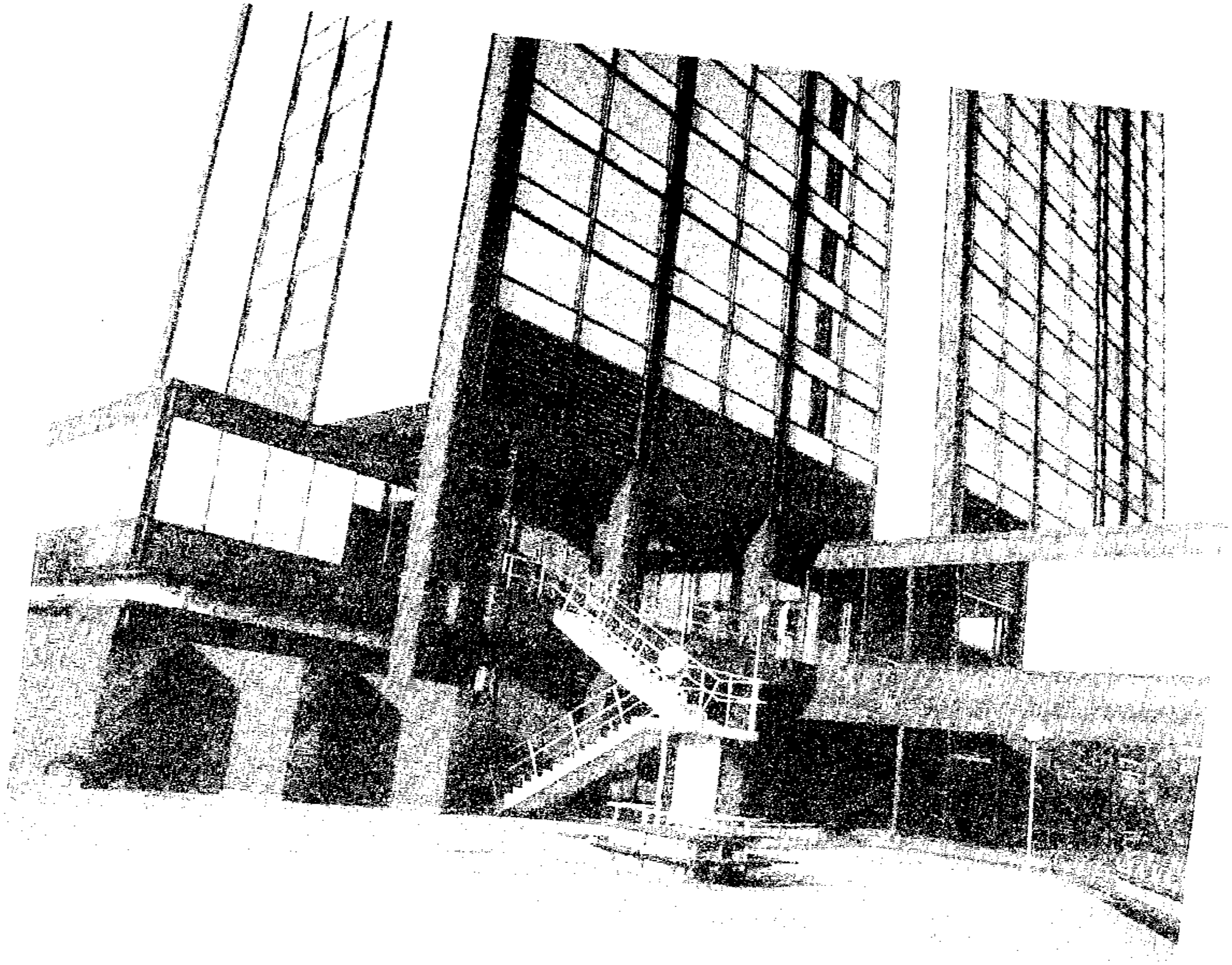

(c). Detail at Second Level NW Corner

Fig. 2-1 Photographs of the Test Building

The soil at the site was determined by bore tests to be hard shale with thin layers of limestone, capable of over 25 tons/sq.ft. bearing. The foundations were poured directly on the rock. The structure-foundation system is depicted in the typical plan shown in Fig. 2-2 and the 3D isometric illustration shown in Fig.2-3.

The foundation system is only 4 feet below grade, consisting of individual spread footings which are not tied together. The building plan is observed to be an approximately 60 ft by 160 ft rectangle. The structural elements and their typical proportions are shown in the plan (Fig. 2-2), indicating a flat-slab system with peripheral walls and two central cores which are coupled by the slab (coupling beams were used at the first four floor levels although these would be least effective at the lower floors). Core footings are 7 ft. deeper than those of the columns, drawings indicate that these followed the contours of rock.

The total height of the building from the ground-floor i.e. level 1 is 280 ft. There are twenty-seven floor levels of typical 9 ft. story height except for those noted in Fig. 2-2. A structural steel appendage of 2400 square feet in plan as well as several TV antenna towers are located on the 27th floor. The nonstructural elements included interior partitions made of light wood-products, and glass attached to the facades through light aluminum framing.

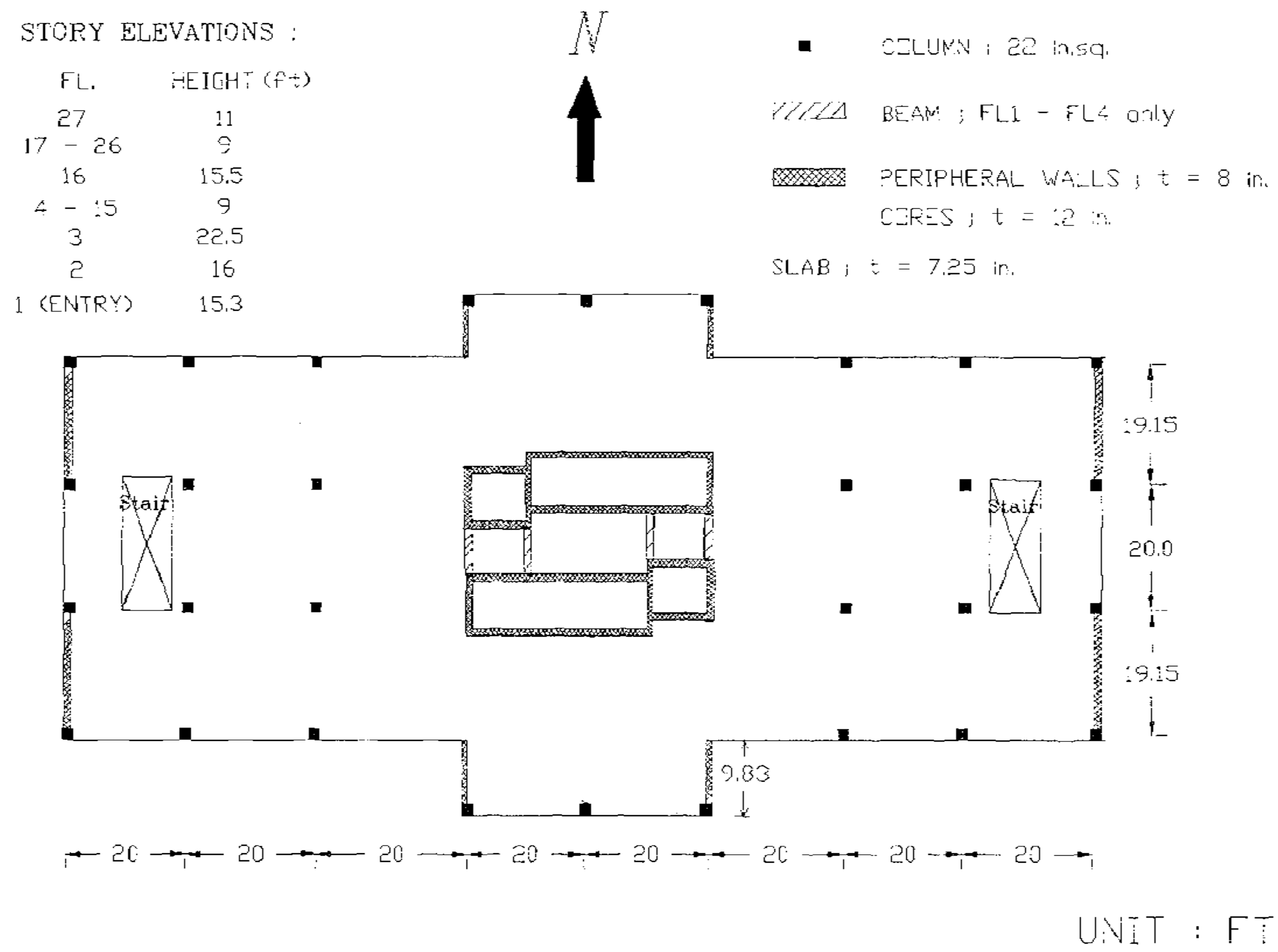

Fig. 2-2 Typical Plan of The Test Building

2.3 Undesirable Attributes of the Building

From Figs. 2-1, 2-2 and 2-3, and the information given above, several attributes related mainly to lateral response are noticed. Those should justify a closer scrutiny of the building had they been noted during a first or second cut rapid seismic vulnerability evaluation effort:

(a) Elements providing the largest portion of lateral shear and overturning stiffness are the central cores which have shallow individual footings susceptible to rocking; (b) all the peripheral walls are terminated before the foundation leading to a significant stiffness discontinuity at the third floor level (particularly of torsional stiffness); (c) plan aspect ratio of 1/3 indicates significant differences in lateral stiffnesses and frequencies in the principal directions; (d) elevation slenderness ratio of nearly 5 along the narrow plan dimension, raising concern for overturning stability; (e) 7.25 in. thick flat slab without stiffening along the exterior edges which raise concern regarding adequate in-plane diaphragm stiffness and strength; (f) the latter attribute also raises concern regarding the shear strength at the slab-column connections under combined gravity and bilateral effects.

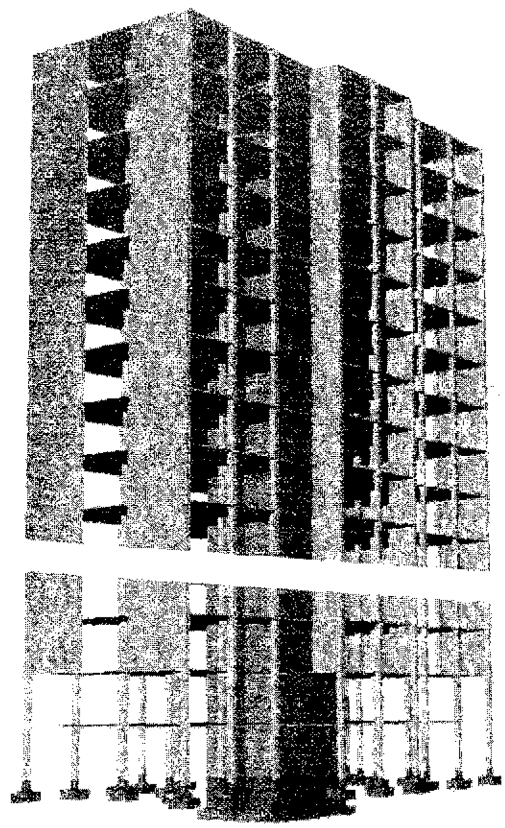

Fig. 2-3 3D Isometric View of the Structure-Foundation System

SECTION 3

ETABS AND PREDICTIVE MODELING

3.1 Description of SUPER-ETABS

"Over the past decade the TABS series [20,23,24] of computer programs, operating on main frame computer systems, have demonstrated a record that unconditionally establishes them as the most practical and efficient tools for the three-dimensional static and dynamic analysis of multistory frame and shear wall buildings [13]". An enhanced version of the program named SUPER-ETABS [18], with the same analytical capability and versatility, was developed for the personal computer. This program permits simulating 3D response of large buildings discretized into column, beam, panel and bracing elements. The independent degrees of freedom and the corresponding forces for each typical element are shown in Fig. 3-1. The column and beam element may have rigid end offsets for stiffness corrections. Columns must be prismatic. Their bending, shear, and axial deformations are included. Beams need not be prismatic but must be symmetric about their vertical midplane. Only bending and shear deformations are considered for beams.

A special panel element is included to model infill panels and discontinuous shear walls. Two alternative types of this element are as follows :

a) a "flexural" model which resists both bending and

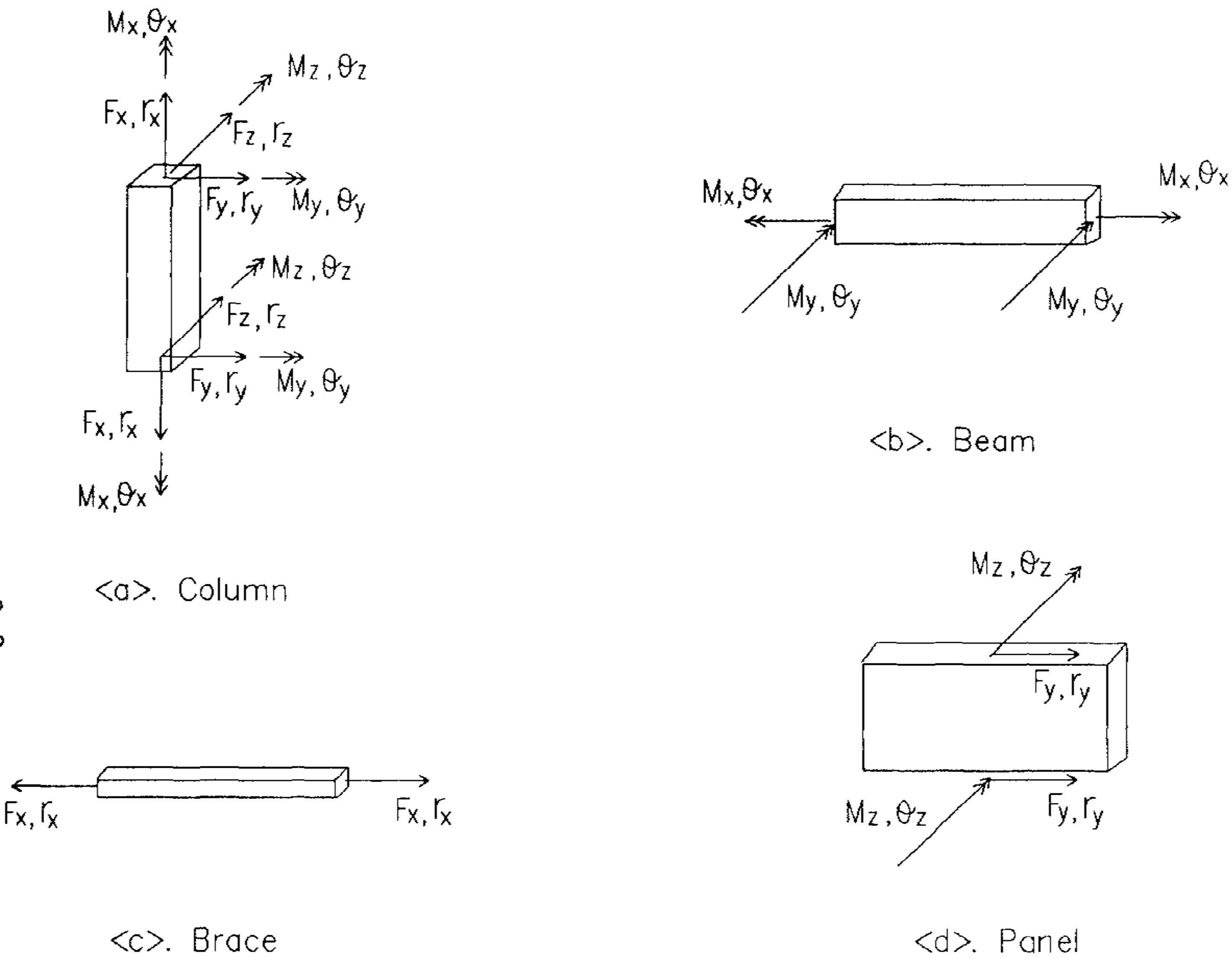

Fig. 3-1 Typical Analytical Elements in SUPER-ETABS

shear.

b) a "pure shear" model which is restricted to resisting only shear.

The typical panel deformations and joint displacements are shown in Fig. 3-2 from Ref.[25]. It must be noted that a panel should be defined only within two column-lines. On the other hand, independent rotations are not incorporated at the four edges of a panel in the formulation of panel elements. It follows that panel element's edge rotation at the joint where panel, edge column, and any beams intersect will not be compatible with the rotation of this joint. Therefore, it is necessary to supply stiff beams sandwiching a panel element to force the column rotations at the edges of a panel to be consistent with overall panel rotations at the top and bottom [25].

3.2 Analytical Modeling of the Building

A building is considered to consist of a number of 3D vertical frames for ETABS modeling. The horizontal displacements of these frames at any floor level are made dependent to the in-plane displacements and rotation of the diaphragm at the floor mass center. The size of problem which may be analyzed by SUPER-ETABS depends on the size of the largest frame. Large buildings may be divided into a large number of frames and analyzed. However, only the in-plane rigidity of the diaphragm is assumed to couple the different

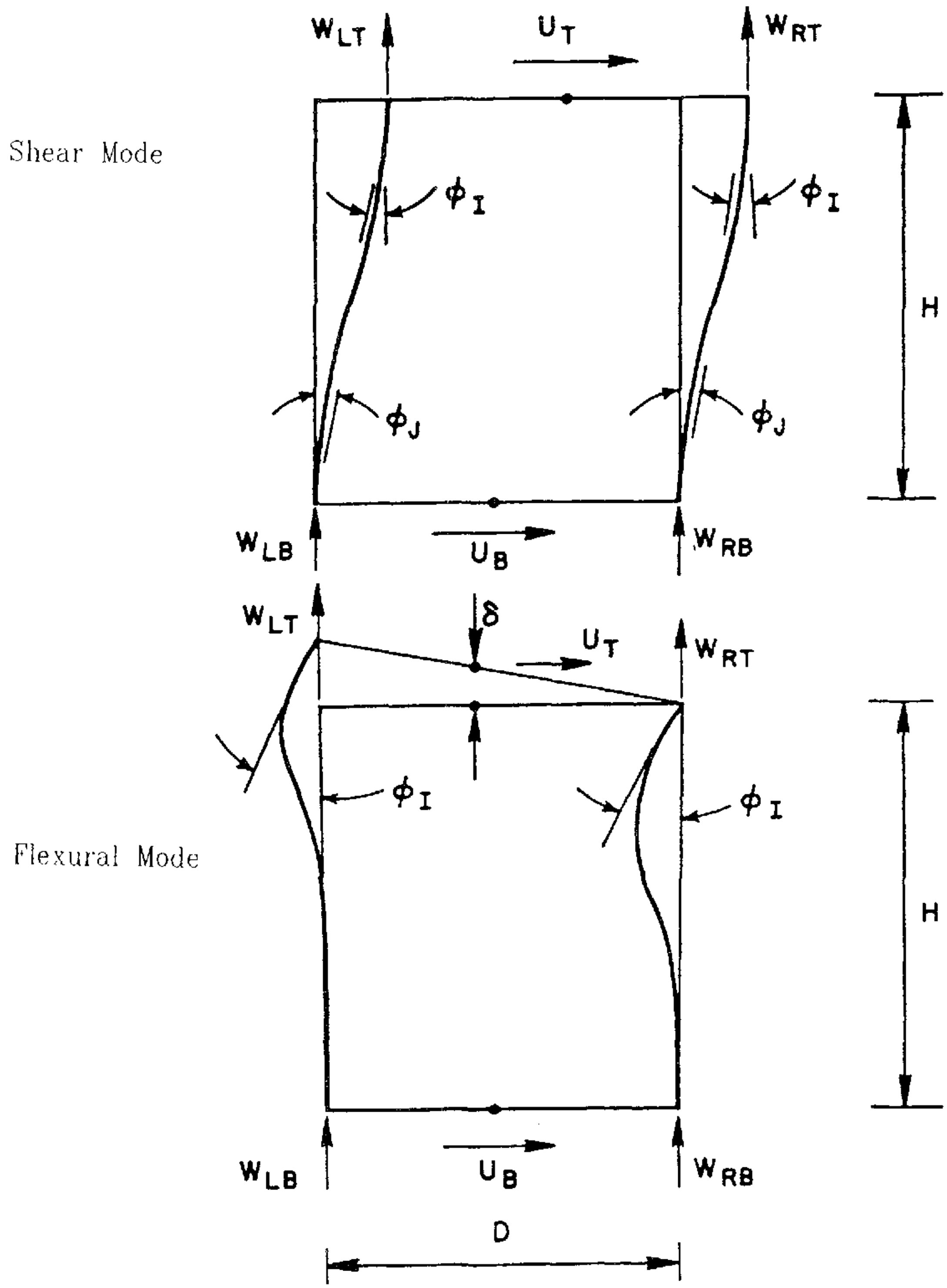

Fig. 3-2 5 Typical Panel Deformations and Joint Displacements Ref.[25]

frames. Therefore, columns or walls which are coupled by beams or which are sufficiently close to each other so that they are effectively coupled by the out-of-plane flexural stiffness of the diaphragm should be modeled as elements of the same analytical "frame".

The analytical model of the building was developed by idealizing the structural system into 4 frames as shown in Fig. 3-3. The story heights indicated in Fig. 3-2 were incorporated in the model.

The total mass of each floor calculated from the structural and non-structural elements was assumed uniformly distributed over the plan and lumped at the geometric center of each floor. A concrete weight density of 150 lb/cubic foot was used to compute mass.

All the physical beams were modeled as T-beams following the ACI guidelines for effective slab participation. When only the slab spanned between two columns, a slab beam was defined with the same depth as the thickness of the slab and a width equal to 30% of the distance between the center-lines of transverse spans.

The value of E was taken as $57000\sqrt{fc'}$, and the value of concrete compressive strength fc', was taken from the report on core tests [21]. These were on the average 50% greater than the corresponding design value. The value of Poisson's ratio was taken as 0.2.

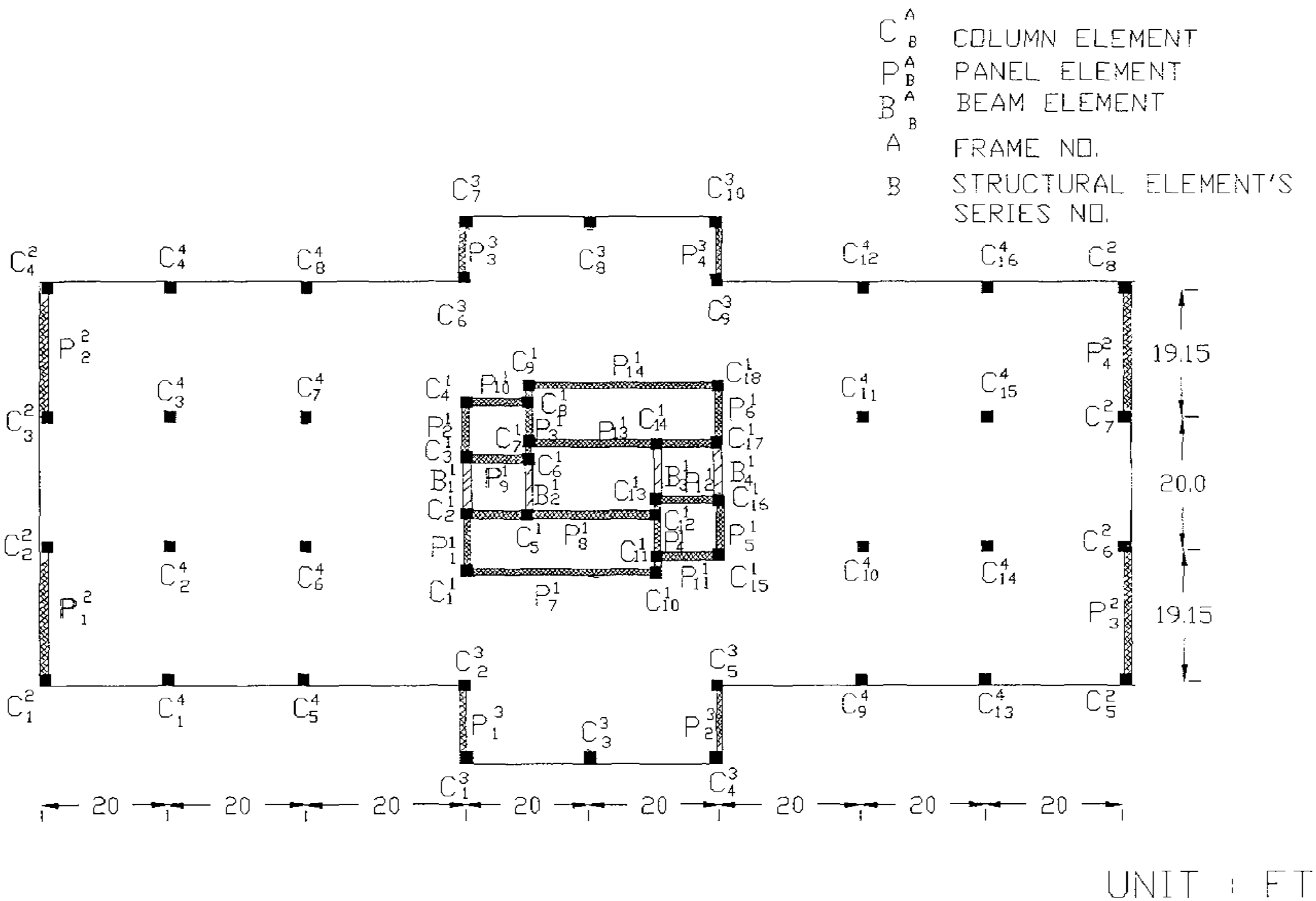

Fig. 3-3 ETABS Analytical Model

The joint zones where columns and beams intersected were assumed to be rigid and these were modeled in ETABS as rigid ends.

A fictitious story under the foundation was defined in order to be able to simulate the soil-foundation mass and flexibility, although during predictions very large stiffnesses were assigned to the elements of this fictitious story to simulate total fixity at the foundation level. The two core systems which are coupled by beams and slab comprised the largest frame. Since the cores were computed to provide almost 90% of the shear and over 50% of the overturning resistance of the building, the importance of their correct modeling is apparent. Modeling the remaining elements of the building do not require elaboration and the following discussion will focus on the cores.

3.3 Investigating the Core Characteristics

To model the cores as an assemblage of analytical elements available in the ETABS library, the following criteria were established: (a) The 6x6 3D basic (cantilever) flexibility of the core (Fig. 3-4) should be replicated by the corresponding flexibility matrix of the ETABS analytical assembly; (b) the geometry (geometric center and shear center locations and principal directions) as well as the estimated deformation kinematics of the actual core should be correctly simulated with the ETABS assembly; (c) Coupling of the cores by

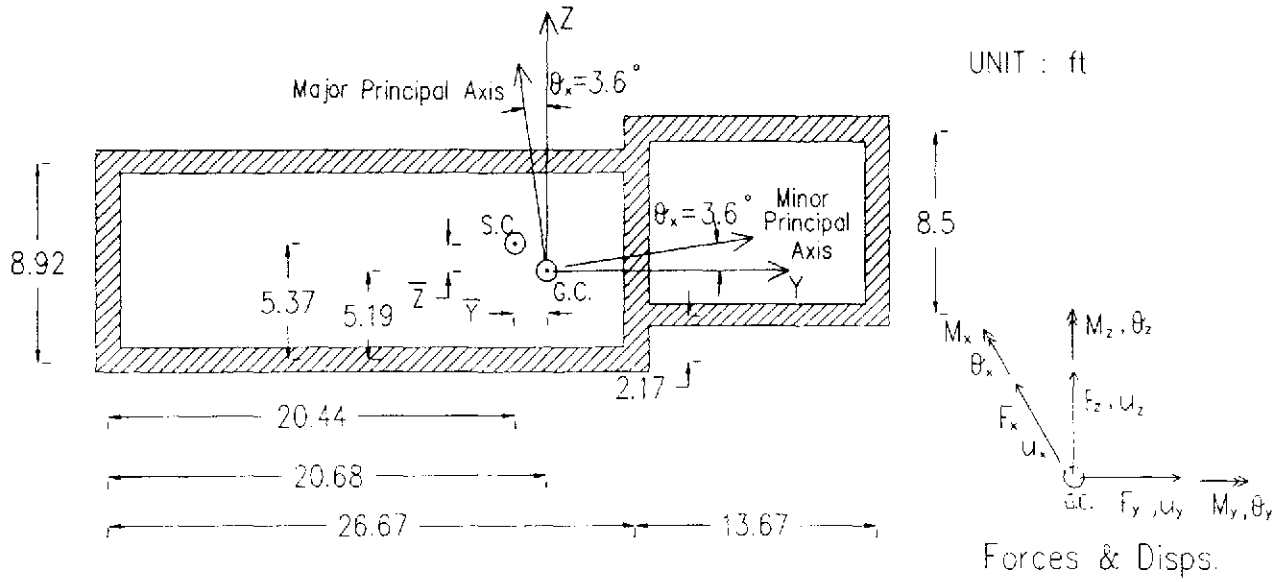

3D Cantilever Flexibility Matrix Based on the Engineering Theory and Principal Axes

$$
\begin{Bmatrix} u_x \\ u_y \\ u_z \\ \theta_x \\ \theta_y \\ \theta_z \end{Bmatrix}
=
\begin{bmatrix}
\frac{1}{EA} & & & & & \\
 & \frac{L}{GA_y} + \frac{L\bar{Z}^2}{GI_x} + \frac{L^3}{3EI_z} & -\frac{L\bar{Z}\bar{Y}}{GI_x} & \frac{L\bar{Z}}{GI_x} & & \frac{L^2}{2EI_z} \\
 & -\frac{L\bar{Z}\bar{Y}}{GI_x} & \frac{L}{GA_z} + \frac{L\bar{Y}^2}{GI_x} + \frac{L^3}{3EI_y} & \frac{-L\bar{Y}}{GI_x} & \frac{-L^2}{2EI_y} & \\
 & \frac{L\bar{Z}}{GI_x} & \frac{-L\bar{Y}}{GI_x} & \frac{L}{GI_x} & & \\
 & & \frac{-L^2}{2EI_y} & & \frac{L}{EI_y} & \\
 & \frac{L^2}{2EI_z} & & & & \frac{L}{EI_z}
\end{bmatrix}
\begin{Bmatrix} F_x \\ F_y \\ F_z \\ M_x \\ M_y \\ M_z \end{Bmatrix}
$$

Characteristics of Core Based on Engineering Theory

A_x = 107.8 ft^2	I_x = 4943 ft^4	$\bar{Y}$ = 0.242 ft
A_y = 52.45 ft^2	I_y = 1855 ft^4	$\bar{Z}$ = 0.176 ft
A_z = 16.18 ft^2	I_z = 18430 ft^4	E = 449571 ksf
L = 30 ft		G = 187321 ksf

Fig. 3-4 3D Cantilever Flexibility of the Core Element coupling beams and diaphragm should be correctly simulated in the model.

The flexibility matrix of the core was first computed based on gross section properties. The engineering theory for member analysis, based on the Bernouilli-Navier assumption for axial-shear-flexure and free warping for torsional response was used [10].

For a single core cross section, the properties A_x, A_y, A_z, I_x, I_y, I_z, Y_c, X_c, Y_s, X_s of the cross section were computed as shown in Fig. 3-4. The procedures and assumptions used to calculate these properties are outlined in Appendix A(a). The properties of two other cross sections which are less complex were also calculated based on the same procedures to better exemplify the procedure. The results from these computations are compared in Appendix A(b).

The core flexibility was therefore quantified based on the axial and effective shear areas and moments of inertia about the reference axes as well as the shear center coordinates as shown in Fig. 3-4.

The analytical assembly which was developed to model the core before the experiments is shown in Fig. 3-5-(a). This assembly was made up by modeling wall segments by panel elements, sandwiched horizontally between stiff beam elements at each floor level connected at floor levels to column elements located along each vertical boundary. The geometry of the analytical assembly therefore coincided with that of

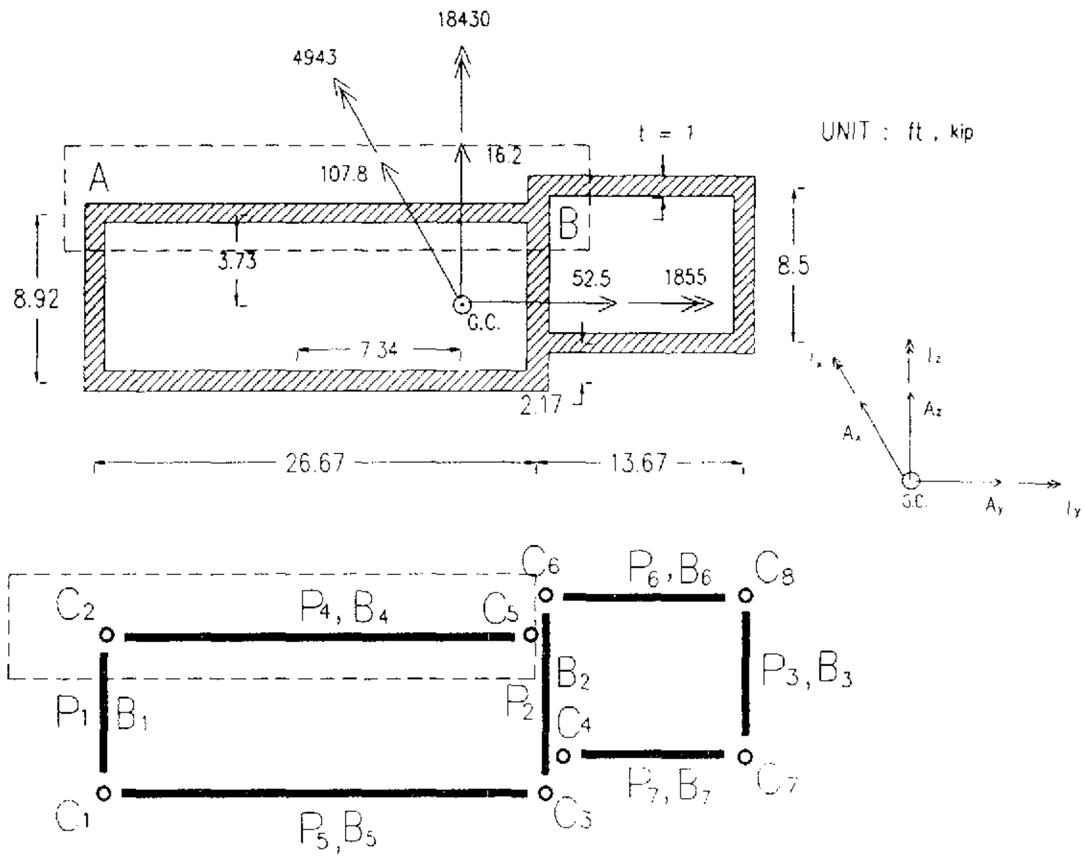

(a). Analytical Model – 1
(Generated Before Experiments)

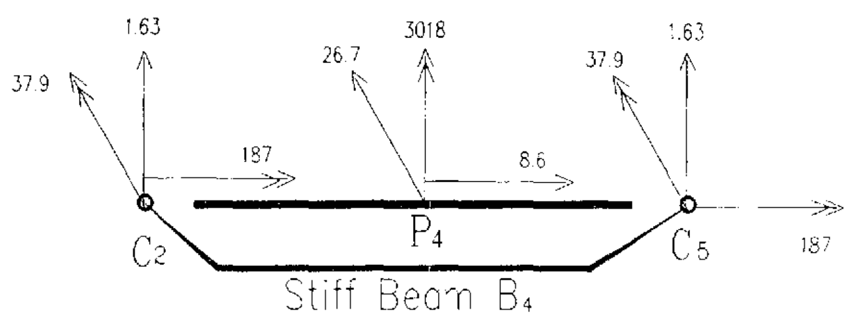

(b) Parameters Assigned for Panel P_4
and Columns C_2 , C_5

Fig. 3-5 Analytical Modeling of the Core
by ETABS before the Experimeters
(Predictive Modeling)

the core, and the deformation kinematics of the core was considered adequately simulated by the analytical assembly through the use of stiff analytical beams sandwiching the panel elements. The shear center coordinates of the analytical assembly was determined by ETABS analyses and verified to correspond to the shear center coordinates computed for the core, this was another verification of the accurate representation of deformation kinematics. The issue was in ascertaining that the ETABS element assembly would have the same flexibility as that of the actual core. This was accomplished as discussed in the following. The assembly model which was generated following the experiments and which is shown in Fig. 5-1(a) will be discussed subsequently.

3.4 Core Modeling by ETABS Prior to Experiments

To define inputs for the panel and column elements which made up the ETABS assembly in Fig. 3-5(a), first the contribution of each wall segment of the physical core to the axial and shear areas and moments of inertia along the principal axes at the geometric centroid of the core were computed. Analytical panel elements are permitted only in-plane flexural and shear stiffness. Although an axial degree-of-freedom and an axial force output is shown in the ETABS manual for panel elements, this is in fact a slave to the axial displacements along the boundaries. An independent axial degree-of-freedom along the centroidal axis is not incorporated. Based on this, the following procedures were devised to define the inputs. Wall section AB shown in Fig. 3-5(a) will be used to illustrate the procedure as follows :

(a) The axial area of core wall segments were assigned as axial area to the corresponding panel elements:

In the real cross section :

wall segment AB : $A_x = 26.7 \text{ ft}^2$

So, in the analytical model :

panel P_4 : $A_x = 26.7 \text{ ft}^2$

column C_2 and C_5 : $A_x = 0$

(b) Contributions made by the in-plane moment-of-inertia of each wall segment to the core crossectional inertia at the centroid were assigned as moment-of-inertia to the corresponding panel.

In the real cross section :

wall segment AB : $I_z = 1/12*1*26.67^3 + 26.67*7.34^2$

$= 3018 \text{ ft}^4$

(with respect to cross section centroid)

So, in the analytical model :

panel P_4 : $I_z = 3018 \text{ ft}^4$

(with respect to its centroid)

column C_2 and C_5 : $I_z = 0$

(c) Contributions made by the out-of-plane inertia of each wall segment were assigned as inertia along the corresponding direction to the analytical columns at the boundaries.

In the real cross section :

wall segment AB : $I_y = 1/12*26.67*1^3+26.67*3.73^2$

$= 374 \text{ ft}^4$

So, in the analytical model :

panel P_4 : $I_y = 0$

(nonzero value is not accepted by ETABS)

column C_2 and C_5 : $I_y = 0.5*374 = 187 \text{ ft}^4$

(d) The total effective shear area along each principal direction of the core was distributed to the wall segments in proportion to their contribution to the principal centroidal moments-of-inertia.

(e) The in-plane effective shear areas computed for a wall segment was assigned as shear area to the corresponding panel element. The total shear area of the core in the y-direction is 52.5 ft^2. The ratio of wall segment AB's I_z to the I_z of the core at the core centroid is given by 3018/18430.

panel P_4 : $A_y = 52.5*3018/18430 = 8.6 \text{ ft}^2$

(f) Out-of-plane effective shear area of a wall segment was assigned as effective shear area to the column elements at the panel boundaries.

column C_2 and C_5 : $A_z = 16.2*187/1855 = 1.63 \text{ ft}^2$

Where 16.2 ft^2 is A_z of the complete core and 187/1855 represent the ratio of the wall segment's I_y to the I_y of the core at the centroid of the core.

(g) The torsional stiffness provided to the analytical assembly due to the shear forces developing in the columns and panels was computed.

Torsional stiffness provided by the 7 panel elements :

$$GI_{xp}/L = \Sigma \left[d_i * \frac{1}{L^3/(12*E*I_i)+L/(G*A_{vi})} \right]$$

$$= 1092 \ G/L$$

where G : shear modulus

E : elastic modulus

L : clear height

I_{xp} : torsional inertia of panel elements

d_i : distance from panel P_i to G.C. of cross section

A_{vi} : shear area of panel P_i

Torsional Stiffness from column elements :

$$G*I_{xc}/L = \Sigma \ G*I_{xci}/L_i = 3548 \ G/L$$

where I_{xci} is torsional inertia of each column element i.

(h) Difference between the torsional constant I_x computed for the real core and the effective torsional constant of the analytical assembly provided by the shear resistances of the analytical elements was assigned as individual torsional constants of the analytical columns, dividing equally between all the columns.

Column C_2 and C_5 : $I_{xi} = (I_x - I_{xc} - I_{xp})/8 = 37.9 \text{ ft}^4$

Where I_{xc} and I_{xp} represent the effective torsional constant of all analytical columns and panels, respectively and I_x represents the torsional constant computed from the real core.

Hence, while the boundary columns were not assigned an axial stiffness, they were assigned flexural, shear and torsional stiffnesses. The flexibility of the ETABS assembly was generated numerically by appropriate ETABS analyses of a cantilever-core, and was determined to nearly coincide with the flexibility computed for the actual core based on gross section properties. This is illustrated in Fig. 3-6 under the ETABS model-1. The results given for ETABS model-2 will be discussed subsequently in relation to the simulative model. Since the compared flexibility coefficients of the real core and the predictive ETABS model were sufficiently close, this was considered appropriate as a reference for dynamic testing and identification of the building, and was used to generate the mode shapes and frequencies.

3.5 Analysis Results

From the ETABS output file, frequencies of the first 9 predicted modes ranged from 0.44 Hz to 6.52 Hz. Since the principal axes and global axes of the complete structure did not exactly coincide, each bending mode had amplitudes in both lateral directions. However, the effective mass of the coupling terms were small, as shown in Fig. 3-7. The mass contributions of the first 9 modes in the lateral direction as well as in torsion added up to more than 92% of the corresponding total mass in each direction. Therefore, only the first nine modes were used in the identification of the building. The mode shapes obtained from these analyses are

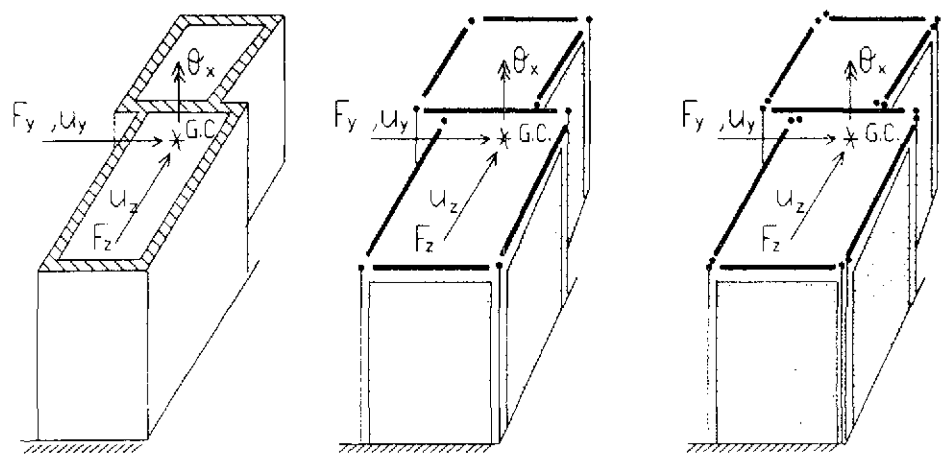

Real Core   ETABS Model - 1   ETABS Model - 2

Load Case *		Displacements		
		u_y (ft)	u_z (ft)	θ_x (rad)
Real Core	F_y = 10^5 Kips	0.304	-0.013	0.0003
	F_z = 10^5 Kips	-0.013	0.093	0.0002
ETABS Model (1)	F_y = 10^5 Kips	0.317	-0.007	0.0004
	F_z = 10^5 Kips	-0.007	0.094	0.0002
ETABS Model (2)	F_y = 10^5 Kips	0.315	-0.003	0.0004
	F_z = 10^5 Kips	-0.003	0.094	0.0002

* Forces are Applied Separately in Each Load Case

Fig. 3-6 Verification of the Analytical Core Element Assemblies

Mode No.	Frequency (Hz)	Modal Mass Ratio		
		W-E Dir.	N-S Dir.	Rotation
1	0.44	0.004	0.693	0.000
2	0.58	0.000	0.000	0.793
3	0.59	0.657	0.004	0.000
4	2.01	0.001	0.201	0.000
5	2.14	0.000	0.000	0.146
6	2.84	0.211	0.002	0.000
7	4.54	0.000	0.000	0.035
8	4.61	0.000	0.047	0.000
9	6.52	0.054	0.001	0.000
Total		0.927	0.946	0.973

Fig. **3-7** Results from Predictive ETABS Model given in Fig. 4-15.

SECTION 4

MODAL TESTING OF THE BUILDING

4.1 General Description

Dynamic tests were conducted in the context of modal testing for the global identification of the building i.e. to verify the ETABS model and to quantify its critical parameters such as core stiffnesses.

4.2 Instruments and Procedures

A number of excitation devices, excitation types and data acquisition procedures were explored to design the test and to arrive at the following procedure. To find an excitation device which would effectively excite the building at frequencies below 1 Hz. proved to be a problem. One of the largest portable excitation devices designed for nuclear facility testing was provided by SDRC of Cincinnati and this was used in the research. Random excitation was continuously generated at the 26th floor of the building by a linear 2500 lbf reactive-mass actuator with a 2 in. maximum stroke leading to a dynamic force of 75 lbf at 0.5 Hz. (exciter is shown in the photograph in Fig. 4-1). The actuator was mounted against the column indicated in Fig. 4-2 and excitation was first applied along the N-S direction. After measuring the lateral and torsional dynamic characteristics, the exciter was rotated to the E-W direction and the complete testing was

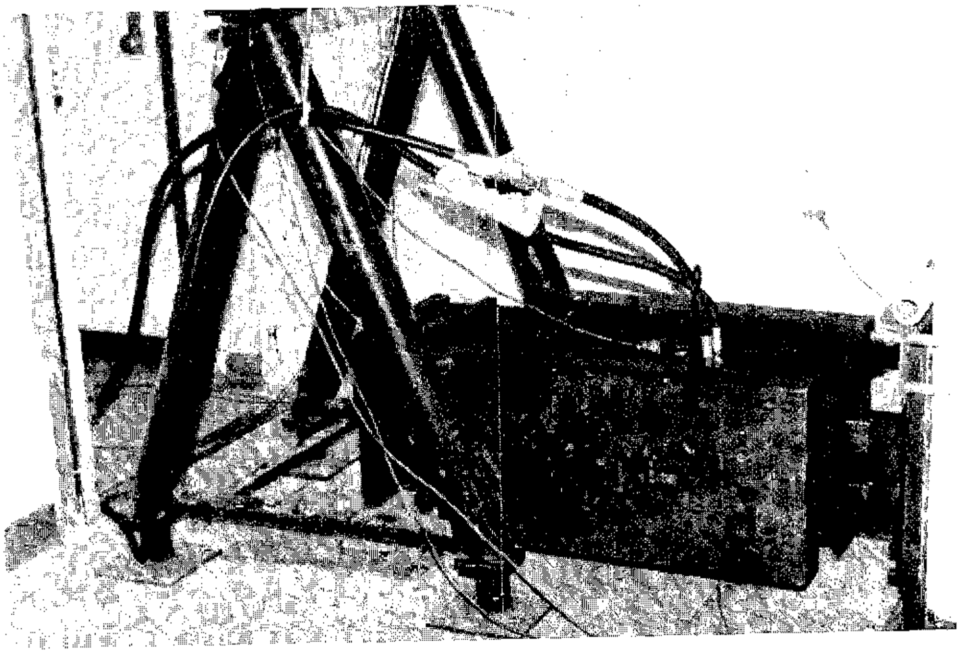

Fig. 4-1 Linear Inertia-Mass Exciter Used for Modal Testing of the Building

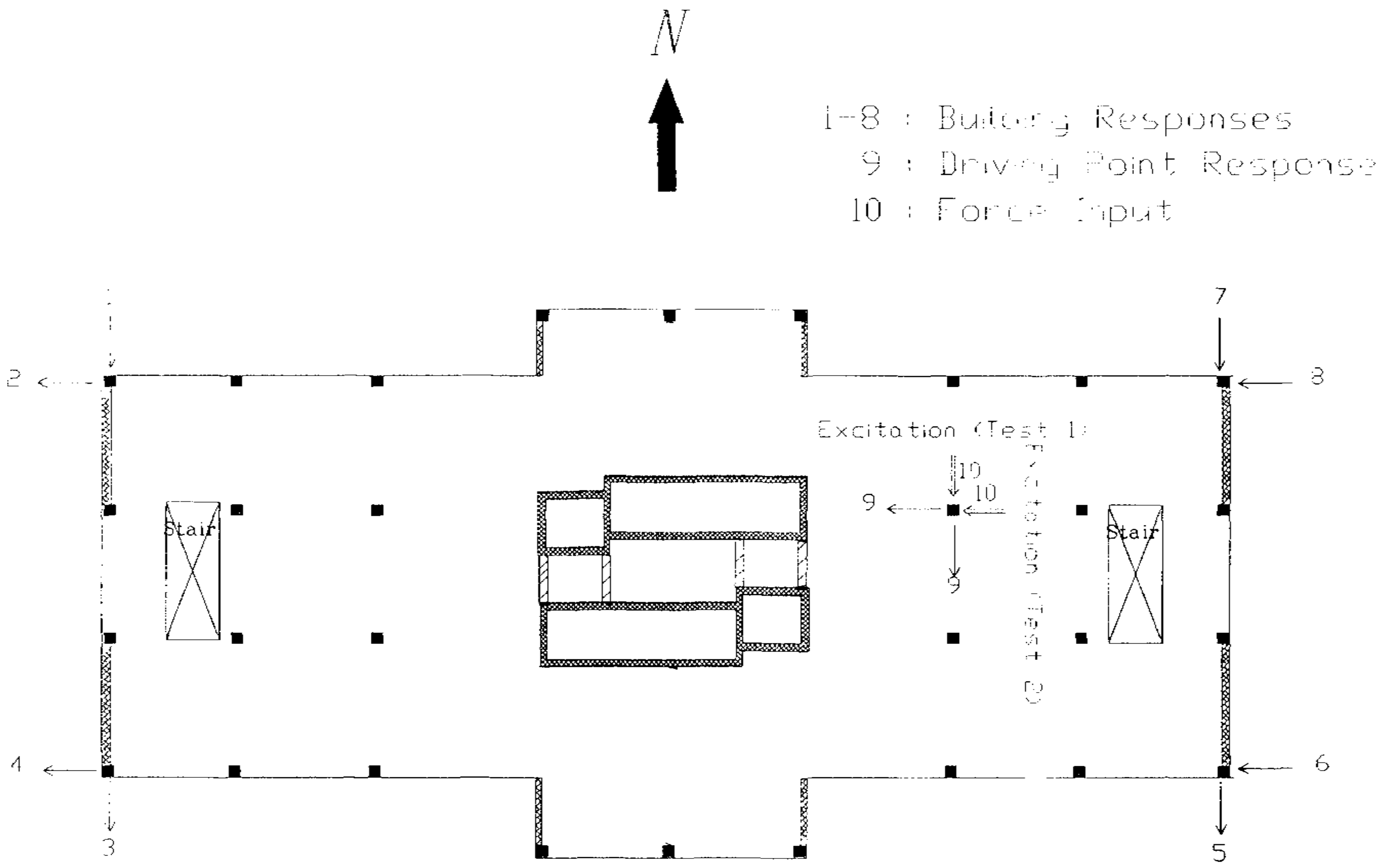

Fig. 4-2 Building Plan Showing Excitation and Typical Response Measurement Locations

repeated along the E-W direction. Responses were measured at nine floor levels while the actuator remained stationary on floor 26. At each floor tested, 10 PCB model 393-B seismic accelerometers were located as shown in Fig. 4-2. A GenRad 2515 dynamic analyzer was used to control the test as well as to measure and store the data in the frequency domain. MODAL-PLUS which is a modal analysis software package developed by SDRC was used to determine the dynamic characteristics of the structure from frequency response functions. A TEAC digital tape drive was used to record the data also in the time domain. Fig. 4-3 shows a photo of the equipment used for the excitation control, while Fig. 4-4 shows the photo of instruments used for the data acquisition and storage. Flow charts of both the excitation control and data acquisition and storage are given in Figs 4-5, and 4-6. The hardware used in modal test are listed in the following :

<A>. For Excitation Control :

<1>. HP 3561a Dynamic Signal Analyzer.

-- Generates very low frequency band limited random force signal

<2>. WAVETEK VCG/Noise Generator, Model 132.

-- Generates broadband random force signal

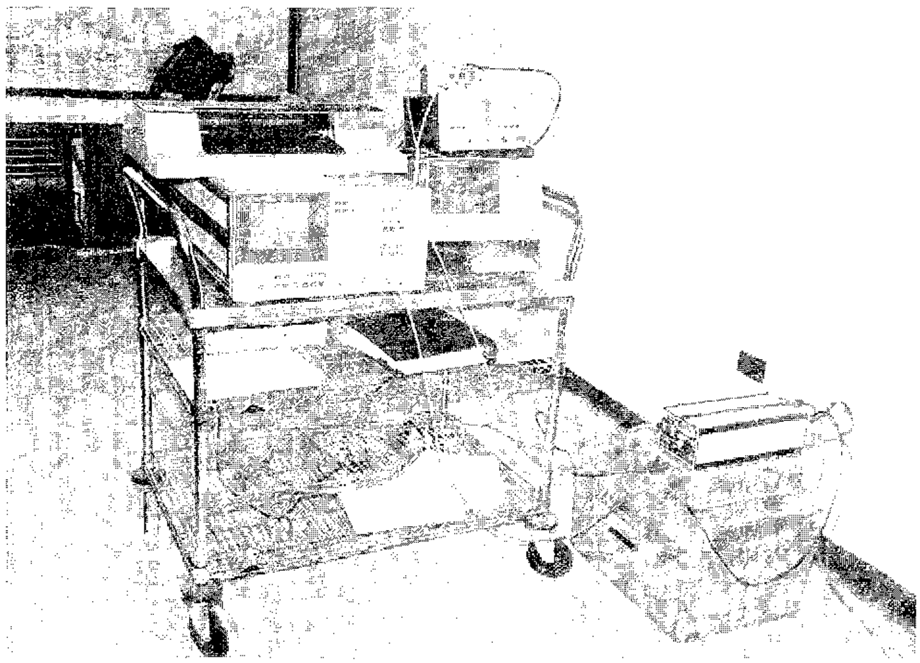

Fig. 4-3 Photograph of Instruments Used to
Control the Excitation

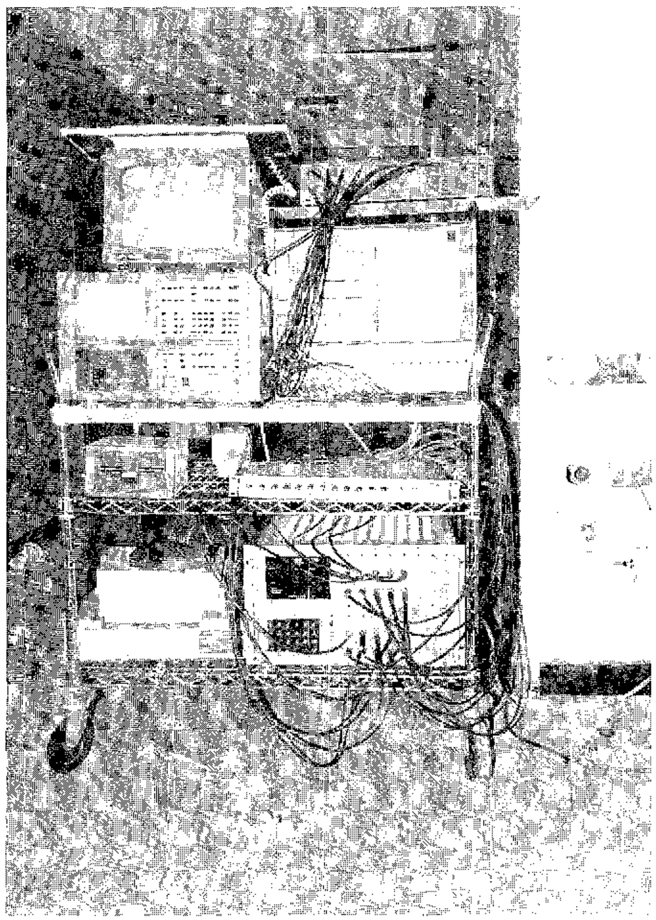

Fig.4-4 Photograph of Instruments Used in the Data Acquisition, Processing and Storage System

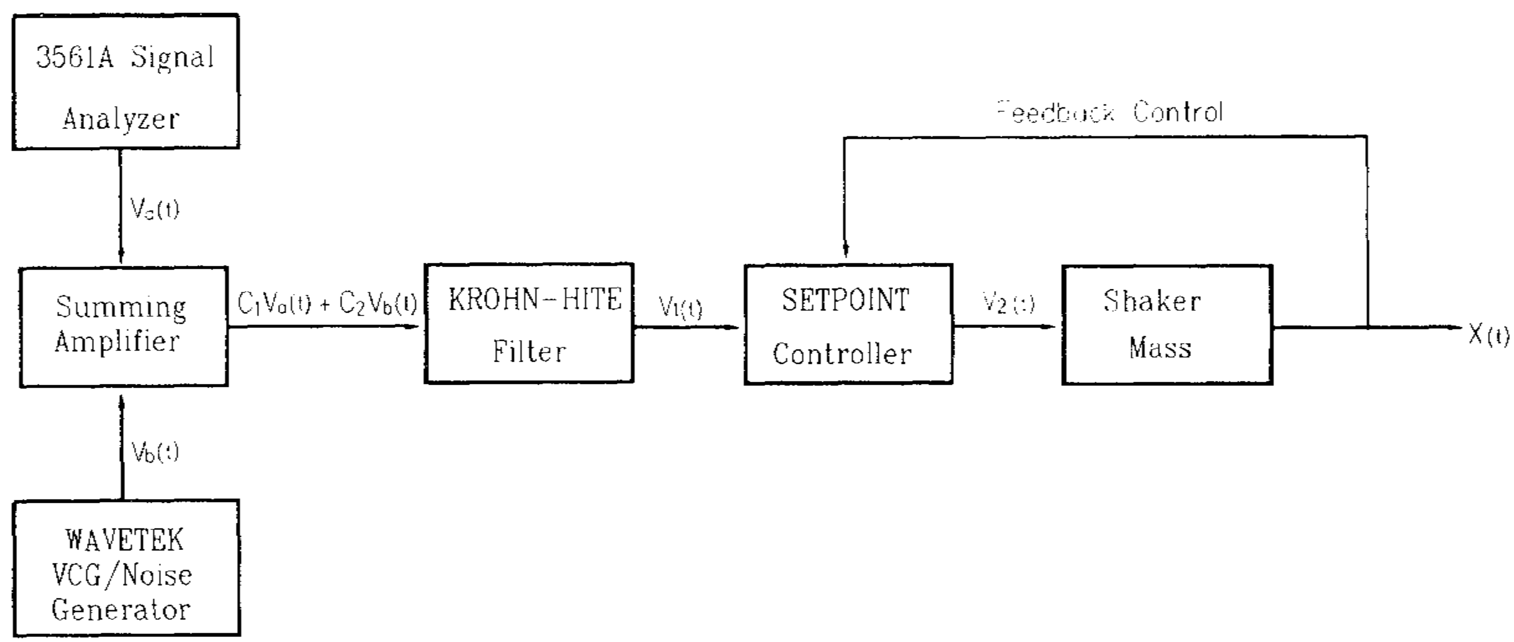

Fig. 4-5 Flow Chart of Instruments Used in the Excitation Generation

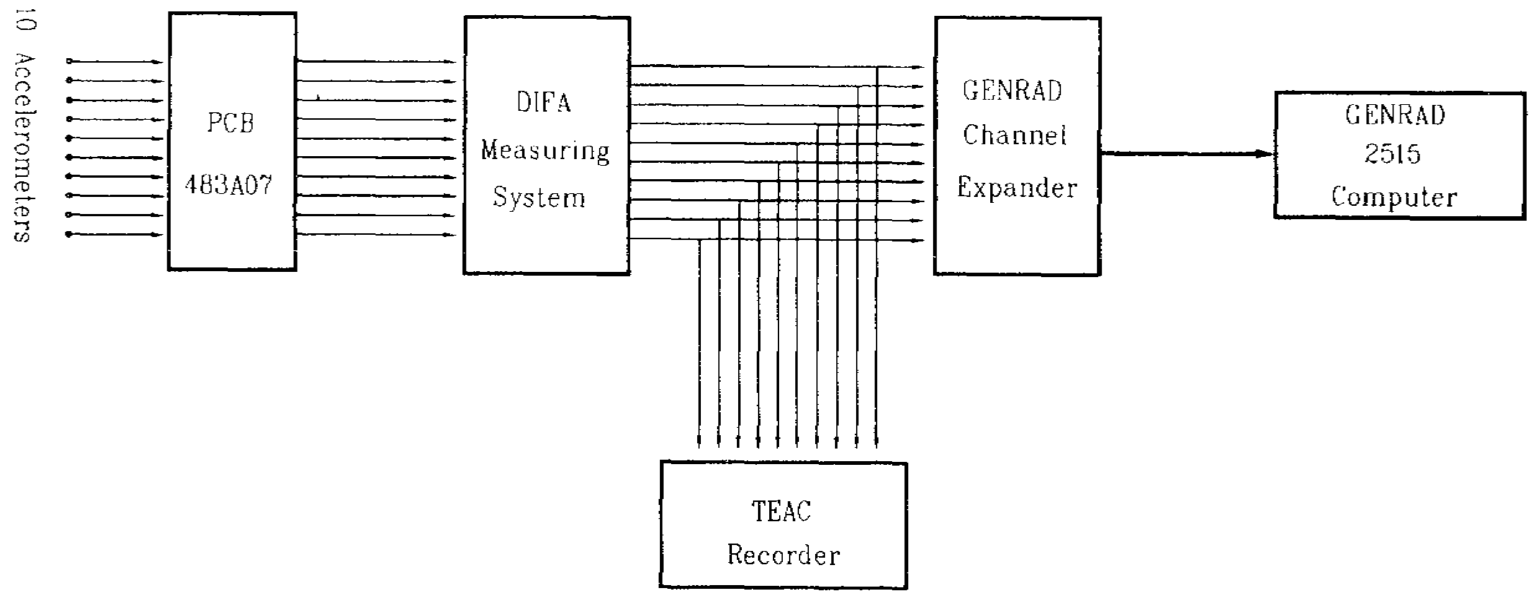

Fig. 4-6 Flow Chart of Instruments Used in the Data Acquisition and Storage

<3>. Summing Amplifier.

-- Added the signals from WAVETEK and 3561A to provide variable gain for each of these signals

<4>. KH (Krohn-Hite) Filter, Model 3550.

-- Low pass filter which concentrates the force energy at low frequencies

<5>. Set Point Controller. (Zonic Technical Laboratories INC.)

-- Feedback servo-controller to control the inertial-mass actuator

<6>. Electro-Hydraulic Servo-Control Inertial-Mass Excitation Generator, (SDRC manufactured 3000 lbs inertia-mass 2 in. stroke actuator used with 2500 lbs mass)

-- Generates force excitation

<B>. For Data Measurement and Store :

<1>. 10 PCB Accelerometers Model 393B.

-- Measures low-level vibration

<2>. PCB PIEZOTRONICS Model 483A07.

-- Power supply for accelerometers

-- Integral amplifiers with max. 100 time gain

<3>. DIFA Measuring System.

-- Low pass filter and signal amplifier

-- Used to make better use of the dynamic range of the recorder (TEAC) and GenRad

<4>. TEAC XR-710 Cassette Data Recorder.

-- 21 channel analog FM data recorder

-- Stores all data time histories on magnetic tape for re-analysis if desired

<5>. GenRad Channel Expansion.

-- Allow up to 16 channels of data input to GenRad

<6>. GenRad Computer-Aided Test System 2515.

-- Acquires Data

-- Calculates frequency response functions (FRF)

-- Stores FRF's to a hard disc

-- Computes modal parameters from stored FRF's using SDRC developed Modal Plus software

Three different sets of data were acquired at each floor (1) Ambient Test data (15 min.); (2) Forced excitation test from 0 to 4 H_z, 200 frequency domain averages; (3) Forced excitation test from 0 to 16 H_z, 400 frequency domain averages.

Coherence (Fig. 4-7) between force and responses were checked and seen to be close to 100% above 1 Hz. and somewhat less below 1 Hz. This remained a problem although tests were conducted by random excitation which was filtered in order to accentuate the frequencies below 1 Hz. It was noticed that the coherence became less when the ambient response due to wind became higher. In fact, the frequencies were noticed to shift in the course of testing through a day with the changes in ambient conditions. Since the level of excitation at lower frequencies did not permit to study the influence of ambient phenomena on mechanical characteristics of the building, these were not explored further.

The modal amplitudes were found at the measurement locations by taking the ratio of corresponding peaks in the transfer functions after these were conditioned by curve-fitting. Possible diaphragm distortion was implicated by slight differences in the modal amplitudes measured at diaphragm corners. The low level of force was not judged adequate to isolate this phenomenon from other possible error sources confidently. Therefore lateral mode amplitudes measured at diaphragm corners were averaged. Similarly, while it was not possible to measure foundation displacement or rotation within the margin of error which affected the test results, possible rigid-body rocking of the core footings was not ruled out at slightly higher excitation levels. A new

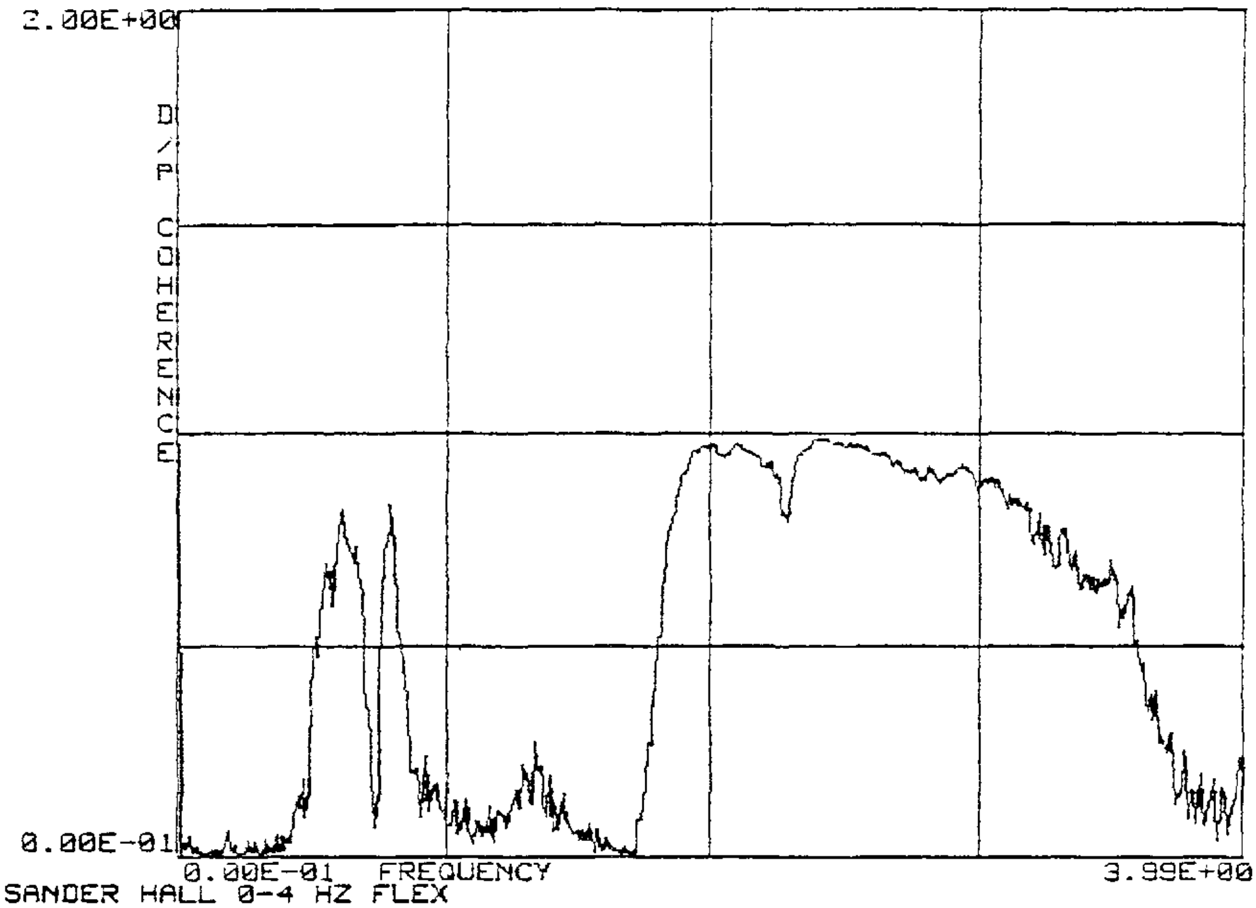

Fig. 4-7 Coherence Between Excitation and Diaphragm Response, Two Stories Above Excitation

excitation device which will have sufficient energy input capability at frequencies under 1 Hz. is being developed to repeat the tests of the building for more rigorous and reliable identification of these phenomena discussed above.

In spite of the fact that input excitation was low under 1 Hz., the characteristics of 9 lower modes along a bandwidth of 0.58 Hz. - 6.56 Hz. could be confidently identified.

It is important to note that due to the design of light wood-product nonstructural elements, their interaction with the structural system was not a problem. It is important that characteristics of some of these modes may change with higher excitation levels, particularly if phenomena such as foundation rocking may be initiated. Also, had stiffer and/or heavior nonstructural components were used, the interaction of these with the structural system would have led to differences in dynamic characteristics with the excitation level.

Reliable measurement of the shapes of the first three modes was accomplished by selecting the "response ratio algorithm". This algorithm is not influenced by the interference of ambient and applied excitations and was in fact aided by the fact that input excitation was complemented by ambient excitation as long as this could be assumed as broad-banded. This is further illustrated in Fig. 4-8 which shows the lower 3 mode shapes obtained from the experiment based on the "transfer function" and "response-ratio" algorithms. The importance of selecting an appropriate

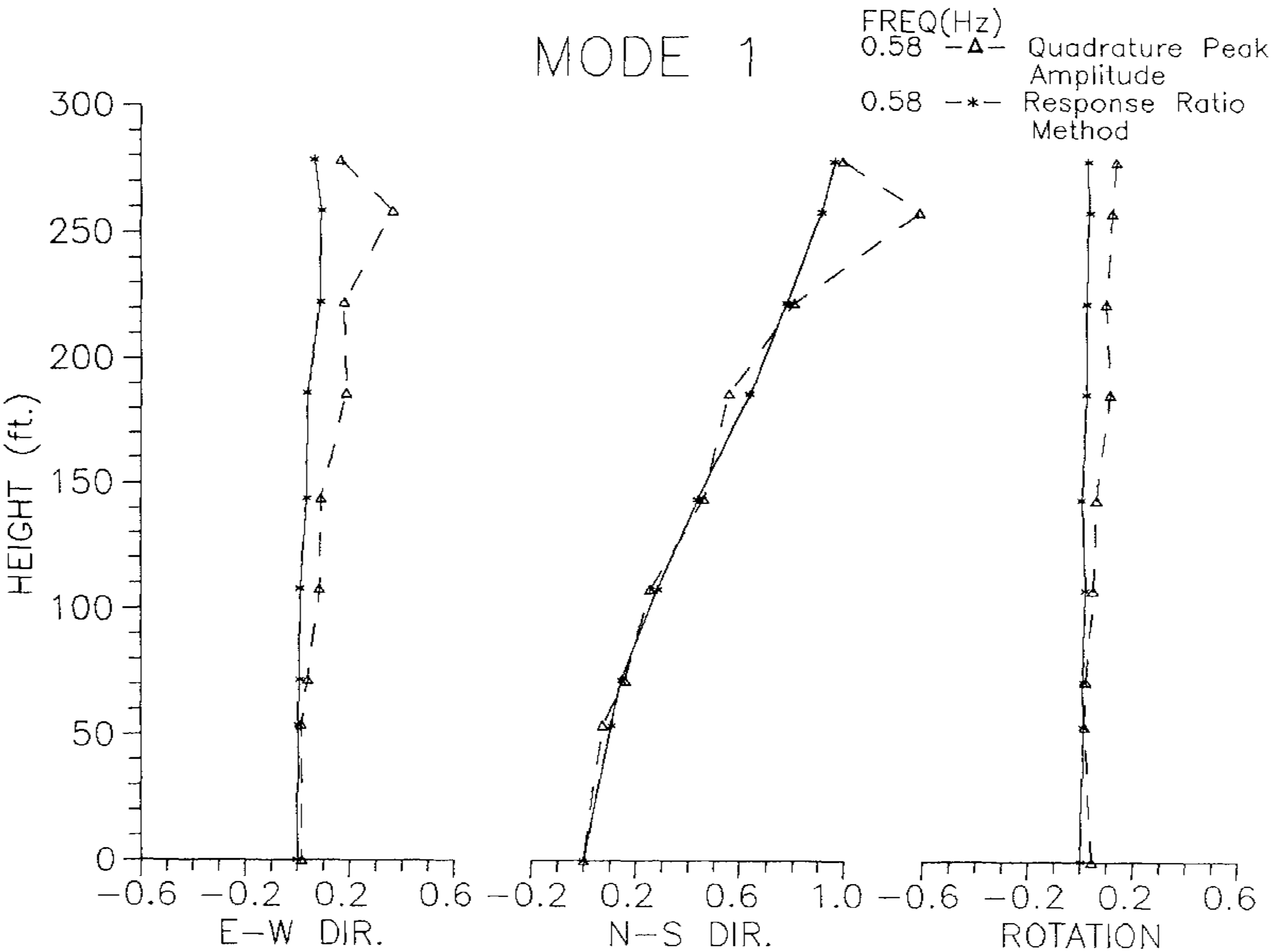

Fig. **4-8** Influence of Curve Fitting and Algorithm on the Mode Shapes Recovered from Modal Test

-- Continued

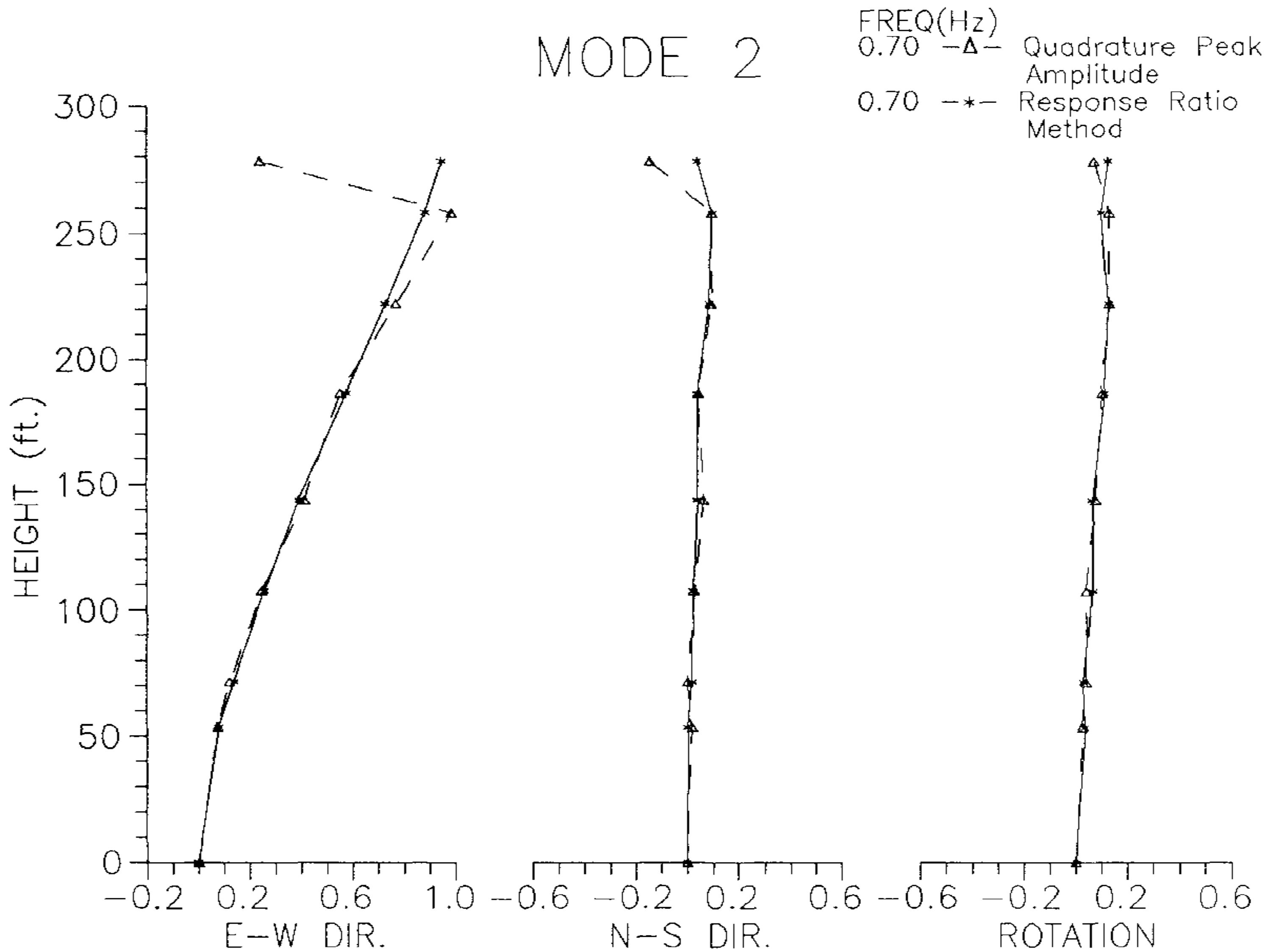

Fig. **4-8** Influence of Curve Fitting and Algorithm on the Mode Shapes Recovered from Modal Test

-- Continued

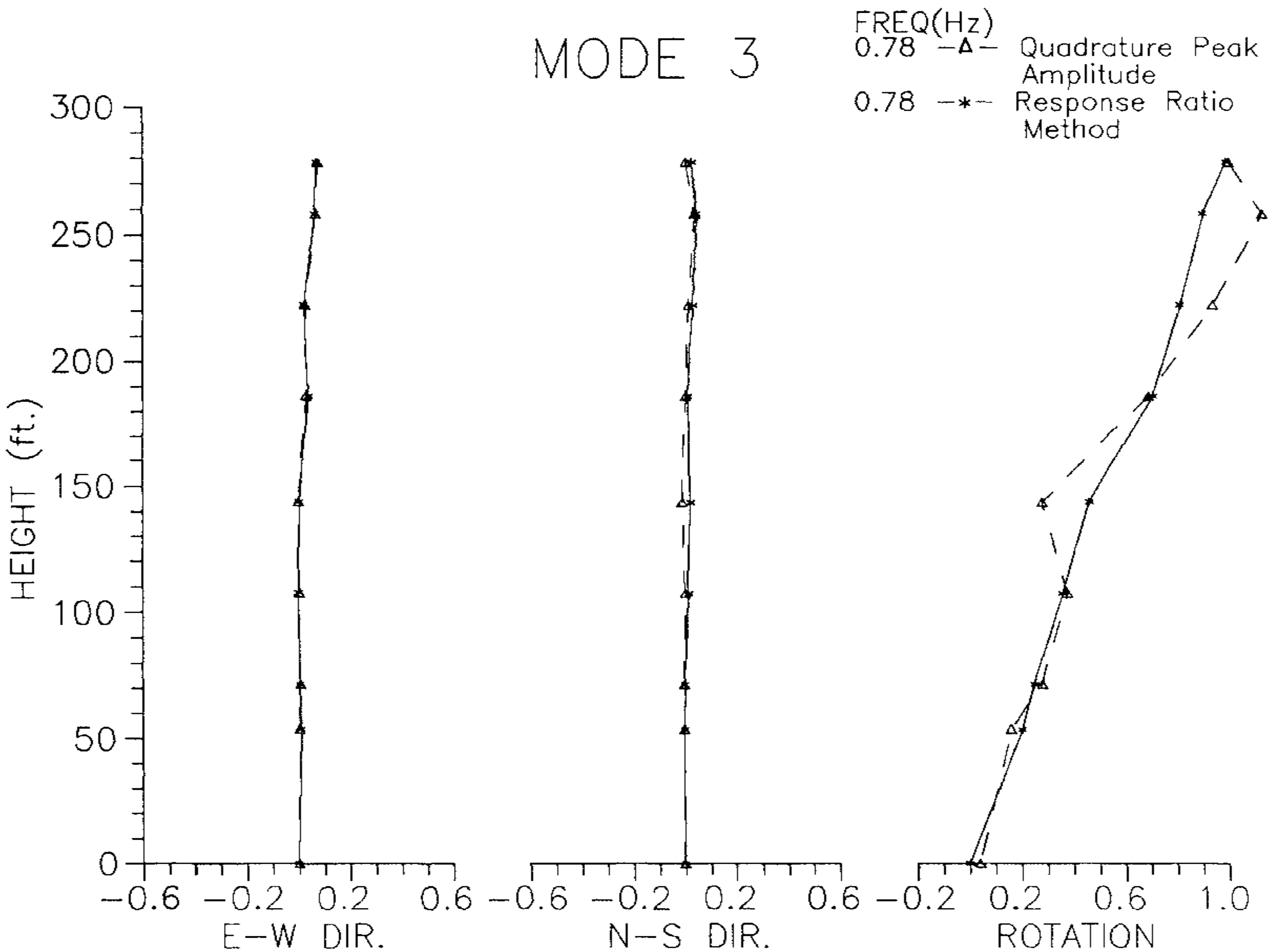

Fig. **4-8** Influence of Curve Fitting and Algorithm on the Mode Shapes Recovered from Modal Test algorithm in improving the reliability of modal test results is evident from this figure. Also evident is the need for specialized expertise in modal testing for reliable identification of constructed facilities.

4.3 Results of Modal Test

The frequency responses measured from 0 to 4 Hz in N-S and E-W directions were shown in Fig. 4-9 and Fig. 4-10 respectively. Frequency responses in the 0 to 16 Hz band in N-S and E-W directions follow in Figs 4-11 and 4-12 respectively. The corresponding force power spectrums are also shown in Figs 4-13 and 4-14.

A reasonably "broad-banded" force input in the frequency band of interest is indicated from these figures. However, a new excitation generator is being developed to improve the power in the 0-2 Hz band. Comparing the force power spectrums in Figs 4-13 & 4-14 and the corresponding frequency responses in Figs 4-9 and 4-10, it is observed that frequencies of the structure correspond to peaks in the power spectrum.

The nine measured mode shapes and frequencies of the building are shown in Fig. 4-15, compared with the predicted values from the predictive ETABS model. The first three predicted frequencies are approximately 25% lower than the measured frequencies while the difference is about 5% for the remaining six frequencies. Predicted modal amplitudes are observed to be quite close to the experimental counterparts.

The large discrepancy in the lower three predicted and measured frequencies indicated a significant shortcoming of the analytical model in spite of the expertise and careful study based on which it was generated. The fact that only the three lower predicted frequencies significantly differed from their measured counterparts, and that the analytical model appeared "more flexible" than the real building in spite of assuming "gross section properties" and "no foundation flexibility" was intriguing.

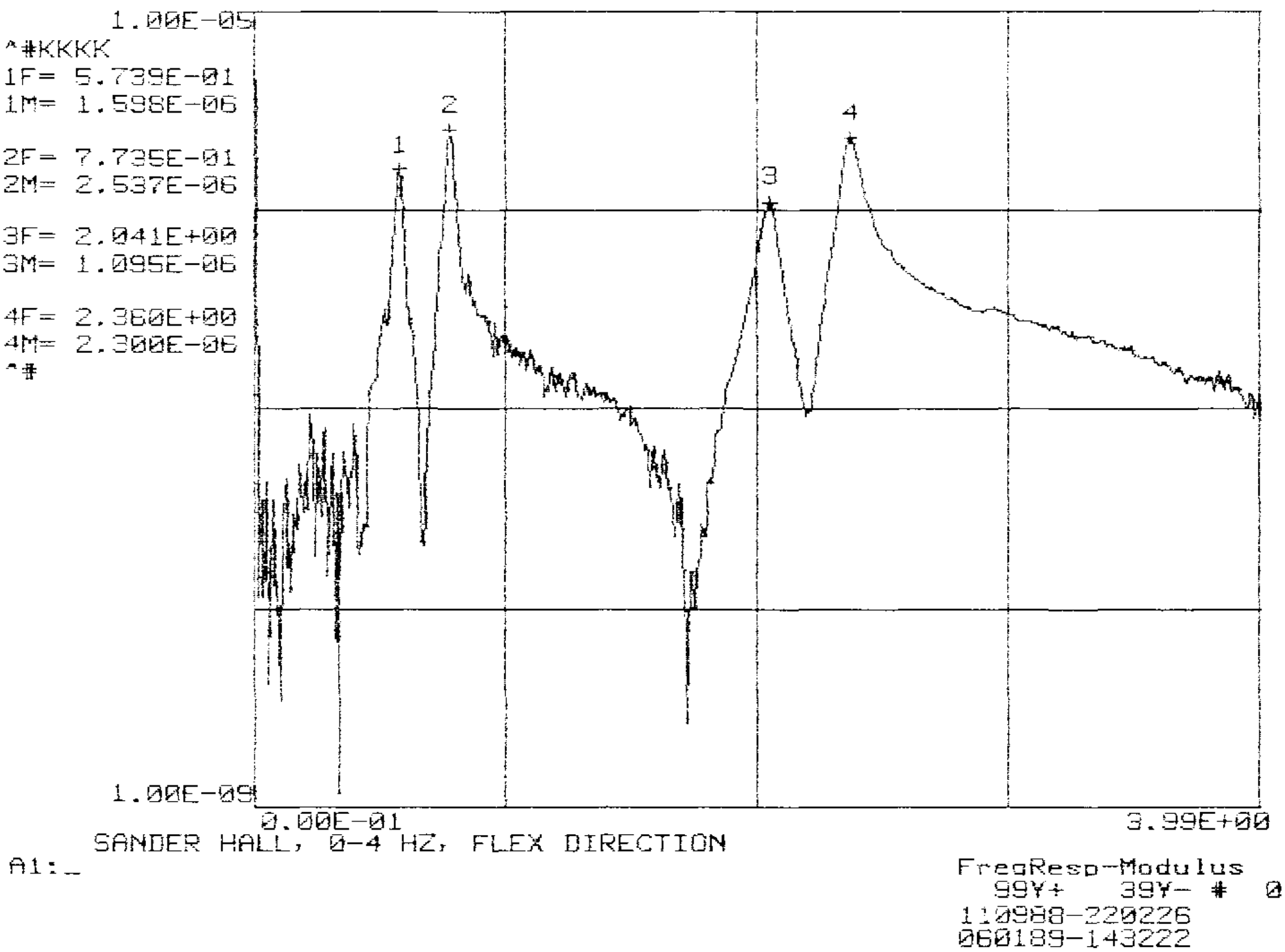

Fig. 4-9 Frequency Responses Measured from 0 to 4 Hz in N-S Dir.

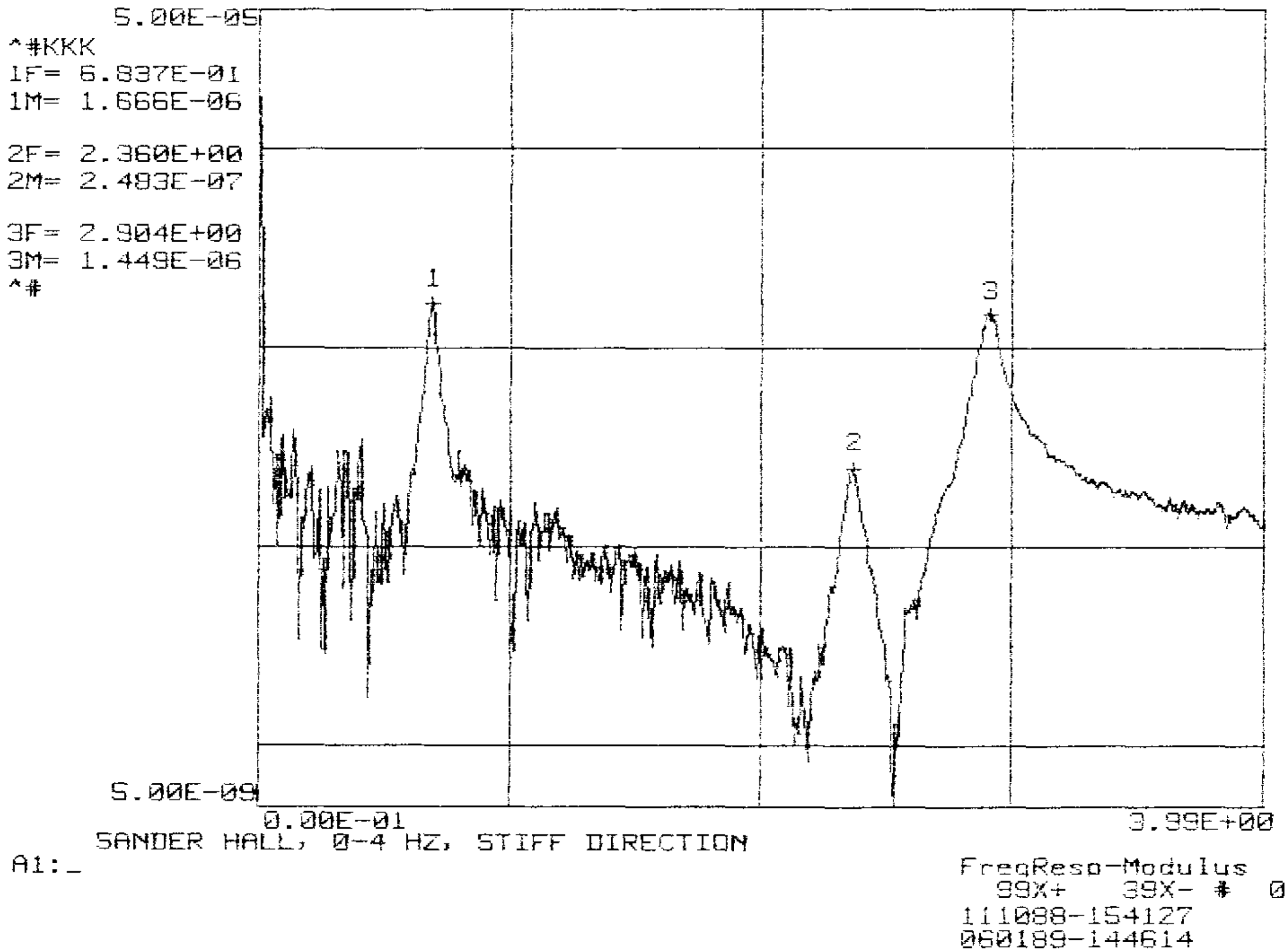

Fig. 4-10 Frequency Responses Measured from 0 to 4 Hz in E-W Dir.

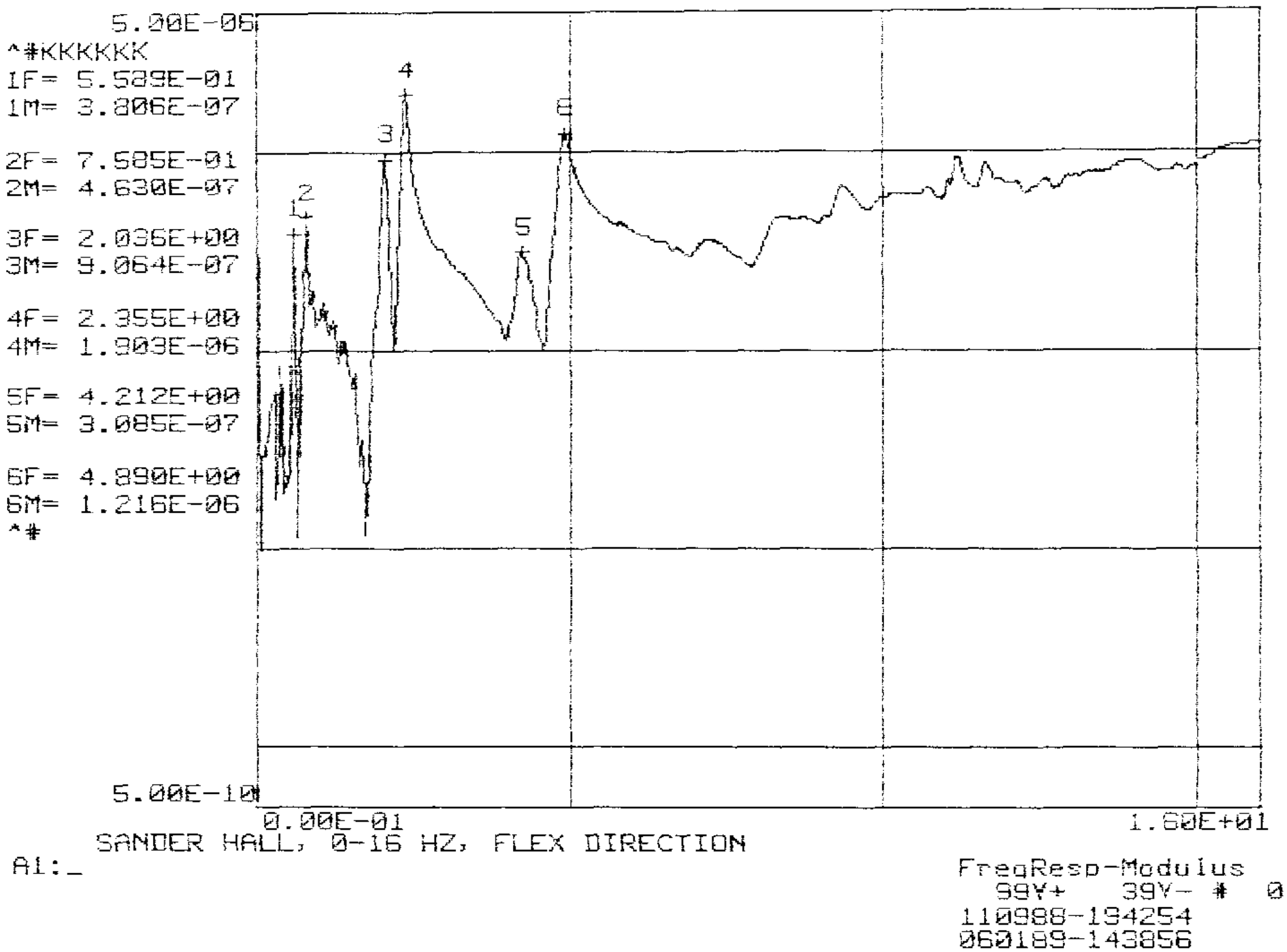

Fig. 4-11 Frequency Responses Measured from 0 to 16 Hz in N-S Dir.

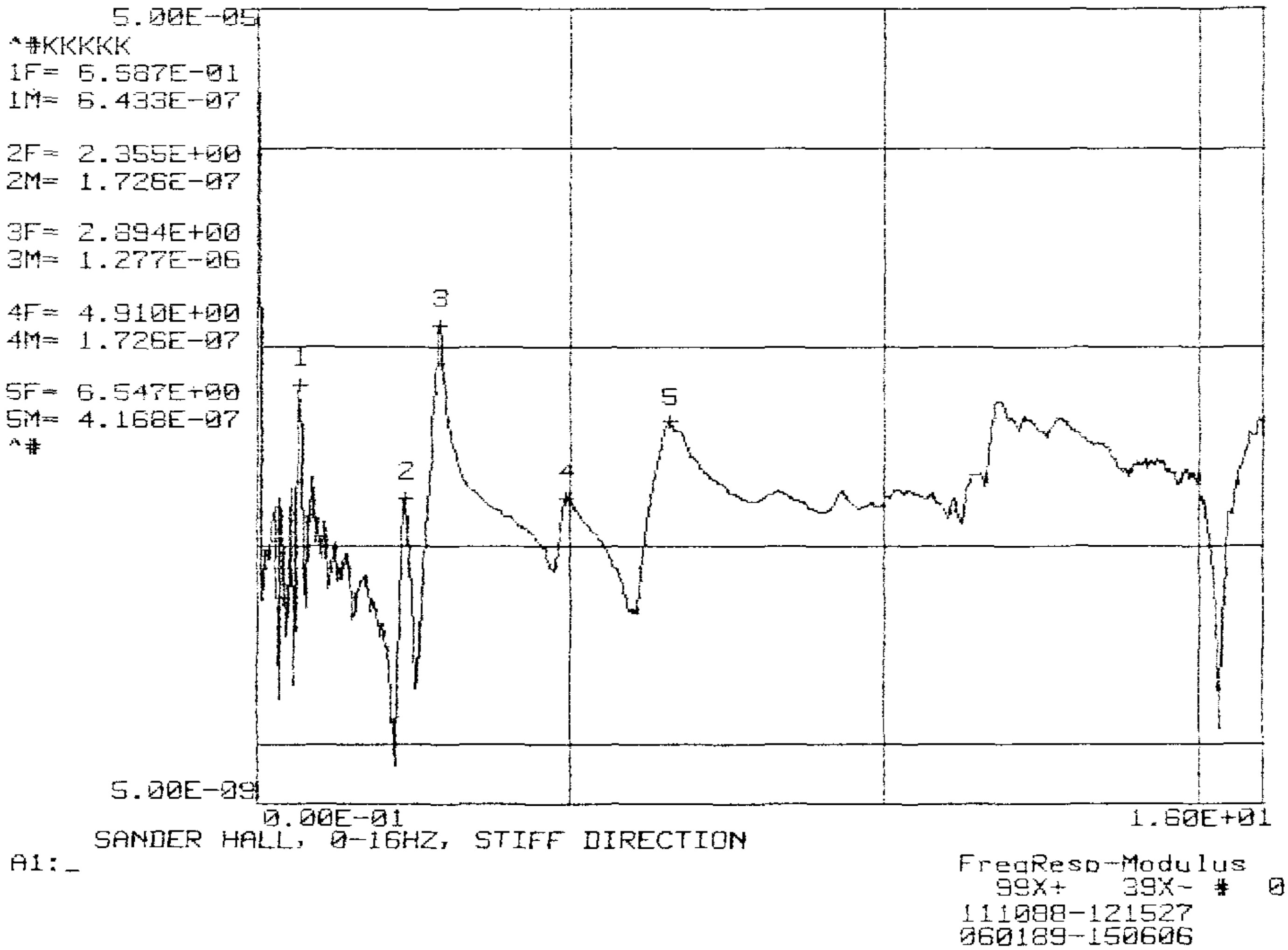

Fig. 4-12 Frequency Responses Measured from 0 to 16 Hz in E-W Dir.

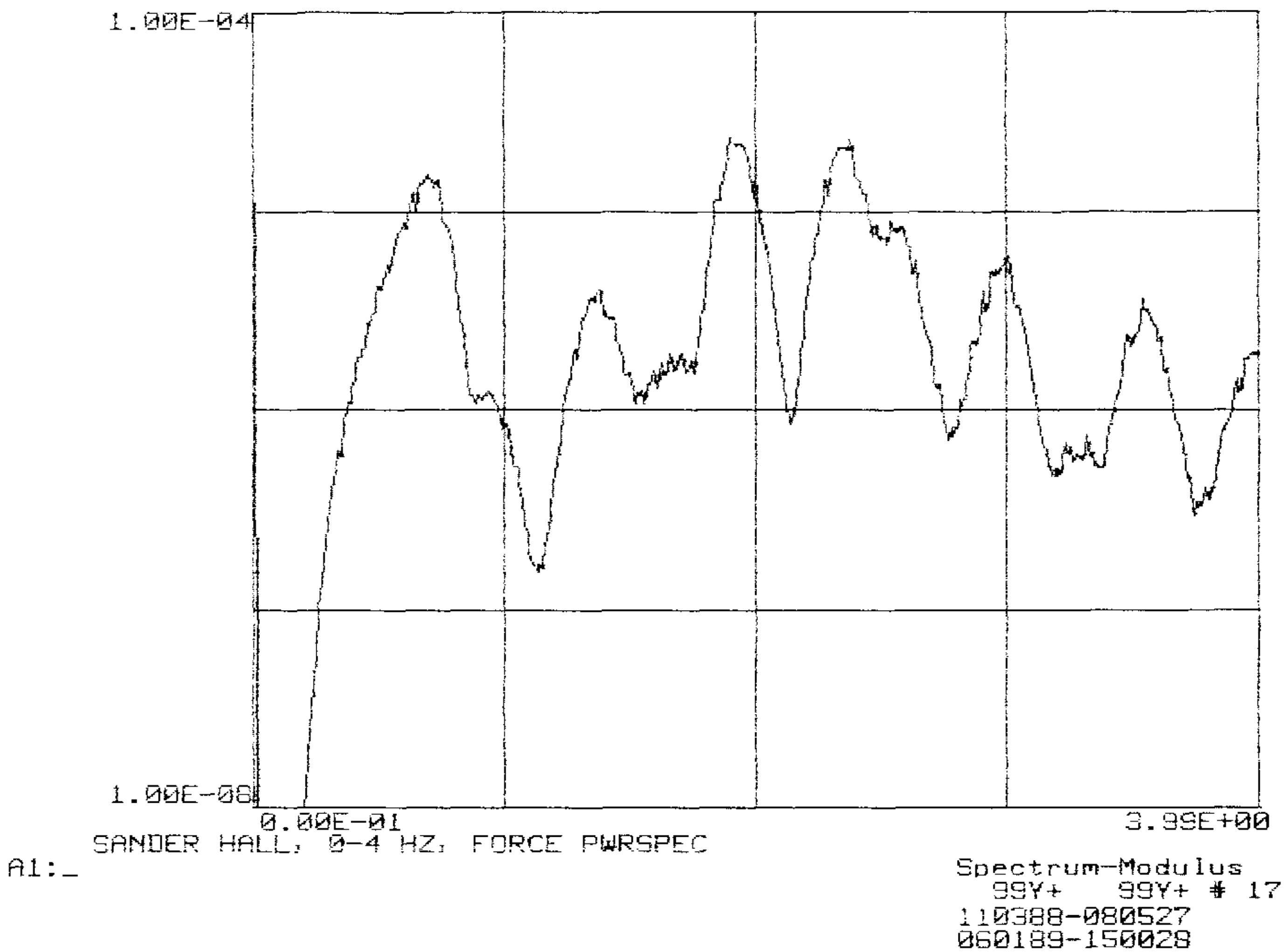

Fig. 4-13 Force Power Spectrum at Frequencies from 0 to 4 Hz

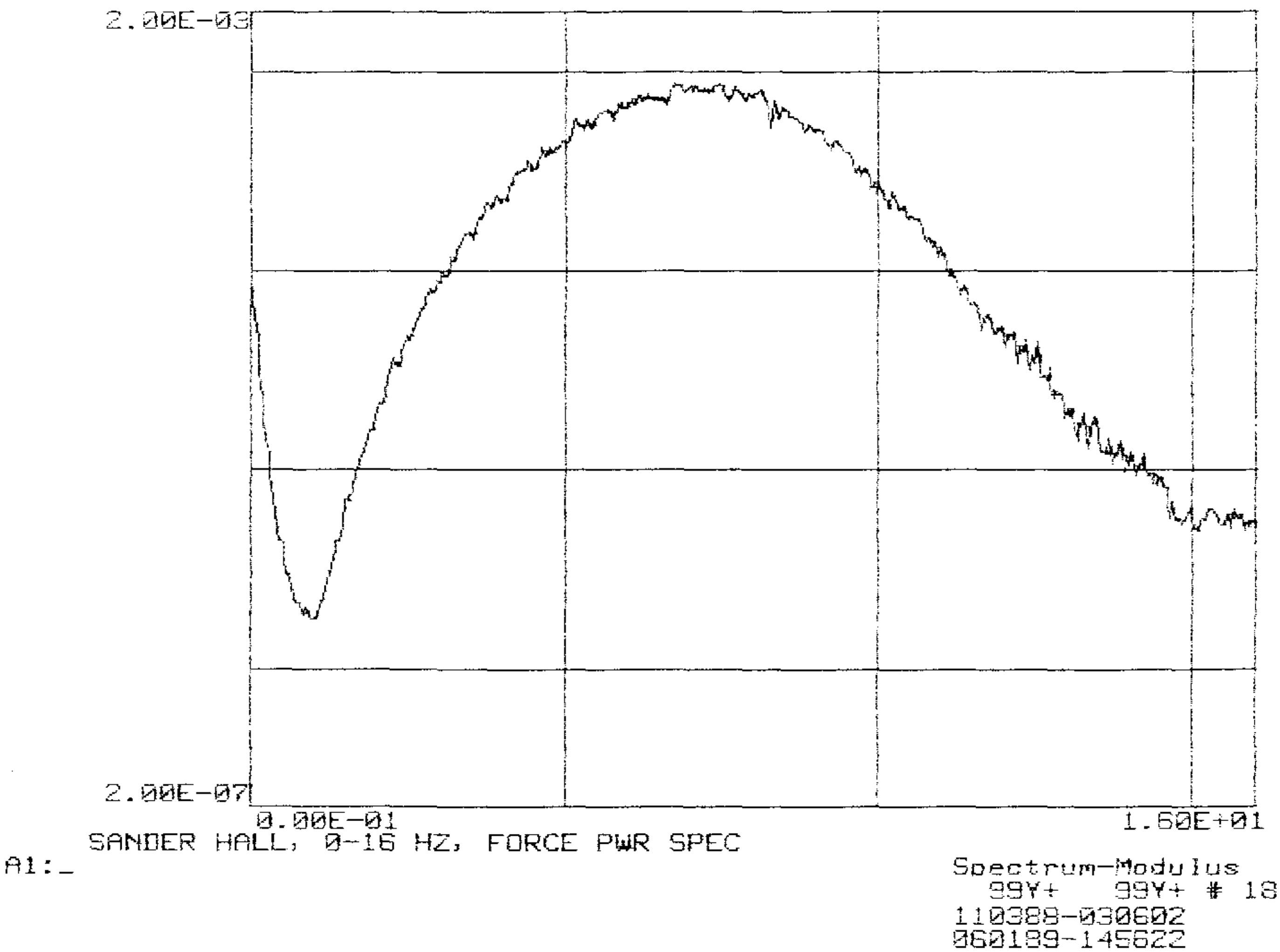

Fig. 4-14 Force Power Spectrum at Frequencies from 0 to 16 Hz

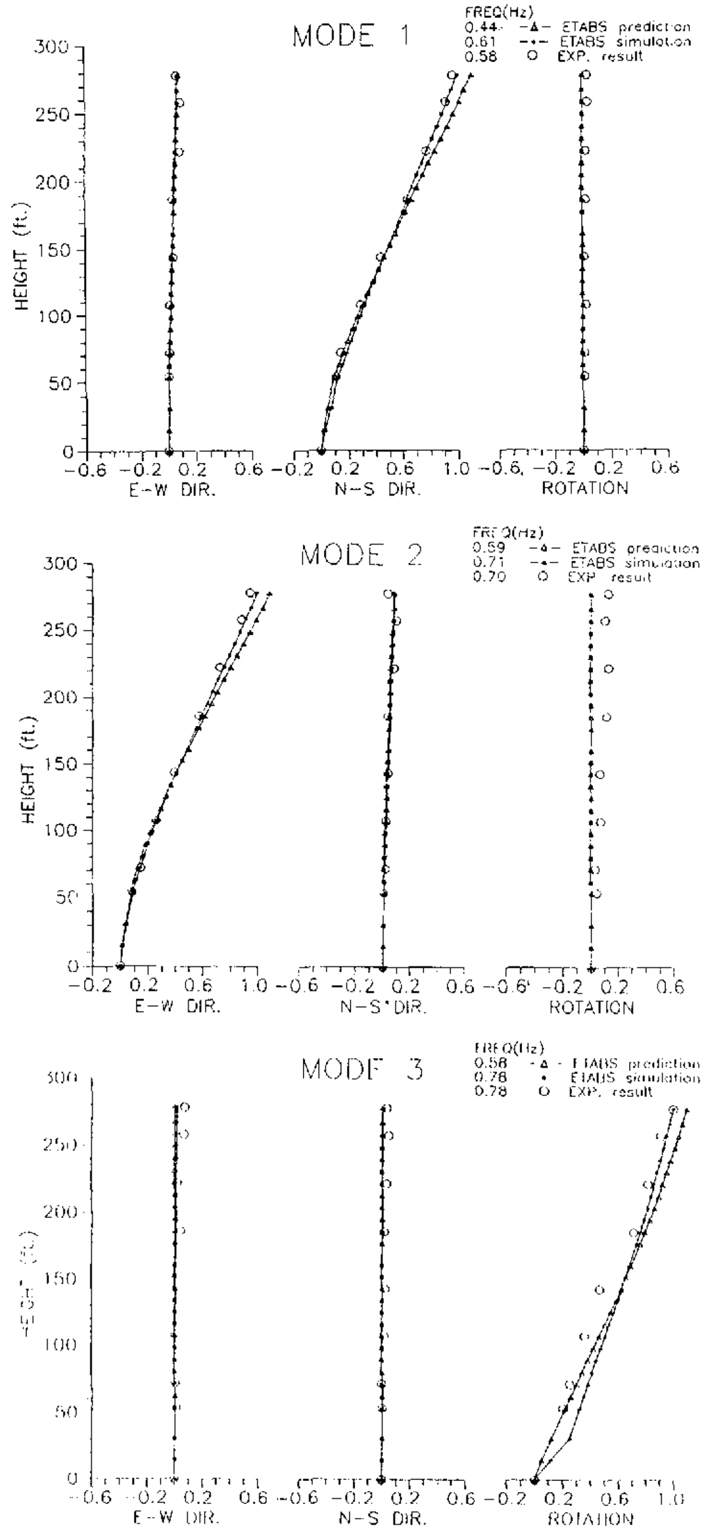

Fig. 4-15 Predicted, Measured and Simulated Natural Frequencies and Normal Mode Shapes of the Building

←– Continued

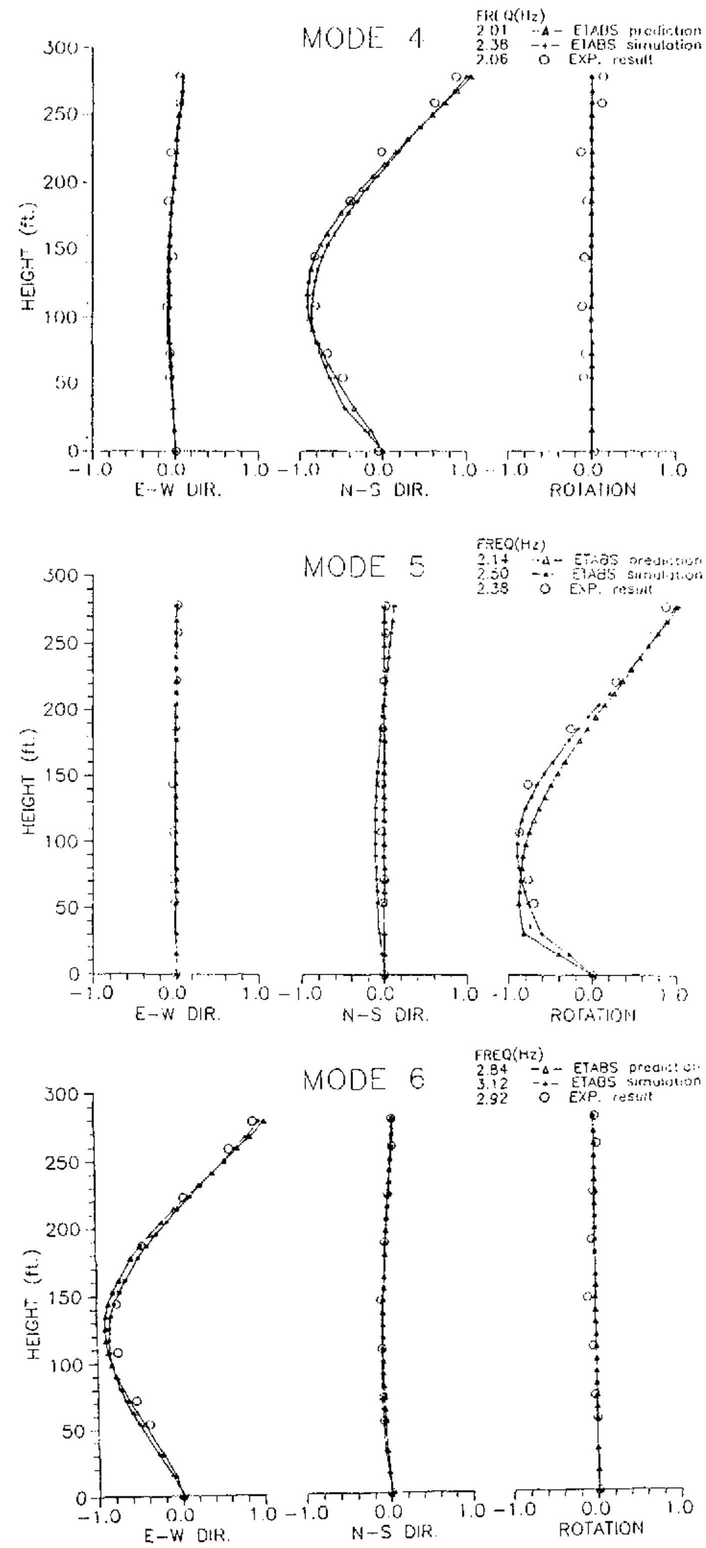

Fig. 4-15 Predicted, Measured and Simulated Natural Frequencies and Normal Mode Shapes of the Building

-- Continued

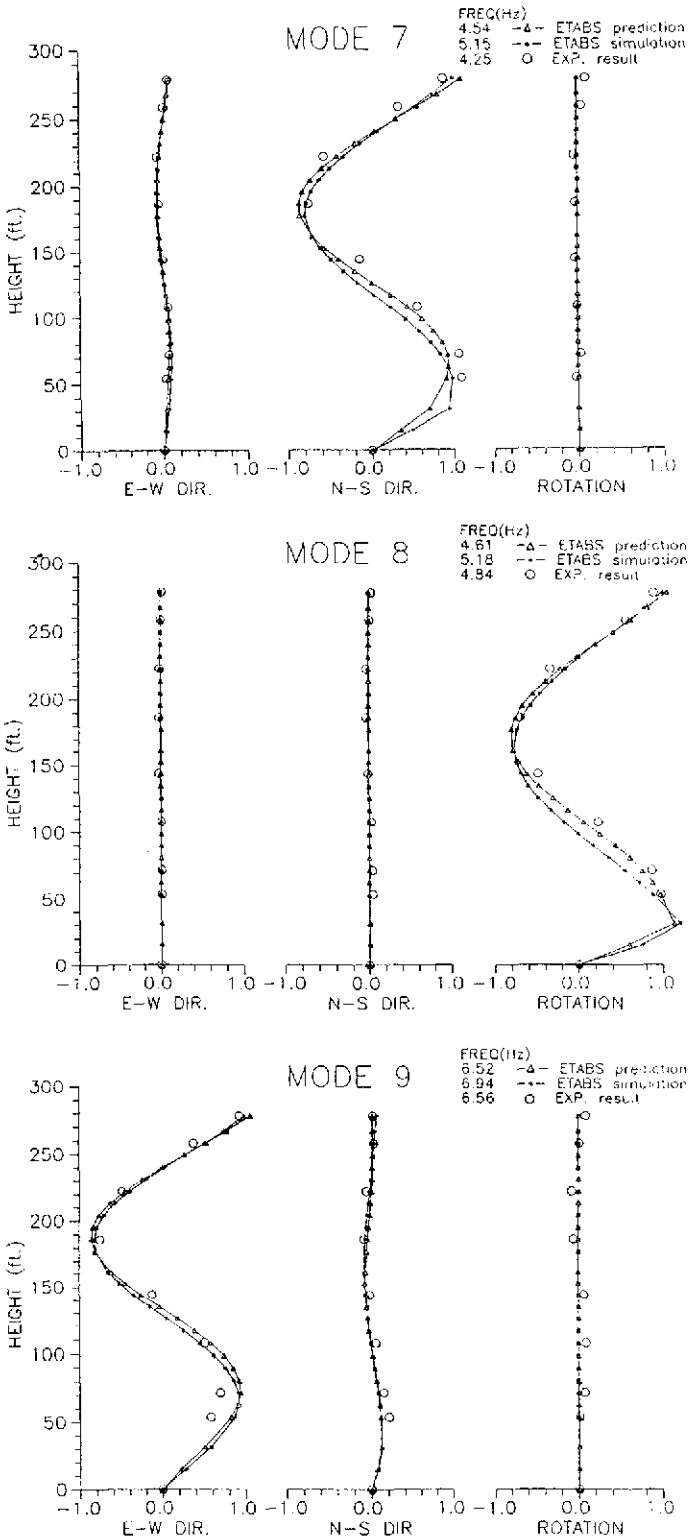

Fig. 4-15 Predicted, Measured and Simulated Natural Frequencies and Normal Mode Shapes of the Building

SECTION 5

CORRELATION OF PREDICTED AND MEASURED RESPONSES AND DEVELOPMENT OF THE SIMULATIVE MODEL

5.1 Improving the ETABS Model to Incorporate Coupling

In the ETABS analytical assembly of the core which was discussed in relation to Fig. 3-5, the columns at panel boundaries were not assigned any axial area and the axial areas of wall segments were assigned to the corresponding panel elements. After observing the experimental results it was realized that this did not permit to simulate the coupling action between different walls of each core & between the two cores correctly. The stiff beams which sandwiched the panels were connected to the edge columns. Since the columns did not have axial rigidity, the coupling action was not simulated. The axial forces which developed in the panels were not adequate for this purpose. So, the core model was modified as illustrated in Fig. 5-1, by defining additional column elements at panel boundaries to which axial areas of the wall segments which contributed to coupling action were assigned. In this manner, the analytical beams which represented the connecting beams and effective slab-beams were connected to columns which could develop the axial forces and therefore effectively simulate the overturning stiffness due to the coupling mechanism.

For example, the axial area of the wall segment BC shown in Fig. 5-1 is assigned as described in the following :

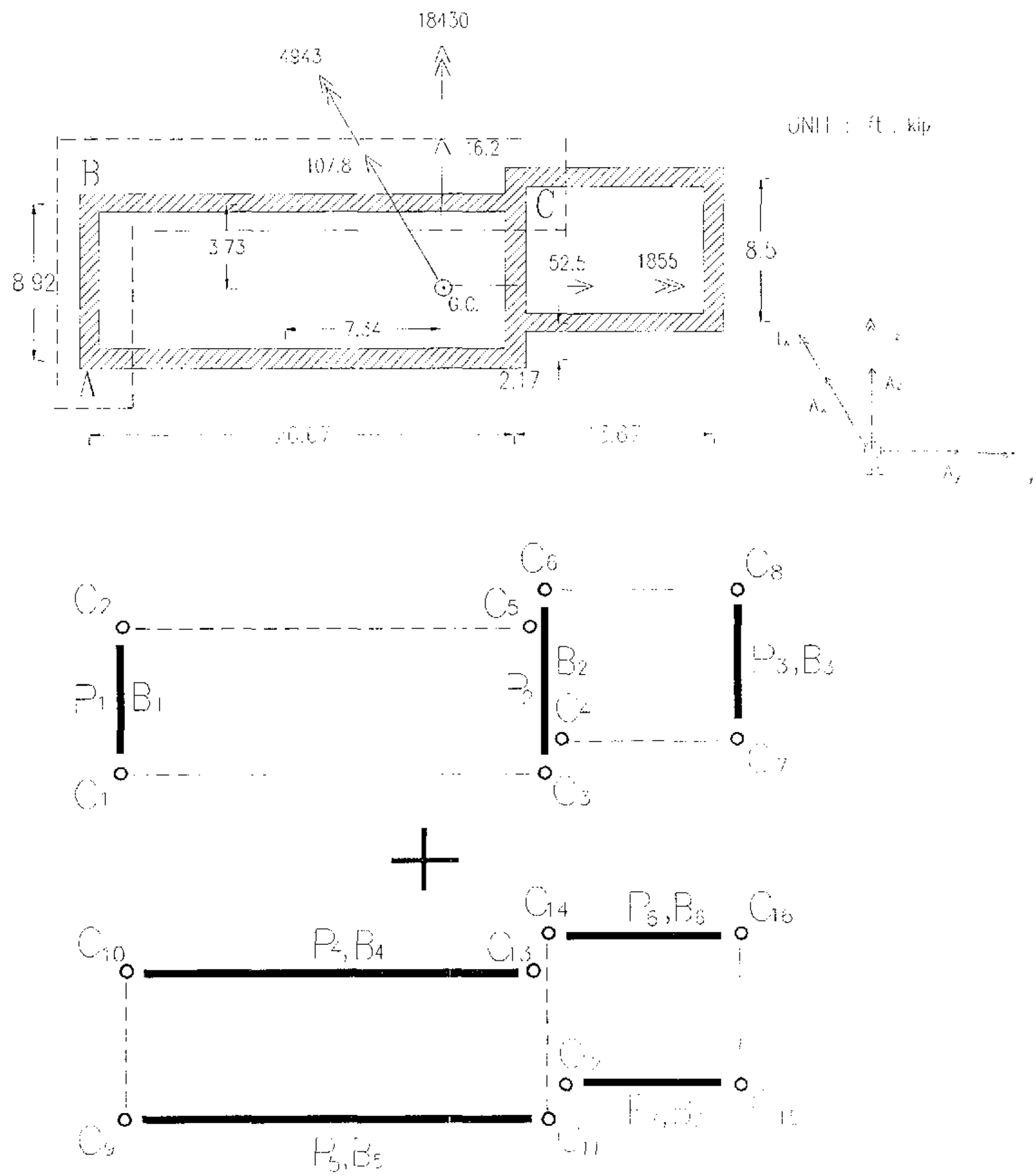

(c). Analytical Model - 2, Obtained by Superposing Above Elements ;

Fig. **5-1** Analytical Modeling of the Core by ETABS Following the Experiments (Simulative Modeling)

Continued

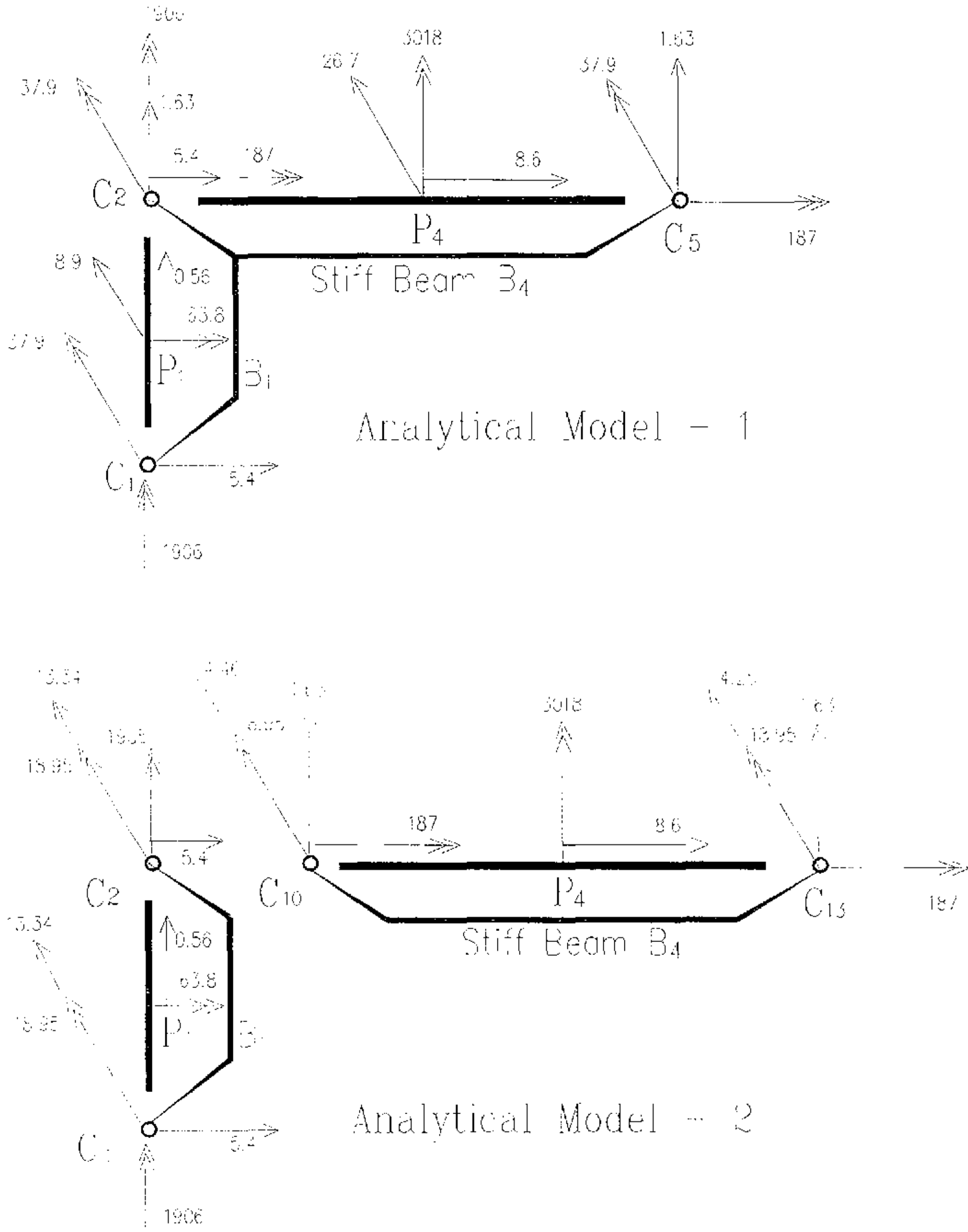

(b) Parameters Assigned for Panels P_1, P_4 and Columns C_1, C_2, C_{10}, C_{13}

Fig. **5-1** Analytical Modeling of the Core by ETABS Following the Experiments (Simulative Modeling) real wall segment BC : $A_x = 26.7$ ft^2

so, in the analytical model :

panel P_4 : $A_x = 0$

and the area of the the wall segment is assigned to

columns C_2 and C_5 : $A_x = 0.5*26.7 = 13.3$ ft^2

Those are shown in Figs 5-1(a) and (b); Analytical Model-2. Since a stiff beam B_1 was assigned to connect column C_1 and C_2, the coupling action due to axial forces developing in panels P_4 and P_5 was represented. The reasoning behind this procedure is clearly explained in Appendix (B).

The element flexibility of the refined model was verified to be sufficiently close to the flexibility of the actual core as shown in Fig. 3-6. It is noted that the displacements from ETABS output only show 2 transverse displacements and the twist angle at the mass center of each floor. Therefore in judging the accuracy of the predictive model, only u_y, u_z and θ_x were compared and were seen similar. On the other hand, the displacements u_x, θ_y and θ_z in ETABS model (1) and the actural core were not compared. Obviously, these were considerably different and led to the errors in the predictive model. The difference between the u_x, θ_y and θ_z of the core obtained by predictive and simulative ETABS models are illustrated in Appendix (B).

5.2 Refining the ETABS Model to Simulate Measured Modal Characteristics

After correlating the analytical results obtained with the improved simulative model and the experimental results, the three lower analytical frequencies were observed to be 8% higher. This pointed out that the analytical model now simulated a higher stiffness than the measured frequencies indicated. It was not possible to justify assuming an infinitely stiff foundation or modeling the walls based on gross sections when a number of narrow cracks were observed. Foundation flexibility was simulated based on the flexibility of columns, walls and footings under the first floor and above the footings. Cracking was simulated by reducing the flexural and shear terms of element stiffness by 30% only at the lower four floors. This reduction of element stiffness was not based on a rigorous study of how cracking influenced the stiffness of cores but was to study the sensitivity of frequencies and mode shapes to such a reduction.

Simulated foundation flexibility led to a reduction in the fundamental frequency by 3% while reducing the flexural and shear stiffness by 30% to simulate cracking reduced the fundamental frequency by an additional 5%. Higher frequencies were affected less.

5.3 Flexibility Matrix

To conceptualize the influence of varying analytical model parameters to the response characteristics, it is important to select a proper "space" for parameter optimization. In most studies, the modal space is selected for this purpose. However, since frequencies and mode shapes are difficult to conceptualize, it has been suggested to conduct parameter optimization in the "flexibility space" [4]. Displacement flexibility coefficients provide a better measure of current conditions, and provide a better guide to selecting the mechanisms and parameters which should be used in optimization. Therefore, the measured modal characteristics were used to derive the lateral flexibility discretized at the nine floor levels at which the modal amplitudes were measured.

The formulation to calculate the flexibility matrix based on frequencies and mass normalized mode shape was as follows [9]:

The standard eigenvalue problem is stated as :

$$K \ \phi_n = w^2 \ M \ \phi_n \qquad (5\text{-}1)$$

where K = Stiffness Matrix

ϕ_n = Mass Normalized Mode Shape n

w = Natural Circular Frequency

M = Mass Matrix

After premultiplying each side of Eq.(5-1) by $(1/w_n^2)\ \phi_n^T$ M f and $(1/w_n^2)\ \phi_m^T$ M f, respectively, and by virtue of the orthogonality of normal modes, the following results are obtained :

$$1/w_n^2 = \phi_n^T\ M\ f\ M\ \phi_n \tag{5-2}$$

$$0 = \phi_m^T\ M\ f\ M\ \phi_n \tag{5-3}$$

where f is the flexibility matrix.

By combining Eqns. (5-2) and (5-3) into matrix form, the following equation is obtained :

$$\phi^T\ M\ f\ M\ \phi = \mathrm{DIAG}\ [1/w_n^2] \tag{5-4}$$

where ϕ is the matrix comprised of the modal vectors.

Making use of the mass ortho-normality of the mode shapes, i.e., $[\phi]^T\ M\ [\phi] = [I]$, the following expressions hold :

$$[\phi]^T = [M\ \phi]^{-1}$$

$$[\phi] = [\phi^T\ M]^{-1} \tag{5-5}$$

Eqns. (5-4) and (5-5) lead to the flexibility matrix :

$$[f] = [\phi]\ \mathrm{DIAG}\ [1/w_n^2]\ [\phi]^T$$

The modal coefficients were subsequently mass-normalized by :

$$\phi_{ir} = a_i\ /\ (\ M_r\ )^{0.5}$$

Where

a_{ir} : Mode coefficients at r^{th} mode

M_r : Mode mass for r^{th} mode

The modal mass was calculated based on following formula :

$$M_r = a_{ir} * a_{ir} * w_r / (2 * A_{ir})$$

w_r : Angular frequency for r^{th} mode

A_{ir} : Driving point residue for r^{th} mode

The theory of the normalization procedure and definition of the residue term are given in ref.[8].

5.4 Correlating the Results of Modal Test with Those from The Simulative Analytical Model

The frequencies and mode shapes obtained after refining the ETABS model are compared to their measured and predicted counterparts in Fig. 4-15. It is observed that a remarkable improvement in correlation is achieved and the difference between analytically simulated and measured frequencies became less than 5%, the analytical model being stiffer. Correlation between analytically simulated and measured mode shapes also improved. In general the close correlation between the experimentally measured and analytically simulated results indicate confidence in both the modal test as well as the analytical model used to simulate the responses. At this point it is possible to initiate a rigorous parameter optimization process and to "calibrate" the analytical model for even closer correlation. Reduction of analytical model stiffness by further reducing the core flexural and shear stiffnesses as well as axial and coupling stiffness is possible.

Some of the columns of the flexibility matrix generated from the measured frequencies and mode shapes are correlated with the corresponding columns of the flexibility generated from analytical frequencies and mode shapes from the refined ETABS model in Fig. 5-2. Flexibility coefficients corresponding to the lateral displacement profiles of the building show good agreement while the coefficients representing in-plane twisting of floor diaphragms show some discrepancy (Fig. 5-2(c)). Particularly, a discontinuity in torsional stiffness at the 16th floor level is apparent from the flexibility based on the experimental modal parameters, this is not correctly simulated by the analytical model. Furthermore, the analytical flexibility indicates a significant torsional stiffness discontinuity at the 3rd floor level, and a need to measure experimental response at this level in future tests is apparent.

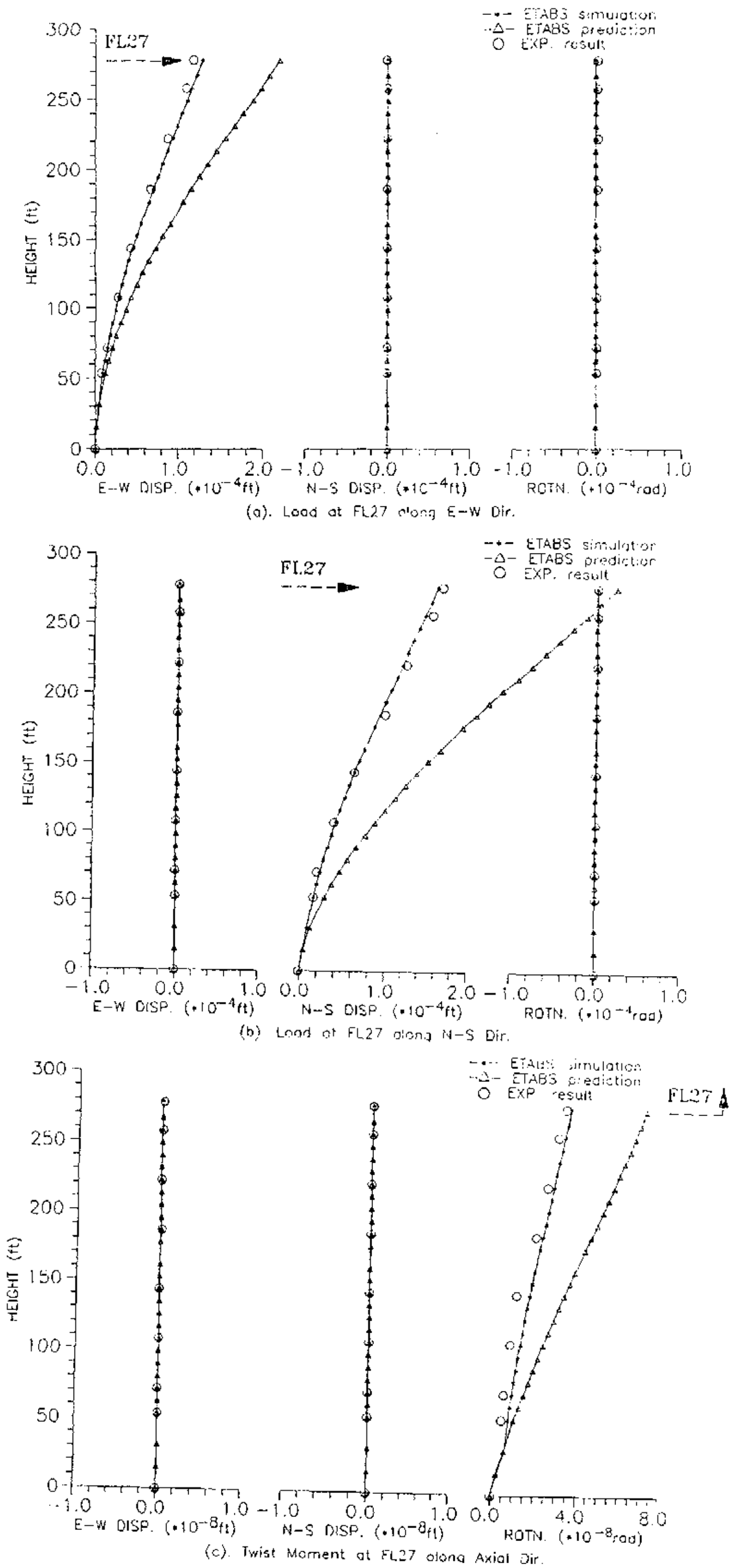

Fig. 5-2 Lateral Flexibilities of the Building Generated from the Two ETABS Models and Measured Modal Parameters

SECTION 6

SUMMARY, CONCLUSIONS AND RECOMMENDATIONS FOR FURTHER STUDY

6.1 Summary

To evaluate seismic vulnerability rationally, it is necessary to estimate the bounds of credible seismic demands and the corresponding supplies of a facility within a reasonable confidence interval. An analytical model which simulates the critical response mechanisms of the soil-foundation-structure and local supplies such as element stiffness, strength, energy dissipation and deformability characteristics with reasonable accuracy is therefore needed. Developing such an analytical model may prove difficult in case a facility has irregular attributes, damage and/or deterioration.

The report outlines efforts for developing a 3D analytical model of a 27-story RC flat-plate building with several irregular attributes, unsymmetric thin-walled cores and shallow foundations. Although literature exists on analysis of thin-walled elements, their validated 3D analytical modeling in conjunction with computer programs such as ETABS has not been reported. Since such programs are used widely by engineers, research into proper macro-element analytical modeling techniques of cores was considered important.

An analytical model of the facility was developed and this was followed by modal testing the building. By correlating the predicted and measured modal characteristics, it was possible to improve, validate and quantify critical parameters of the analytical model. The identified model simulated the measured characteristics of the building accurately. Results from the initially developed model, however, correlated poorly with the measured characteristics and errors in the order of 100% were noted in the predicted and experimentally determined lateral flexibility of the building.

Although forced-vibration testing and identification of mid-rise buildings with isolated walls have been reported, these did not have RC cores and the experiments have not been carried out in the context of modal testing. The study therefore helped to reach conclusions regarding correct modeling procedures for RC cores as well as walls which are not planar, i.e. such as those with T or L shapes. The study also revealed the critical requirements for successfully exciting and modal testing large constructed facilities with periods near two seconds.

6.2 Conclusions Regarding Analysis Modeling

In 3D analytical modeling of constructed facilities, collecting, documenting and synthesizing information regarding the as-built characteristics and current conditions of the facility is the most important step. Before completing the model, it is helpful to first establish the critical attributes of the facility so that they may be included in the model. This, however, is an art and some important attributes are not easy to detect without experience even when information and time are available.

Reliable analytical modeling of buildings with cores is observed to depend on first an accurate calculation of core characteristics: (a) The geometry (shear and geometric center locations and principal directions); (b) the force distribution within the core section and its 3D flexibility including the axial, flexural, shear, torsional flexibilities and their coupling; and, (c) 3D displacement kinematics of the core element.

It is then possible to construct an analytical macro-element assembly to simulate the core geometry, force distribution, 3D flexibility and deformation kinematics using column, panel and beam elements. If software and hardware permit, it would also be possible to represent the core by a microscopic finite-element assembly while other elements of the facility may be modeled at the element or macroscopic level.

Ascertaining that the analytical representation of the core correctly simulates all of the 3D geometry, force distribution, flexibility and the deformation kinematics is important. In the reported study, an incomplete check of the deformation kinematics was carried out. This comparison indicated good agreement between calculated core displacements and those simulated by the analytical assembly. Experiments indicated, however, that due to neglect in checking and simulating the complete 3D deformation kinematics of the actual core and its analytical representation, more than 100% error accumulated in the predicted roof-level lateral flexibility of the building.

6.3 Conclusions Regarding Experimentation

The most appropriate tool which is suggested for experimental identification of most constructed facilities is modal testing. There are important prerequisites for successful modal testing and identification, starting with conceptualizing the facility and developing its 3D linearized analytical modeling. This forms the basis of instrumentation, excitation, data acquisition and processing which are designed in a facility-specific manner utilizing the linearized analytical model.

Except for excitation generation, the currently available hardware and software used in the modal testing industry for modal testing mechanical structures are suitable for accurately modal testing constructed facilities. For best results, the level of excitation should considerably exceed the excitation due to ambient sources or special hardware and signal processing techniques which can differentiate between responses induced by forced excitation and those induced by ambient effects should be used.

Importantly, for identification to serve as a basis of evaluation, the level of excitation should be such that the measured responses should not be significantly affected by nonstructural elements which are not considered in analytical modeling. Furthermore, the excitation should be able to activate any service-level soil-foundation-structure interactions so that these may be measured. Measurement of soil-foundation flexibility requires special instrumentation during modal testing.

6.4 Conclusions Regarding The Significance of Identification

The significance of identifying linearized models of constructed facilities utilizing modal testing appear debatable since: (a) constructed facilities are nonlinear and their linearized identification is not rational; (b) very few cases of successful modal tests have been reported for constructed facilities where the information generated led to a reliable identification; modal tests of irregular facilities or those with undesirable attributes have not been reported at all; (c) even if successful modal testing of a facility leads to meaningful identification of a linearized model, this model cannot be used to simulate local supplies and compute local demands at nonlinear limit states; (d) periodic modal tests cannot be used to monitor for damage either since global modes are not perceptively influenced by local damage.

The study reported here refutes these points. A linearized 3D analytical model of the irregular facility was successfully identified at the element level. Although this linearized model cannot be used directly for nonlinear analysis, it does reliably simulate the critical response mechanisms and the existing conditions of the facility. This model can therefore be used for: (a) Estimating local demands at the onset of inelastic limit states; (b) as a basis for local identification by localized modal testing and non-destructive probes; (c) as a reliable starting point for modeling nonlinear response.

By adopting a correct strategy for nonlinear analysis, uncertainties related to estimating nonlinear element responses may be minimized. However, unless the 3D geometry, deformation kinematics and all critical response mechanisms of the facility at its existing state are not correctly simulated through linearized identification, reliability of unusual, large and complex, irregular, deteriorated or damaged constructed facilities cannot be confidently evaluated. The fact that experimental identification is essential in evaluating vulnerability of such facilities with reasonable confidence has been exemplified by the reported research.

6.5 Recommendations for Further Research

Confidently evaluating vulnerability of those types of construction in the Midwestern and Eastern United States which have not yet experienced an earthquake is an important problem. Unless vulnerability is reliably estimated it is not possible to overcome societal complacence towards seismic hazard in many regions of USA. Since there is no data-base regarding past earthquake performance of many types of facilities designed and constructed without regard to seismic risk, their accurate analytical modeling and correctly simulating their failure limit-state responses become critical. It is recommended that studies similar to those reported here to be carried out on different types of construction in a facility-specific manner.

Research on reliable 3D nonlinear analysis of facilities to simulate their failure limit-state responses and capacity supplies is recommended. Although nonlinear analysis has been researched for the last fourty years, the state-of-the-art has not yet advanced to yield reliable nonlinear analyses of constructed facilities.

Particularly in view of the uncertainties in estimating expected ground motion characteristics at a site, and the sensitivity of nonlinear time-history analyses to this and many other parameters, it does not make sense to promote this type of analysis for evaluating facilities. Research should first concentrate on improving the state-of-the-art in 3D static nonlinear analyses to predict failure limit-state response characteristics of constructed facilities. Such analyses may reveal sufficient information regarding the vulnerability of construction if they are based on an identified linearized analytical model of the facility.

SECTION 7

REFERENCES

1. Aktan, A. E., "Building Identification : Needs and Means," Dynamic Response of Structures," G. C. Hart and R. B. Nelson, Editors, ASCE, 1986.

2. Aktan, A. E., "Present and Future in RC Building Analysis," Proceedings of the 9th World Conference on Earthquake Engineering, Tokyo-Kyoto, Japan, 1988.

3. Aktan, A. E., and Ho, I. K., "Evaluating Reliability of Constructed Facilities by Dynamic Testing and Identification," Proceedings of a Workshop on Rescue of Americas Infrastructure, University of Puerto Rico at Mayaquez, 1989.

4. Aktan, A. E., Hogue, T., and Hoyos, A., "Identification of Civil-Engineered Structures," Proceedings of the 1987 SEM Spring Conference, Houston, June 1987.

5. Aktan, A. E. and Nelson, G. E., "Problems in Predicting Seismic Responses of RC Buildings," Journal of Structural Engineering, September 1988.

6. Ahmadi, A. K. and Torkamani, M. A. M., "Application of System Identification in Mathematical Modeling of Buildings," Research Report SETEC-CE-86-002, University of Pittsburgh, Dept. of Civil Engineering.

7. Bertero, V. V., and Clough, R. W., "The Interdependence of Analysis and Experiments in Structural Dynamics Research," Dynamic Response of Structures, G. C. Hart, and R. B. Nelson, Editors, 1986.

8. Brown, D. L., Class Notes of "Analytical and Experimental Modal Analysis," University of Cincinnati, 1987.

9. Clough, R. W. and Penzien, J., Dynamics of Structures, McGraw-Hill, New York, 1975.

10. Connor, J., "Analysis of Structural Member Systems," Ronald Press, 1976.

11.Cook, R. D. and Young, W. C., Advanced Mechanics of Materials, Macmillan, 1985.

12. Flesch, R. G. and Kernbichler, K., "A Dynamic Method for the Safety Inspection of Large Prestressed Bridges," Proceedings, Int. NSF Workshop on Nondestructive Evaluation

for Performance of Civil Structures, USC, Los Angeles, 1988.

13. Habibullah, A., "User's Manual of ETABS - Three Dimensional Analysis of Building System," 1986.

14. Hart, G. C., and Yao, J. T. P., "System Identification in Structural Dynamics," Journal of the Engineering Mechanics Division, ASCE, Vol. 103, No. EM6, Dec. 1977.

15. Hoyos, A. and Aktan, A. E., "Regional Identification of Civil-Engineered Structures Based on Impact-Induced Transient Responses," Research Report 87-1.

16. Ibanez, Paul, "Identification of Dynamic Structural Models from Experimental Data," Engineering Report, UCLA-ENG-7225, University of California, Los Angeles, CA, March 1972.

17. Ibanez, Paul, "Use of System-Identification in Civil Engineering Structures," Proceedings of the 1987 SEM Spring Conference, Houston, TX.

18. Maison, B. F. and Neuss, C. F., "SUPER-ETABS - An Enhanced Version of The ETABS Program," A Report to the National Science Foundation, 1983.

19. Natke, H. G. and Yao, J.T.P., (Eds): "Structural Safety Evaluation Based on System Identification Approaches," Friedr.Vieweg & John, Braunschweig, Wiesbaden, 1988.

20. Peterson, F. E., Blissmer, F. B. and Kirby, R. W., "Lateral-A Computer Program for the Three-Dimensional Analysis of Multistory Frame and Shear Wall Buildings," Engineering Analysis Corporation, Redondo Beach, California, 1969.

21. Smith, Stevens & Young, "Sander Tower Study for University of Cincinnati," 1988.

22. Stephen, R. M., Wilson, E. L. and Stander, N., "Dynamic Properties of a Thirty-Story Condominium Tower Building," Report No. UBC/EERC-85/03, April 1985, University of California, Berkeley, CA.

23. Wilson, E. L. and Dovey, H. H., "Three-Dimensional Analysis of Building Systems - TABS," EERC, Report No. 72-8, University of California, Berkeley, California, Dec. 1972.

24. Wilson, E. L. and Habibullah, A., "Three-Dimensional Static and Dynamic Analysis of Multistory Frame and Shear Wall Buildings," NISEE, University of California, Berkeley, California, Feb. 1977.

25. Wilson, E. L., Hollings, J. P. and Dovey, H. H., "ETABS - Three Dimensional Analysis of Building System," Report No. UBC/EERC-75-13, Revised March 1979, University of California, Berkeley, CA.

APPENDIX A

COMPUTING SECTION PROPERTIES FOR CLOSED THIN WALLED CORE BASED ON THE ENGINEERING THEORY

The objectives of this Appendix are :

<1> To illustrate calculating the properties of a closed two-celled thin-walled cross section based on the engineering theory. This is shown in part <a>.

<2> To illustrate the difference between 3 cross sections which have only slight differences in geometry. Two of the cross sections are less complex than the one shown in part <a>. The properties of these were calculated as shown in part <b>.

<a>

In the following, a single core cross section is used to illustrate how to calculate the properties A_x, A_y, A_z, I_x, I_y, I_z, Y_c, X_c, Y_s, X_s :

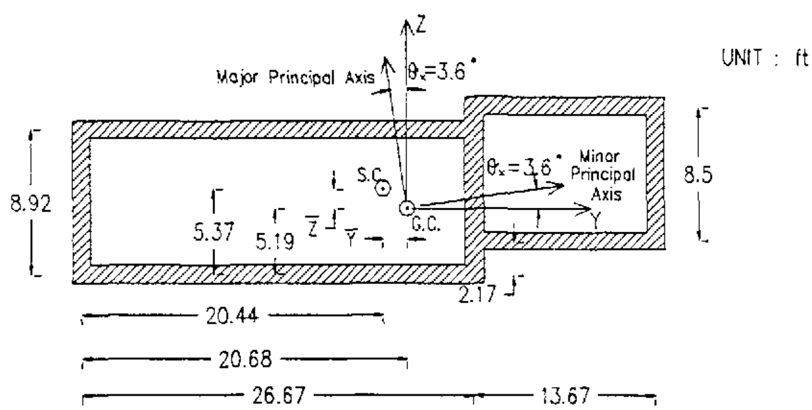

<1> Axial Area along X-axis :

$$
\begin{aligned}
A_x &= 9.917+(9.917+1.75)+9.5+2*25.67+2*12.67 \\
&= 107.8 \ ft^2
\end{aligned}
$$

<2> Location of G.C. :

$$
\begin{aligned}
Z_c &= [9.917*(9.917*0.5-0.5)+(11.667*0.5-0.5)+9.5* \\
&\quad (9.5*0.5+2.167-0.5)+25.67*(9.917-1)+12.67* \\
&\quad (11.667-1)+12.67*2.167]/107.8 \\
&= 5.19 \ ft
\end{aligned}
$$

$$
\begin{aligned}
Y_c &= [11.667*(25.67+1)+9.5*(13.67+26.67)+25.67*2* \\
&\quad *(25.67*0.5+0.5)+12.67*2*(26.67+0.5+0.5* \\
&\quad 12.67)]/107.8 \\
&= 20.68 \ ft
\end{aligned}
$$

<3> Moment of Inertia along the Y-axis :

$$
\begin{aligned}
I_y &= 1/12*27.67*9.917^3+27.67*9.917*(9.917*0.5-0.5- \\
&\quad 5.186)^2-1/12*25.67*7.917^3-5.67*7.917*(7.917 \\
&\quad *0.5+0.5-5.186)^2+1/12*14.67*9.5^3+14.67*9.5* \\
&\quad (9.5*0.5+2.167-0.5-5.186)^2-1/12*12.67*7.5^3- \\
&\quad 12.67*7.5*(7.5*0.5+0.5+2.167-5.186)^2-1/12* \\
&\quad 7.75^3-7.75*(7.75*0.5+2.167-0.5-5.186)^2 \\
&= 1855.2 \ ft^4
\end{aligned}
$$

<4> Moment of Inertia along the Z-axis :

$$
\begin{aligned}
I_z &= 1/12*9.917*27.67^3+27.67*9.917*(27.67*0.5-0.5- \\
&\quad 20.67)^2-1/12*7.917*25.67^3-5.67*7.917*(25.67* \\
&\quad 0.5+0.5-0.67)^2+1/12*9.5*14.67^3+14.67* \ 9.5* \\
&\quad (14.67*0.5+25.67+0.5-20.675)^2-1/12*7.5*12.67^3 \\
&\quad -2.67*7.5*(12.67*0.5+27.67-0.5-20.675)^2-
\end{aligned}
$$

$1/12*7.75-7.75*(5.495+0.5)^2$

$= 18430.1\ ft^4$

<5> Cross Moment of Inertia :

$I_{yz} = 8.917*(-20.675)*(-0.728)+10.667*5.995*$

$0.148+8.5*19.665*1.231+26.67*(-7.34)*(-$

$5.186)+ 26.67*(-7.34)*3.731+13.67*12.83*$

$5.481+13.67*12.83*(-3.019)$

$= 1066.1\ ft^4$

<6> Orientation of the Principal Axes :

$\theta_p = 2*I_{yz} / (I_z - I_y)$

$= 3.6$ degree

Since the principal axes are rotated only 3.6 degrees with respect to the reference axes, they were assumed to coincide with the reference axes in the following shear flow calculation.

<7>. Location of the S.C. :

Computed as $Y_s = 0.242$ ft, $Z_s = 0.176$ ft as described in the following :

In order to determine the coordinates of the shear center, the following superposition is carried out. For shear forces applied at the shear center, the shear flow q can be represented by the sum of two shear flows :

$$q = q_0 + q_c$$

q_0 is shear flow of the cross section which is rendered an open section by cutting as shown in Fig. A1.

Assuming plane sections remain plane, q_0 is calculated from the general expression [11].

$$q_0 = \frac{(-V_z * I_{yz} + V_y * I_y) * Y_c \quad + \ (V_z I_z - V_y I_{yz}) * Z_c}{(\ I_y * I_z - \ I_{yz}^2) \ * \ t} * A_s * t$$

V_y, V_z : shear forces along Y, Z direction.

Y_c, Z_c : coordinates of the centroid of sectorial area A_s.

A_s is the sectorial area of the cross section.

t is the uniform thickness of the wall.

q_c is a constant shear flow in the closed section which is released when the section is rendered open, which can be calculated based on the condition of zero twist. This condition arises from the fact that the shear force was applied through the shear center.

The shear-flow q_0 and q_c were calculated and are shown in Fig. A-1.

Therefore, the location of shear center Y_s ,Z_s can now be calculated from the moment at G.C.

$$V_z * Y_s = \Sigma \int q_i * r_i \, ds = 0$$

Where V_z : Shear force in z direction

Y_s : Distance at y direction from S.C. to G.C.

q_i : Shear flow at segment i

r_i : Distance from segment to G.C.

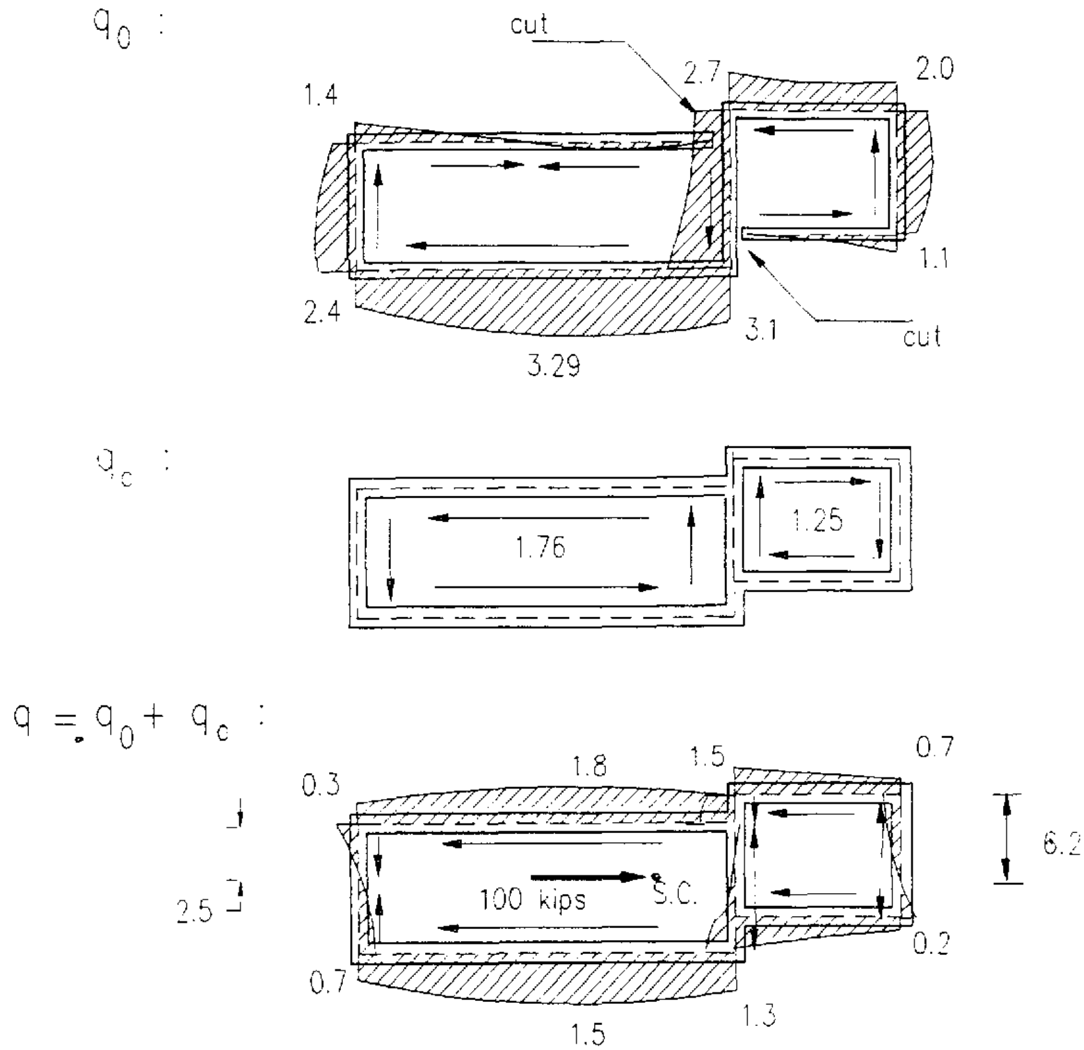

(Unit : kip/ft)

<a>. Horizontal Force 100 kips Acted on S.C.

Fig.A-1 Shear Flow Diagram

-- Continued

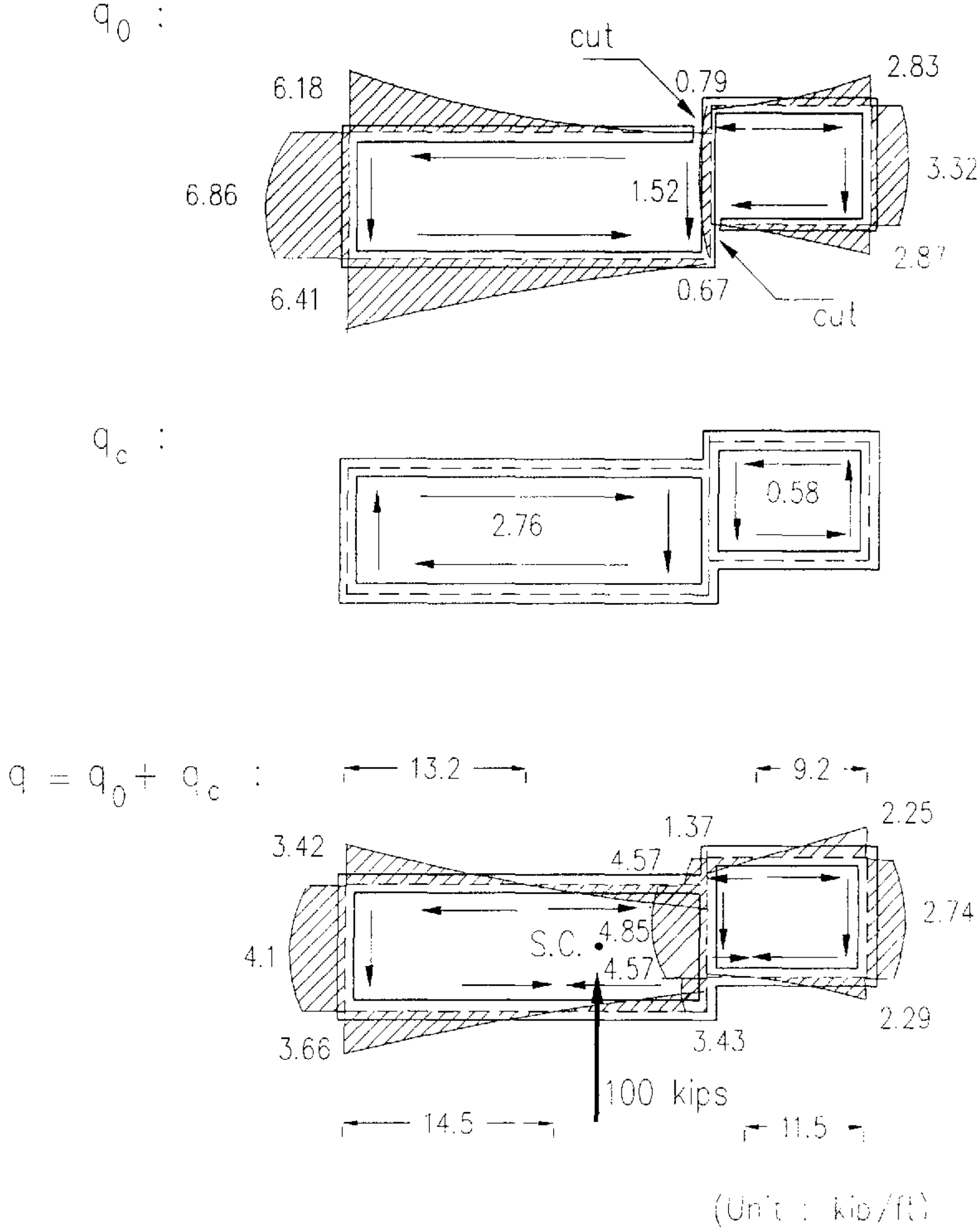

<b>. Vertical Load 100 kips Acted on S.C.

Fig. A-1 Shear Flow Diagram

<8>. Effective shear area in the y and z directions :

$A_y = 52.45\ ft^2$, $A_z = 16.18\ ft^2$

Based on the " Principle of Virtual Forces [10]" :

The internal work is computed as :

$$W_i = \int (\tau * r)\ dV$$

$$= \int \frac{Q}{t*I} * \frac{V*Q}{G*t*I} * t * ds * dx$$

$$= \frac{V*dx}{G*t*I^2} \int Q^2 * ds$$

Where τ : Shear stress due to dummy force

r : Shear strain due to shear force V

Q : First moment of area

t : Width of segment

G : Shear modulus

The External Work is :

$$W_e = \frac{V}{G * A_v} * dx$$

Where A_v is effective shear area

Because $W_i = W_e$

$$\Longrightarrow \frac{1}{A_v} = \frac{1}{I*I*t} \int Q^2 * ds$$

$$\Longrightarrow \frac{1}{A_v} = \frac{1}{V^2*t} \int (q_i)^2 * ds \qquad (q = \frac{V*Q}{I})$$

<9>. Torsional Constant was computed as :

$$I_x = 4943 \text{ ft}^4$$

The Twist Angle ϕ and Torque T were obtained from [11]

$$\phi = \frac{1}{2*G*\Gamma} \left(\int \frac{q}{t} \, ds \right)$$

Torque $T = 2 * \Sigma \left(\Gamma_i * q_i \right)$

Γ : Area enclosed by the medial line.

t : Uniform thickness of the cross section.

G : Shear Modulus.

Torsional constant $I_x = T / G\phi$

<b>. Case 1 and case 2 correspond to two similar cross sections, the dimensions of which are shown in Fig. A-2. The properties of each cross section was calculated by the procedures discussed in part <a> and compared in the following:

Properties	Case 1	Case 2	Case 3
A_x (ft^2)	98.4	107.3	107.8
A_y (ft^2)	75.2	48.74	52.45
A_z (ft^2)	15.52	15.98	16.18
I_x (ft^4)	5229	5244	4943
I_y (ft^4)	1720	1779	1855
I_z (ft^4)	18137	18488	18430

The change in the properties of the section in case 2 as compared to that in case 3 is very small. This indicates that the assumption of principal inertia axes coinciding with the reference axes was justified.

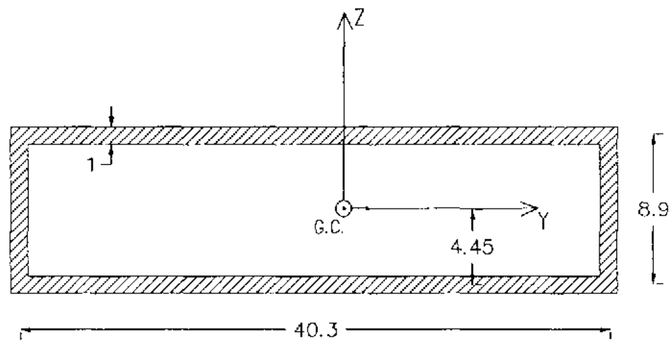

<A>. Case - 1

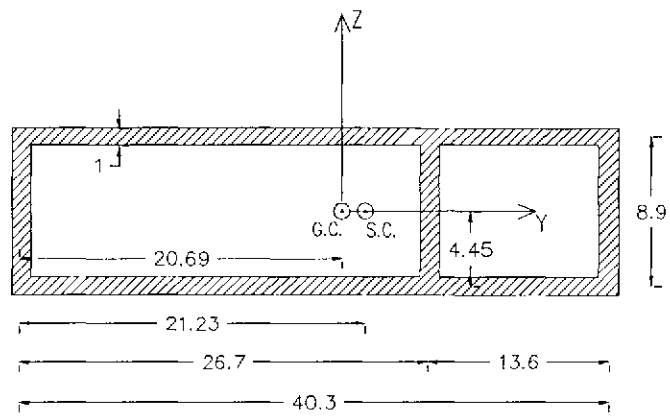

<B>. Case - 2

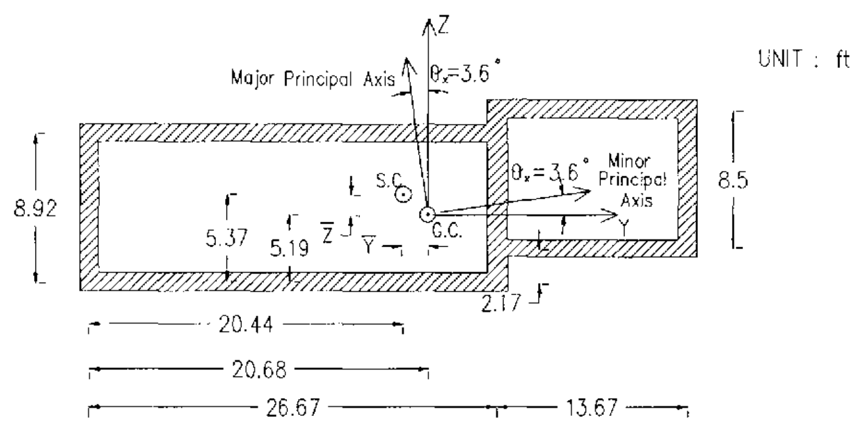

<C>. Case - 3

Fig.**A-2** Cross Sections of Three Different Core Systems

APPENDIX B

STUDY OF ALTERNATIVE ETABS MODELS FOR A CLOSED-BOX CORE SECTION

B.1 Introduction

In order to illustrate the procedure for correct ETABS modeling of a closed box-section core, a one-story, cantilever element with a symmetric box cross section was considered as an example. The displacements due to an eccentric lateral force acting on the top of this element are shown in Fig. B-1. These were obtained from a variety of ETABS analytical assemblies.

Based on the engineering theory, displacements at the mass center of top floor were calculated. There were used to check the accuracy in the results of analyses using five different ETABS analytical assemblies.

B.2 Closed Form Displacement Calculation

Based on the 3D cantilever flexibility matrix shown as Fig. B-1, the displacements of the core structure were calculated as following:

$\bar{Y} = \bar{Z} = 0$ due coinciding shear and geometric centers

$F_y = 2000$ Kips

$M_x = 10000$ Kip-ft

$F_x = F_z = M_y = M_z = 0$

$$U_y = \frac{F_y * L}{G * A_y} + \frac{F_y * L^3}{3*E*I_z}$$

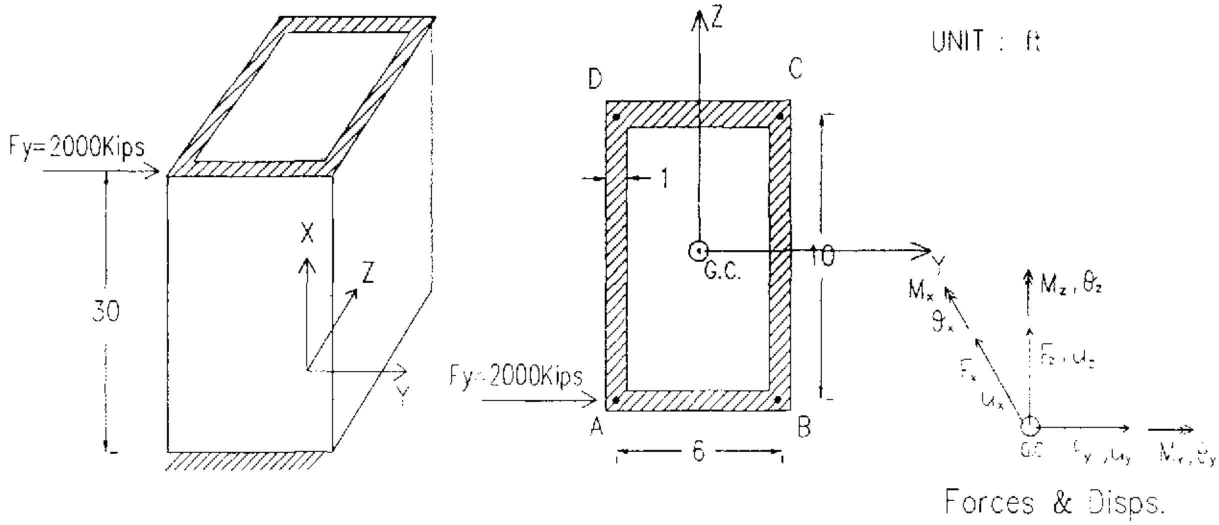

3D Cantilever Flexibility Matrix Based on Engineering Theory

$$
\begin{Bmatrix} u_x \\ u_y \\ u_z \\ \theta_x \\ \theta_y \\ \theta_z \end{Bmatrix}
=
\begin{bmatrix}
\frac{1}{EA} & & & & & \\
 & \frac{L}{GA_y}+\frac{L\bar{Z}^2}{GI_x}+\frac{L^3}{3EI_z} & -\frac{L\bar{Z}\bar{Y}}{GI_x} & \frac{L\bar{Z}}{GI_x} & & \frac{L^2}{2EI_z} \\
 & -\frac{L\bar{Z}\bar{Y}}{GI_x} & \frac{L}{GA_z}+\frac{L\bar{Y}^2}{GI_x}+\frac{L^3}{3EI_y} & \frac{-L\bar{Y}}{GI_x} & \frac{-L^2}{2EI_y} & \\
 & \frac{L\bar{Z}}{GI_x} & \frac{-L\bar{Y}}{GI_x} & \frac{L}{GI_x} & & \\
 & & \frac{-L^2}{2EI_y} & & \frac{L}{EI_y} & \\
 & \frac{L^2}{2EI_z} & & & & \frac{L}{EI_z}
\end{bmatrix}
\begin{Bmatrix} F_x \\ F_y \\ F_z \\ M_x \\ M_y \\ M_z \end{Bmatrix}
$$

Characteristics of Core Based on Engineering Theory

$A_x = 32\ ft^2$	$I_x = 450.0\ ft^4$	$\bar{Y} = \bar{Z} = 0$
$A_y = 12\ ft^2$	$I_y = 472.7\ ft^4$	$E = 449571$ ksf
$A_z = 20\ ft^2$	$I_z = 220.7\ ft^4$	$G = 187321$ ksf

Fig. **B-1** 3D Cantilever Flexibility of The Element With Box Cross Section

$$= 0.2081 \text{ ft}$$

$$\theta_x = \frac{M_x * L}{G * I_x} = 0.0035 \text{ rad.}$$

$$\theta_z = \frac{F_y * L^2}{2*E*I_z} = 0.0091 \text{ rad.}$$

$$U_x = U_z = \theta_y = 0$$

B.3 ETABS Modeling

In order to model the core structure shown in Fig. B-1 by using SUPER-ETABS, panel, column, and beam elements were used to assemble each wall segment. Five different modeling cases were considered and wall sections AB and BC (Fig. B-1) will be used to illustrate the parameter assignment in each following modeling cases :

Case 1 :

Based on the false assumption that the program will transform the moment of inertia and torsional inertia to the mass center automatically, only the in-plane moment of inertia, axial area, and shear area of each wall segment were assigned to the corresponding panel elements. Four fictitious column lines were defined at each corner and a stiff beam was defined to connect the boundary columns in each wall segment.

The analytical model is shown in Fig. B-2 and assigned parameters are based on the following procedures:

(a) The axial area of core wall segments were assigned as axial area to the corresponding panel elements:

In the real cross section :

wall segment AB : $A_x = 6.0\ ft^2$

wall segment BC : $A_x = 10.0\ ft^2$

So, in the analytical model :

panel P_1 : $A_x = 6.0\ ft^2$

panel P_3 : $A_x = 10.0\ ft^2$

column C_1, C_2 and C_3 : $A_x = 0$

(b) Contributions made by the in-plane moment-of-inertia of each wall segment to the core crossectional inertia at the centroid were assigned as moment-of-inertia to the corresponding panel.

In the real cross section :

wall segment AB : $I_z = 1/12*1*6.0^3 = 18.5\ ft^4$

wall segment BC : $I_y = 1/12*1*10.0^3 = 83.8\ ft^4$

(with respect to cross section centroid)

So, in the analytical model :

panel P_1 : $I_z = 18.5\ ft^4$

panel P_3 : $I_y = 83.8\ ft^4$

(with respect to panel centroid)

column C_1, C_2 and C_3 : $I_z = I_y = 0$

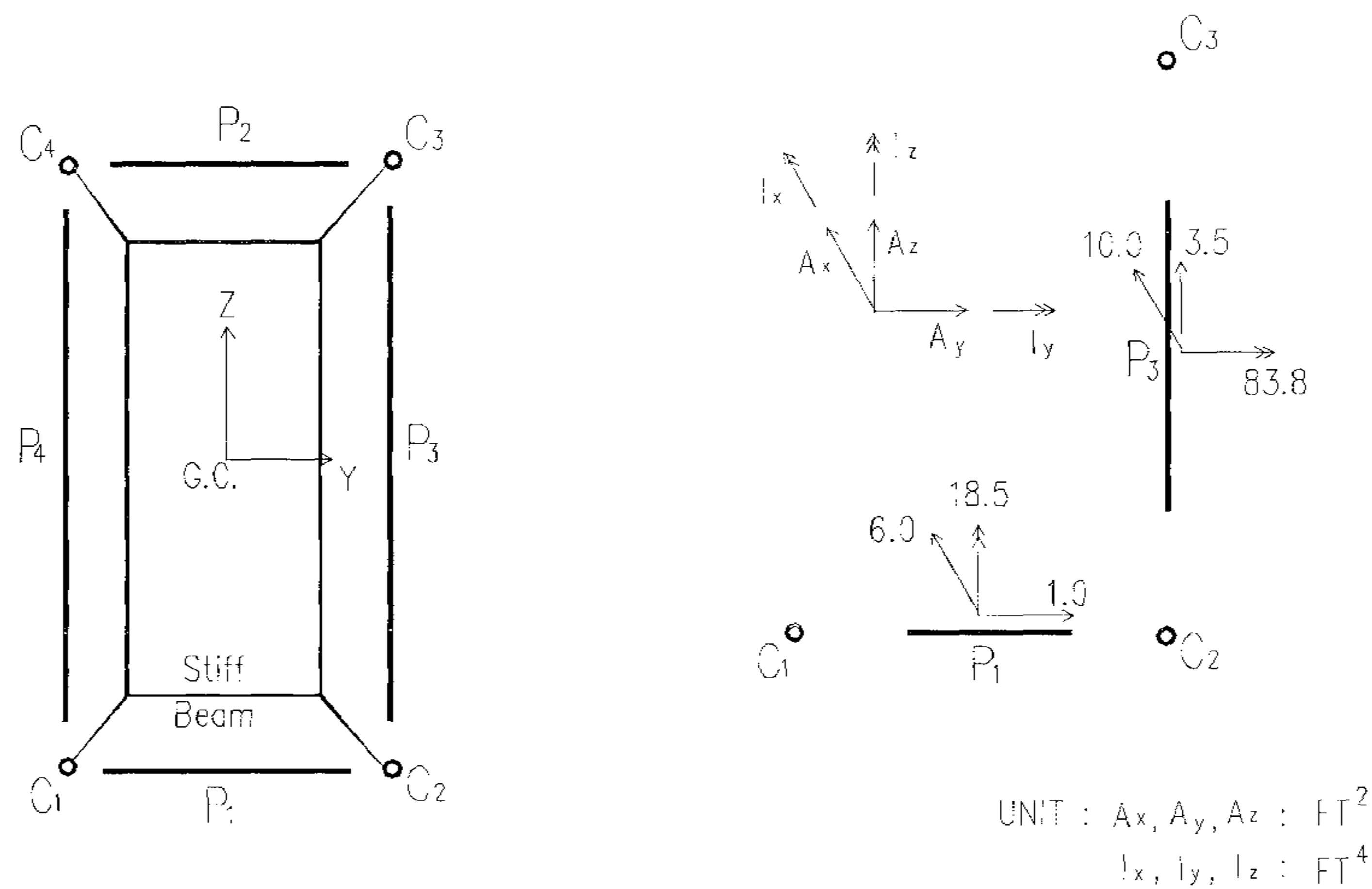

Fig.**B-2** Parameter Assignment and ETABS Analytical Modeling for Case 1

(c) The in-plane effective shear areas computed for a wall segment was assigned as shear area to the corresponding panel element. The total shear area of the core is 12.0 ft^2 in the y-direction and 20 ft^2 in the z-direction. The ratio of wall segment AB's I_z to the I_z of the core at the core centroid is given by 18.5/220.7. The ratio of wall segment BC's I_y to the I_y of the core at the core centroid is given by 83.8/472.7.

panel P_1 : $A_y = 12.0*18.5/220.7 = 1.0\ ft^2$

panel P_3 : $A_z = 20.0*83.8/472.7 = 3.5\ ft^2$

column C_1, C_2 and C_3 : $A_z = A_y = 0$

Case 2 :

The analytical assembly was modeled similar to Case 1. However, some parameters were assigned to the analytical column elements as follows (Fig. B-3) :

(a) The out-of-plane moment of inertia of each wall segment was calculated with respect to section centroid and assigned as inertia along the corresponding direction to the analytical columns at the boundaries.

In the real cross section :

wall segment AB : $I_y = 1/12*6.0*1^3+6.0*5.0^2 = 152.5\ ft^4$

wall segment BC : $I_z = 1/12*10.0*1^3+10.0*3.0^2 = 91.8\ ft^4$

(with respect to cross section centroid)

So, in the analytical model :

panel P_1 : $I_y = 0$

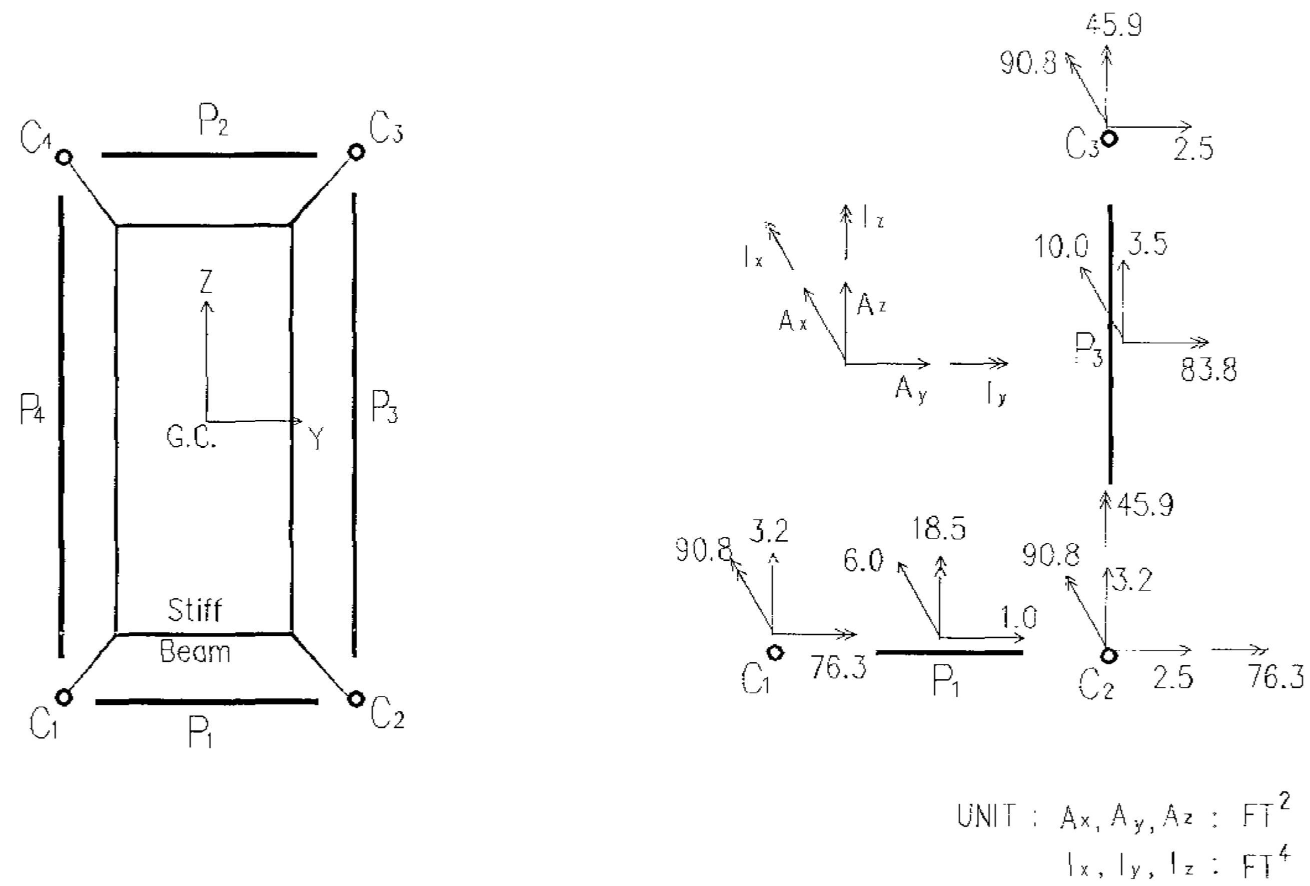

Fig.**B-3**Parameter Assignment and ETABS Analytical Modeling for Case 2 panel P_3 : $I_z = 0$

(nonzero value is not accepted by ETABS)

column C_1 and C_2 : $I_y = 0.5*152.5 = 76.3$ ft^4

column C_2 and C_3 : $I_z = 0.5*91.8 = 45.9$ ft^4

Where I_y and I_z are with respect to column centroids and local y and z directions are as shown in Fig. B-3.

(b) The torsional stiffness provided to the analytical assembly due to the shear forces developing in the columns and panels was computed first, the difference of torsional inertia between the real cross section and analytical assembly due to the element shears was assigned as torsional stiffnesses of the analytical columns equally.

Based on the formulations shown in Chap. 3.4(g) and as given in Fig.B-1, torsional constant of the complete section is 450 ft^4, the torsional constant provided by the 4 panel elements is 32.5 ft^4 and provided by the column elements is 54.5 ft^4.

So, in the analytical model :

Column C_1, C_2 and C_3 : $I_x = (450-32.5-54.5)/4 = 90.8$ ft^4

(c) Out-of-plane effective shear area of a wall segment was assigned as effective shear area to the column elements at the panel boundaries.

column C_1 and C_2 : $A_z = 20.0*76.3/472.7 = 3.2$ ft^2

Where 20.0 ft^2 is A_z of the complete core and 76.3/472.7 represents the ratio of the wall segment's local I_y to the I_y of the core at the centroid of the core.

column C_2 and C_3 : $A_y = 12.0*45.9/220.7 = 2.5\ ft^2$

Where $12.0\ ft^2$ is A_y of the complete core and 45.9/220.7 represents the ratio of the wall segment's local I_z to the I_z of the core at the centroid of the core.

Case 3 :

Same modeling and parameter assignment as in Case 2, but the stiff beams were removed. The analytical model and assigned parameters are shown in Fig. B-4.

Case 4 :

Same modeling and parameter assignment as in Case 2, but removing the axial area of each panel element. These areas were assigned by equally dividing between the corresponding column elements.

In the real cross section :

wall segment AB : $A_x = 6.0\ ft^2$

wall segment BC : $A_x = 10.0\ ft^2$

So, in the analytical model :

panel P_1 and P_3 : $A_x = 0.0\ ft^2$

column C_2 : $A_x = 0.5*(A_x$ of wall segment AB or BC)

$= 0.5*(10.0+6.0) = 8.0\ ft^2$

The analytical model and assigned parameters were shown in Fig. B-5.

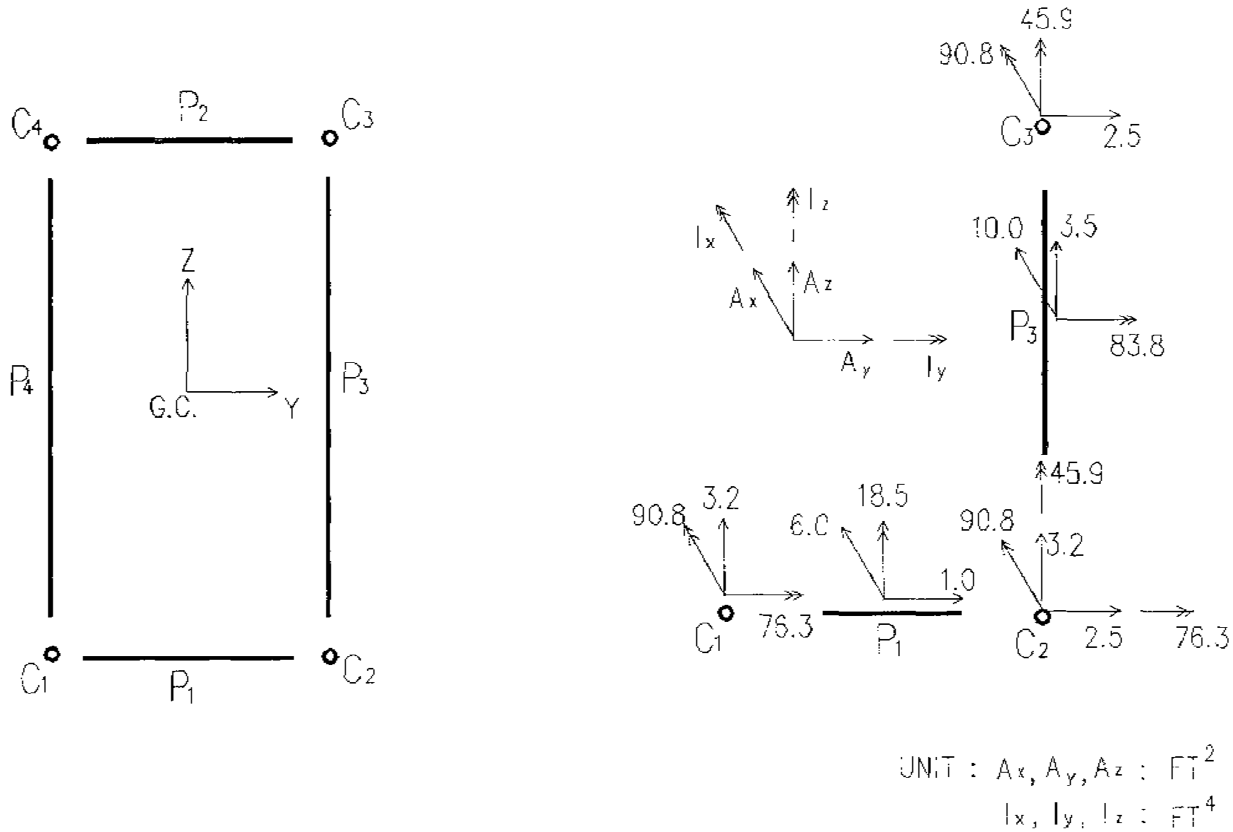

FigB-4 Parameter Assignment and ETABS Analytical Modeling for Case 3

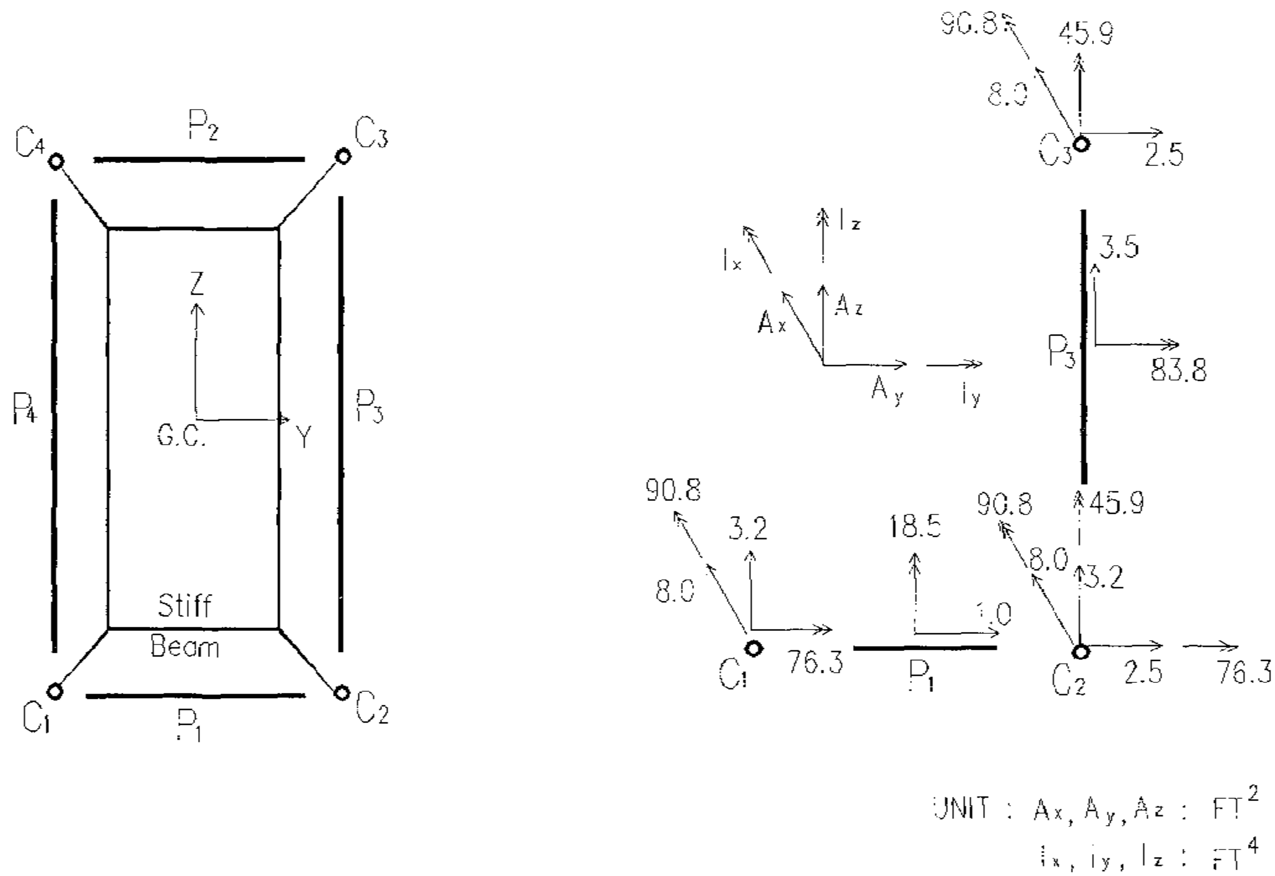

Fig B-5 Parameter Assignment and ETABS Analytical Modeling for Case 4

Case 5 :

Similar modeling and assigned parameters as in Case 4, except that additional column elements are defined at panel boundaries. Half the axial area of a panel element is assigned to the corresponding column element, which would simulate the contribution of that panel to the coupling action. For example, as shown in Fig.B-6, the column elements C_5 and C_6 simulate the contribution of panel P_1 to the coupling action in the z-direction. Note that column elements C_5 and C_8 are connected by the stiff beam sandwiching panel P_4 and providing the coupling mechanism due to the axial force contributions of wall segments AB and BC in the z-direction.

In the real cross section :

wall segment AB : $A_x = 6.0\ ft^2$

wall segment BC : $A_x = 10.0\ ft^2$

So, in the analytical model :

panel P_1 and P_3 : $A_x = 0.0\ ft^2$

column C_1, C_2 : $A_x = 0.5*(A_x$ of wall segment AD or BC)

$= 0.5*10.0 = 5.0\ ft^2$

column C_6, C_7 : $A_x = 0.5*(A_x$ of wall segment AB or DC)

$= 0.5*6.0 = 3.0\ ft^2$

The corresponding displacements for the five different cases studied and the computation based on the flexibility of the complete element at its centroid are compared in the following. The internal forces of analytical elements arising

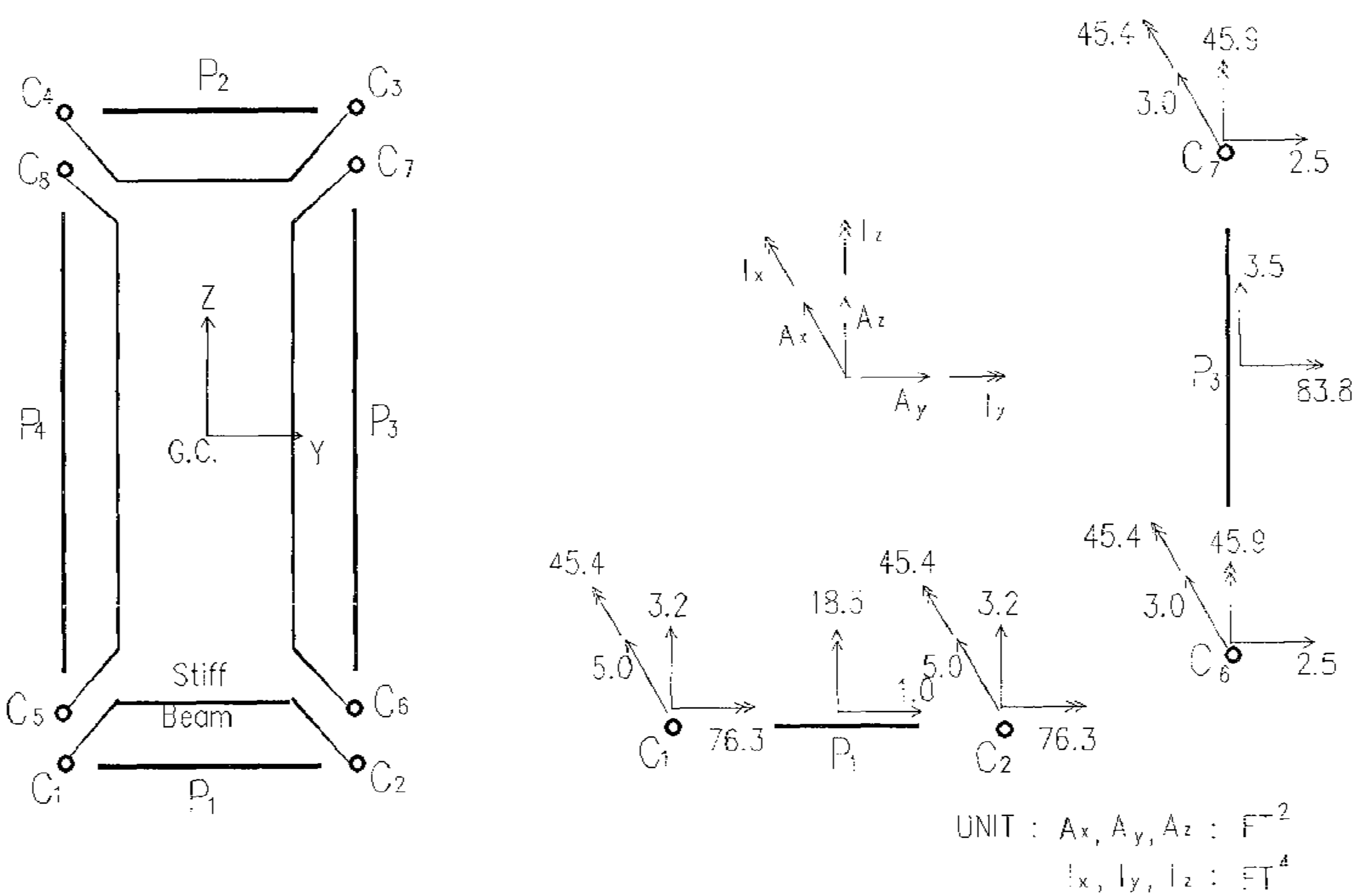

Fig.B-6 Parameter Assignment and ETABS Analytical Modeling for Case 5

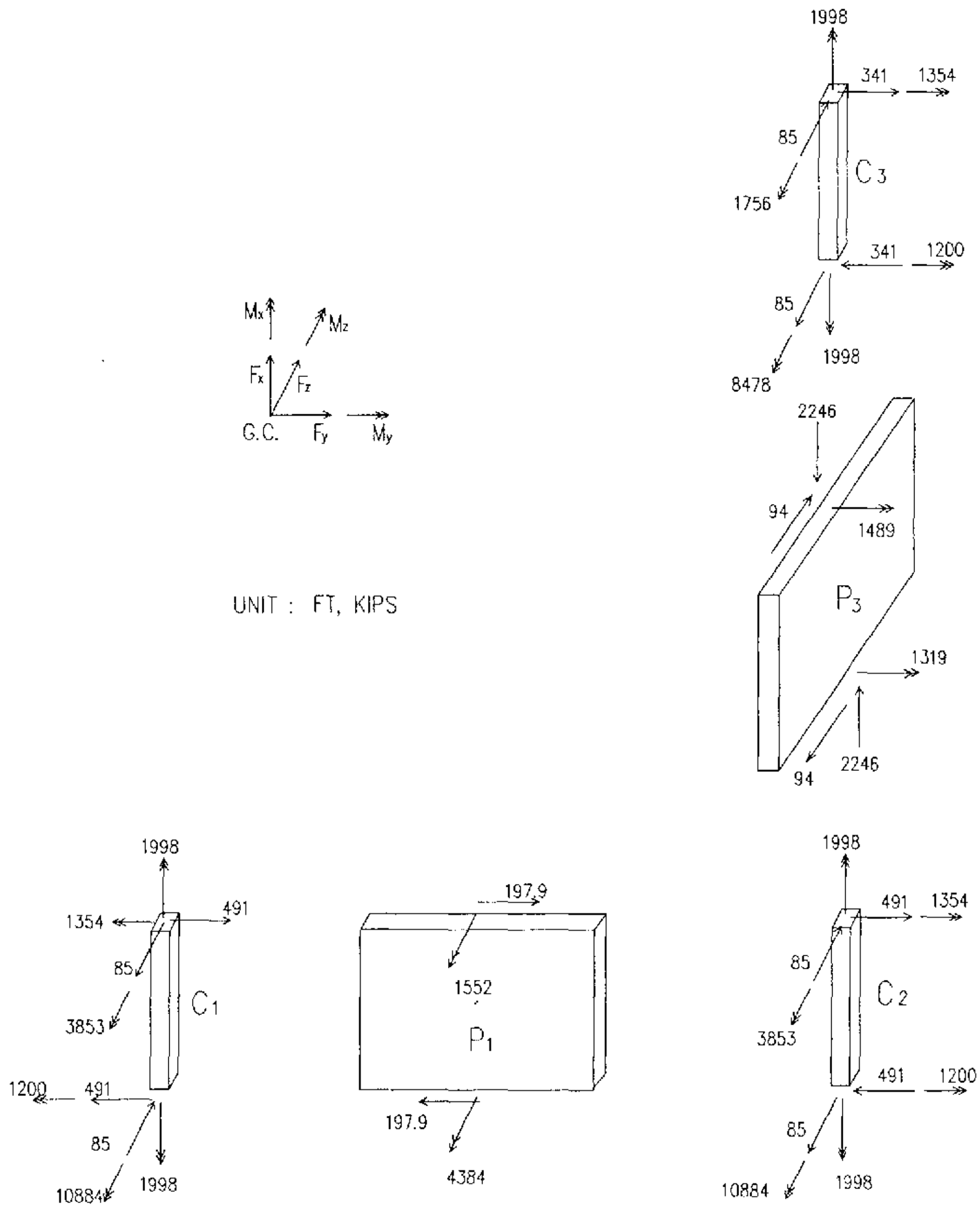

Fig.B-7 Element Forces Obtained for Case 2

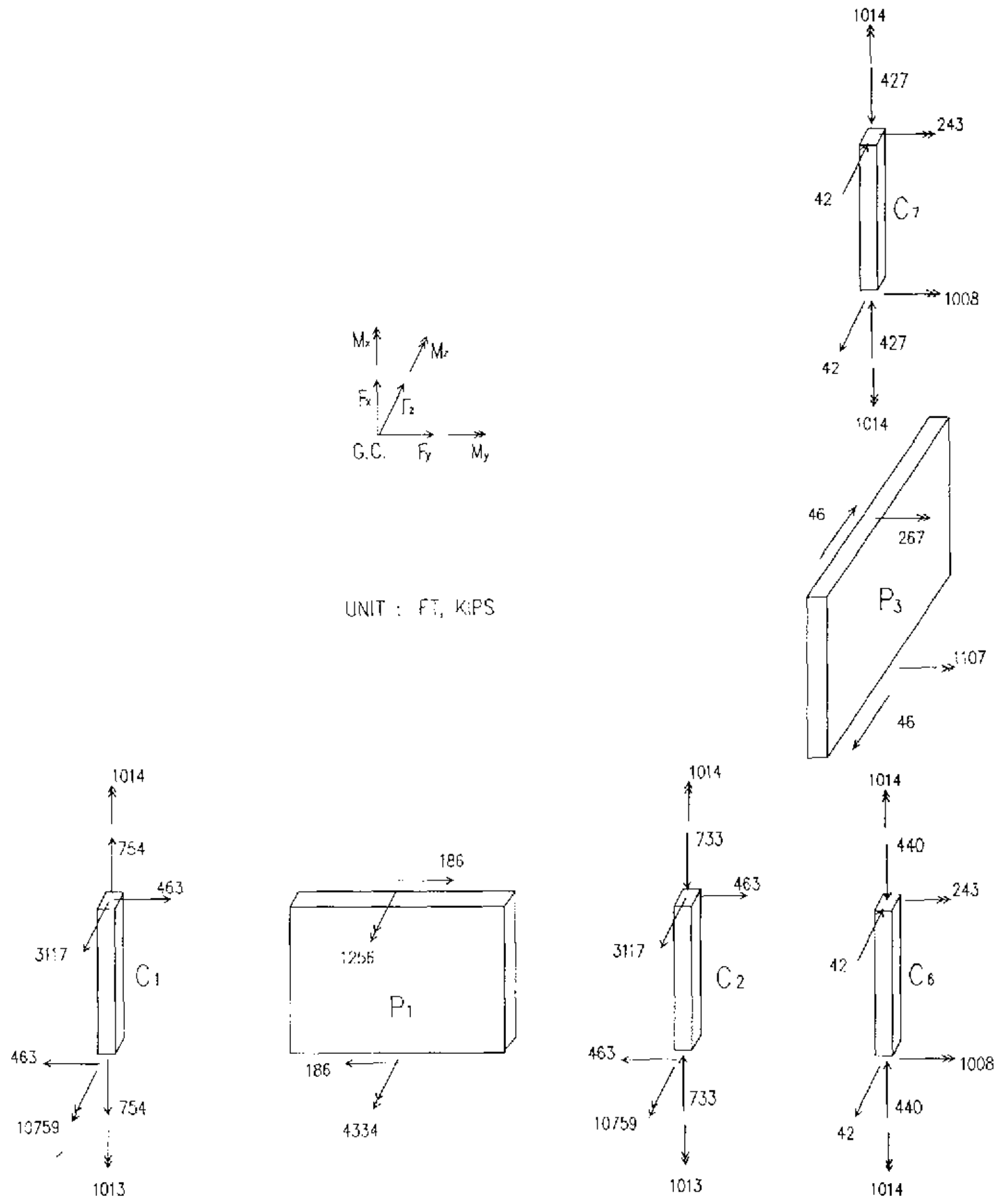

Fig. B-8 Element Forces Obtained for Case 5 from the analyses of Case 2 and Case 5 are shown in Figs B-7 and B-8.

TABLE B.1 Displacement and Rotations Obtained by the Analysis of 5 ETABS Assemblies Modeling the Wall

	Displacement	Rotations	
Type	U_y (ft)	θ_x (rad)	θ_z (rad)
Case 1	0.568	0.036	0.0403
Case 2	0.208	0.004	0.0109
Case 3	0.269	0.005	0.0118
Case 4	0.131	0.003	0.0075
Case 5	0.208	0.004	0.0093
Theoretical Disp.	0.208	0.004	0.0091

Here, U_y and 0_z are given as output from the program. However, θ_z is not. Therefore θ_z was computed from the final row of the element flexibility shown in Fig. B-1 [10].

$$M_z = \frac{u_y}{L} * (S_a + S_c) + S_a * \theta_z$$

In this expression M_z and u_y are already provided by the ETABS output. S_a, S_c are obtained from member stiffness expressions [25].

$$S_a = \frac{2 * E * I_z}{L} * \frac{(2 + \beta)}{(1 + 2\beta)}$$

$$S_c = \frac{2 * E * I_z}{L} * \frac{(1 - \beta)}{(1 + 2\beta)}$$

$$\beta = \frac{6 * E * I}{L^2 * A_v * G}$$

where β is the shear flexibility factor, A_v is the effective shear area with respect to the axis of bending under consideration and the other symbols were already defined.

B.4 Conclusions

To model a wall segment using analytical panel and column elements, it is important to note that rotations of the panel and the boundary columns at common nodes should be consistent. An undeformed analytical element assembly for a real wall segment is shown in Fig. B-9(a). Since in the program the rigid diaphragm assumption provides the same lateral displacement at each floor, panel and column were considered to be constrained by the links at each side. Fig. B-9(b) shows the deflected shapes of each element when a lateral force acts at the top of the wall. It is obvious that the rotations of panel and column elements at the common nodes are not consistent. In order to enforce the same vertical displacement and rotations at the common nodes of panel and column

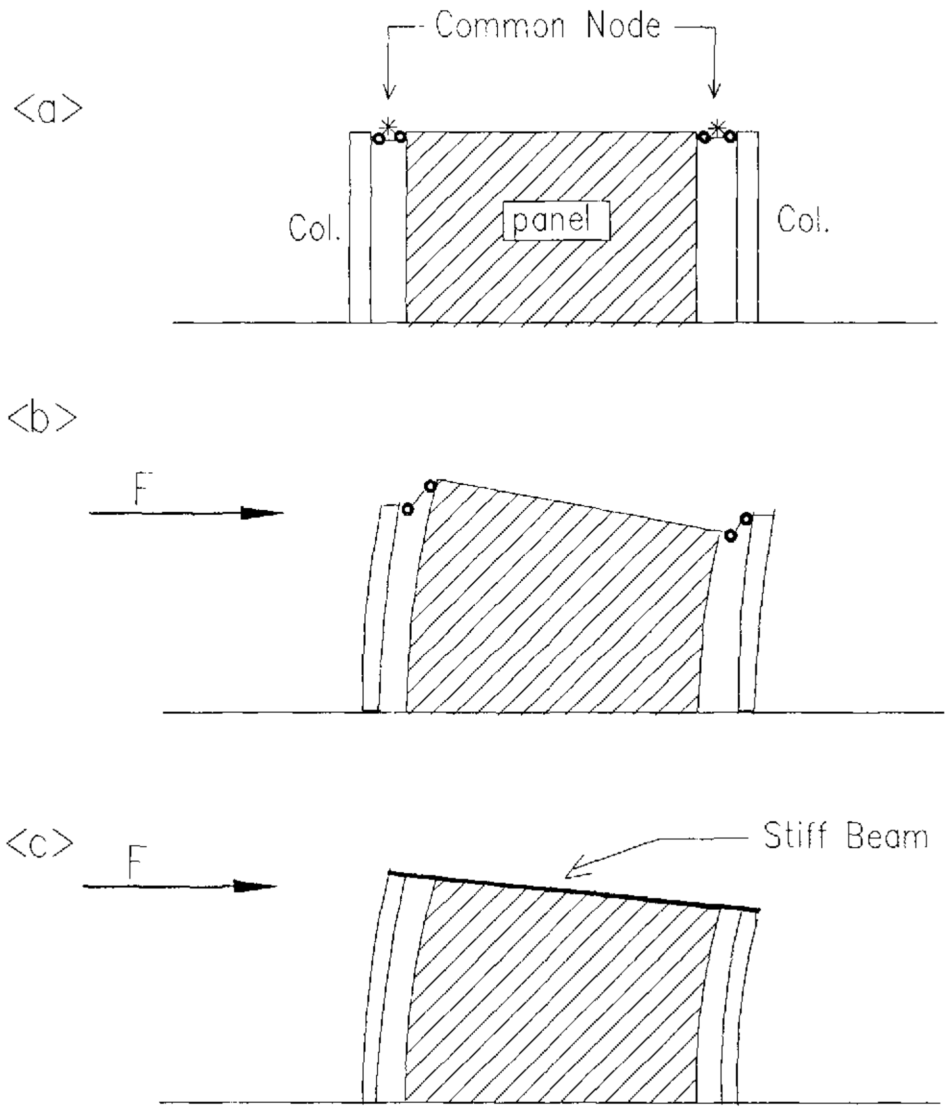

Fig. B-9 The Deformation Kinematics of the ETABS Panel and Column Element Assemblies With and Without Stiff Beam elements, a stiff beam should be defined sandwiching the panel and connecting to the two boundary columns. Then the deformation kinematics of the assembly comprised of the panel and two boundary columns will be consistent with the deformation kinematics of the real wall segment. This is shown in Fig. B-9(c).

To further explain the above reasoning, the flexural stress distribution at the core of a cantilever element with a box cross section when subjected to a lateral force as shown in Fig. B-1 was computed (Fig.B-10(a)). The deformed shape of the element if it was modeled in ETABS using the modeling procedure described in Case 3 (no stiff beam connected between boundary columns) is shown in Fig.B-10(b). The deformed shape of the element simulated by ETABS when it is modeled by using stiff beams as described for cases 2, 4 & 5 is shown in Fig.B-10(c). In the model of case 2, the coupling mechanism is not simulated correctly due to assigning the axial area to panel elements instead of the column elements as described in Chap.5.1. In case 4, each boundary column is assigned moment inertia in both directions. Therefore, the flexural rigidity will increase due to the connection by a stiff beam and the analytical model becomes stiffer than the real structure. In case 5, by defining additional column elements at panel boundaries, the axial coupling is simulated and the flexural rigidity is not artificially increased, since the boundary columns were assigned out-of-plane moment of inertia only.

(a)

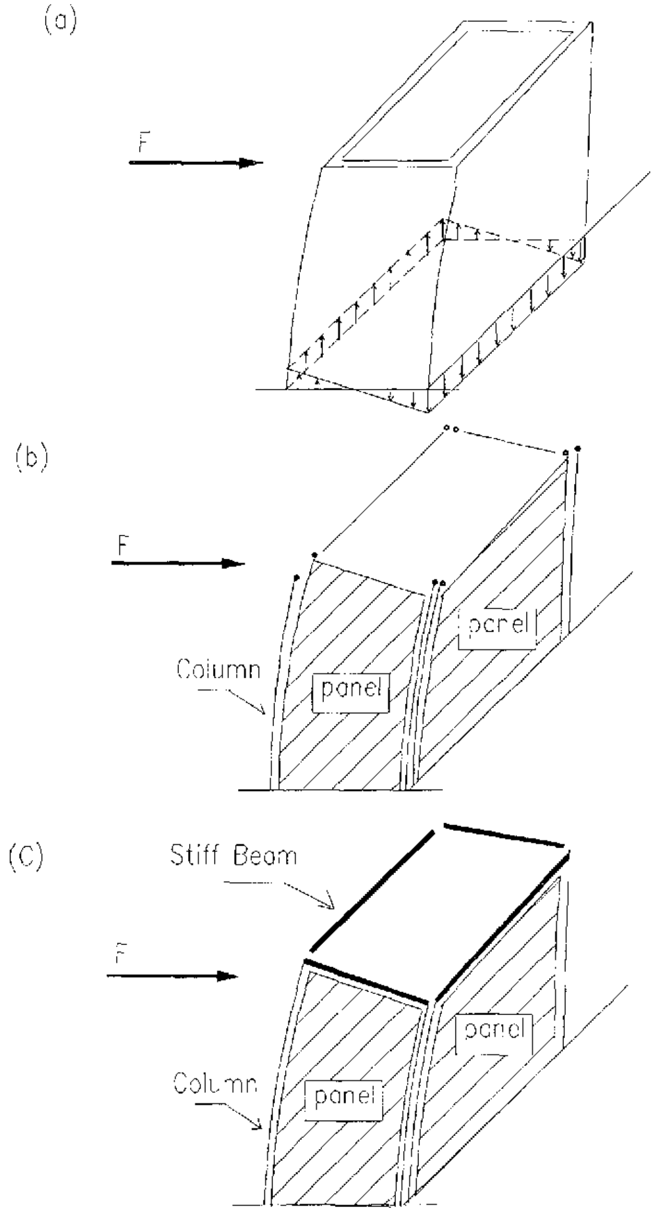

Fig.B-10 The Deformation Kinematics of a Structure With Box Cross Section Modeled by Different ETABS Assemblies this is why Case 5 is the only correct analytical model and the othercases are not.

It is noted that the analytical assembly in case 2 corresponds to the predictive model of the core described in Chap. 3.4. The analytical assembly in case 5 corresponds to the simulative model described in Chap. 5.1. Comparing the results shown above, case 2 and case 5 are observed to have similar lateral displacements and twist angles as given by the closed-form computation. However, the element forces which are shown in Figs B-7 & B-8 reveal that these models have significantly different force distributions. By comparing the rotation angles θ_z, case 5 is shown to have the same θ_z as given by closed-form computation. This further indicates that Case 5 is the correct model for the core.

These results illustrate why the simulative model described in Chap. 5.1 led to successful correlation with the experimental results while the predictive model did not.

NATIONAL CENTER FOR EARTHQUAKE ENGINEERING RESEARCH
LIST OF PUBLISHED TECHNICAL REPORTS

The National Center for Earthquake Engineering Research (NCEER) publishes technical reports on a variety of subjects related to earthquake engineering written by authors funded through NCEER. These reports are available from both NCEER's Publications Department and the National Technical Information Service (NTIS). Requests for reports should be directed to the Publications Department, National Center for Earthquake Engineering Research, State University of New York at Buffalo, Red Jacket Quadrangle, Buffalo, New York 14261. Reports can also be requested through NTIS, 5285 Port Royal Road, Springfield, Virginia 22161. NTIS accession numbers are shown in parenthesis, if available.

NCEER-87-0001 "First-Year Program in Research, Education and Technology Transfer," 3/5/87, (PB88-134275/AS).

NCEER-87-0002 "Experimental Evaluation of Instantaneous Optimal Algorithms for Structural Control," by R.C. Lin, T.T. Soong and A.M. Reinhorn, 4/20/87, (PB88-134341/AS).

NCEER-87-0003 "Experimentation Using the Earthquake Simulation Facilities at University at Buffalo," by A.M. Reinhorn and R.L. Ketter, to be published.

NCEER-87-0004 "The System Characteristics and Performance of a Shaking Table," by J.S. Hwang, K.C. Chang and G.C. Lee, 6/1/87, (PB88-134259/AS). This report is available only through NTIS (see address given above).

NCEER-87-0005 "A Finite Element Formulation for Nonlinear Viscoplastic Material Using a Q Model," by O. Gyebi and G. Dasgupta, 11/2/87, (PB88-213764/AS).

NCEER-87-0006 "Symbolic Manipulation Program (SMP) - Algebraic Codes for Two and Three Dimensional Finite Element Formulations," by X. Lee and G. Dasgupta, 11/9/87, (PB88-219522/AS).

NCEER-87-0007 "Instantaneous Optimal Control Laws for Tall Buildings Under Seismic Excitations," by J.N. Yang, A. Akbarpour and P. Ghaemmaghami, 6/10/87, (PB88-134333/AS).

NCEER-87-0008 "IDARC: Inelastic Damage Analysis of Reinforced Concrete Frame - Shear-Wall Structures," by Y.J. Park, A.M. Reinhorn and S.K. Kunnath, 7/20/87, (PB88-134325/AS).

NCEER-87-0009 "Liquefaction Potential for New York State: A Preliminary Report on Sites in Manhattan and Buffalo," by M. Budhu, V. Vijayakumar, R.F. Giese and L. Baumgras, 8/31/87, (PB88-163704/AS). This report is available only through NTIS (see address given above).

NCEER-87-0010 "Vertical and Torsional Vibration of Foundations in Inhomogeneous Media," by A.S. Veletsos and K.W. Dotson, 6/1/87, (PB88-134291/AS).

NCEER-87-0011 "Seismic Probabilistic Risk Assessment and Seismic Margins Studies for Nuclear Power Plants," by Howard H.M. Hwang, 6/15/87, (PB88-134267/AS).

NCEER-87-0012 "Parametric Studies of Frequency Response of Secondary Systems Under Ground-Acceleration Excitations," by Y. Yong and Y.K. Lin, 6/10/87, (PB88-134309/AS).

NCEER-87-0013 "Frequency Response of Secondary Systems Under Seismic Excitation," by J.A. HoLung, J. Cai and Y.K. Lin, 7/31/87, (PB88-134317/AS).

NCEER-87-0014 "Modelling Earthquake Ground Motions in Seismically Active Regions Using Parametric Time Series Methods," by G.W. Ellis and A.S. Cakmak, 8/25/87, (PB88-134283/AS).

NCEER-87-0015 "Detection and Assessment of Seismic Structural Damage," by E. DiPasquale and A.S. Cakmak, 8/25/87, (PB88-163712/AS).

NCEER-87-0016 "Pipeline Experiment at Parkfield, California," by J. Isenberg and E. Richardson, 9/15/87, (PB88-163720/AS). This report is available only through NTIS (see address given above).

NCEER-87-0017 "Digital Simulation of Seismic Ground Motion," by M. Shinozuka, G. Deodatis and T. Harada, 8/31/87, (PB88-155197/AS). This report is available only through NTIS (see address given above).

NCEER-87-0018 "Practical Considerations for Structural Control: System Uncertainty, System Time Delay and Truncation of Small Control Forces," J.N. Yang and A. Akbarpour, 8/10/87, (PB88-163738/AS).

NCEER-87-0019 "Modal Analysis of Nonclassically Damped Structural Systems Using Canonical Transformation," by J.N. Yang, S. Sarkani and F.X. Long, 9/27/87, (PB88-187851/AS).

NCEER-87-0020 "A Nonstationary Solution in Random Vibration Theory," by J.R. Red-Horse and P.D. Spanos, 11/3/87, (PB88-163746/AS).

NCEER-87-0021 "Horizontal Impedances for Radially Inhomogeneous Viscoelastic Soil Layers," by A.S. Veletsos and K.W. Dotson, 10/15/87, (PB88-150859/AS).

NCEER-87-0022 "Seismic Damage Assessment of Reinforced Concrete Members," by Y.S. Chung, C. Meyer and M. Shinozuka, 10/9/87, (PB88-150867/AS). This report is available only through NTIS (see address given above).

NCEER-87-0023 "Active Structural Control in Civil Engineering," by T.T. Soong, 11/11/87, (PB88-187778/AS).

NCEER-87-0024 Vertical and Torsional Impedances for Radially Inhomogeneous Viscoelastic Soil Layers," by K.W. Dotson and A.S. Veletsos, 12/87, (PB88-187786/AS).

NCEER-87-0025 "Proceedings from the Symposium on Seismic Hazards, Ground Motions, Soil-Liquefaction and Engineering Practice in Eastern North America," October 20-22, 1987, edited by K.H. Jacob, 12/87, (PB88-188115/AS).

NCEER-87-0026 "Report on the Whittier-Narrows, California, Earthquake of October 1, 1987," by J. Pantelic and A. Reinhorn, 11/87, (PB88-187752/AS). This report is available only through NTIS (see address given above).

NCEER-87-0027 "Design of a Modular Program for Transient Nonlinear Analysis of Large 3-D Building Structures," by S. Srivastav and J.F. Abel, 12/30/87, (PB88-187950/AS).

NCEER-87-0028 "Second-Year Program in Research, Education and Technology Transfer," 3/8/88, (PB88-219480/AS).

NCEER-88-0001 "Workshop on Seismic Computer Analysis and Design of Buildings With Interactive Graphics," by W. McGuire, J.F. Abel and C.H. Conley, 1/18/88, (PB88-187760/AS).

NCEER-88-0002 "Optimal Control of Nonlinear Flexible Structures," by J.N. Yang, F.X. Long and D. Wong, 1/22/88, (PB88-213772/AS).

NCEER-88-0003 "Substructuring Techniques in the Time Domain for Primary-Secondary Structural Systems," by G.D. Manolis and G. Juhn, 2/10/88, (PB88-213780/AS).

NCEER-88-0004 "Iterative Seismic Analysis of Primary-Secondary Systems," by A. Singhal, L.D. Lutes and P.D. Spanos, 2/23/88, (PB88-213798/AS).

NCEER-88-0005 "Stochastic Finite Element Expansion for Random Media," by P.D. Spanos and R. Ghanem, 3/14/88, (PB88-213806/AS).

NCEER-88-0006 "Combining Structural Optimization and Structural Control," by F.Y. Cheng and C.P. Pantelides, 1/10/88, (PB88-213814/AS).

NCEER-88-0007 "Seismic Performance Assessment of Code-Designed Structures," by H.H-M. Hwang, J-W. Jaw and H-J. Shau, 3/20/88, (PB88-219423/AS).

NCEER-88-0008 "Reliability Analysis of Code-Designed Structures Under Natural Hazards," by H.H-M. Hwang, H. Ushiba and M. Shinozuka, 2/29/88, (PB88-229471/AS).

NCEER-88-0009 "Seismic Fragility Analysis of Shear Wall Structures," by J-W Jaw and H.H-M. Hwang, 4/30/88, (PB89-102867/AS).

NCEER-88-0010 "Base Isolation of a Multi-Story Building Under a Harmonic Ground Motion - A Comparison of Performances of Various Systems," by F-G Fan, G. Ahmadi and I.G. Tadjbakhsh, 5/18/88, (PB89-122238/AS).

NCEER-88-0011 "Seismic Floor Response Spectra for a Combined System by Green's Functions," by F.M. Lavelle, L.A. Bergman and P.D. Spanos, 5/1/88, (PB89-102875/AS).

NCEER-88-0012 "A New Solution Technique for Randomly Excited Hysteretic Structures," by G.Q. Cai and Y.K. Lin, 5/16/88, (PB89-102883/AS).

NCEER-88-0013 "A Study of Radiation Damping and Soil-Structure Interaction Effects in the Centrifuge," by K. Weissman, supervised by J.H. Prevost, 5/24/88, (PB89-144703/AS).

NCEER-88-0014 "Parameter Identification and Implementation of a Kinematic Plasticity Model for Frictional Soils," by J.H. Prevost and D.V. Griffiths, to be published.

NCEER-88-0015 "Two- and Three- Dimensional Dynamic Finite Element Analyses of the Long Valley Dam," by D.V. Griffiths and J.H. Prevost, 6/17/88, (PB89-144711/AS).

NCEER-88-0016 "Damage Assessment of Reinforced Concrete Structures in Eastern United States," by A.M. Reinhorn, M.J. Seidel, S.K. Kunnath and Y.J. Park, 6/15/88, (PB89-122220/AS).

NCEER-88-0017 "Dynamic Compliance of Vertically Loaded Strip Foundations in Multilayered Viscoelastic Soils," by S. Ahmad and A.S.M. Israil, 6/17/88, (PB89-102891/AS).

NCEER-88-0018 "An Experimental Study of Seismic Structural Response With Added Viscoelastic Dampers," by R.C. Lin, Z. Liang, T.T. Soong and R.H. Zhang, 6/30/88, (PB89-122212/AS).

NCEER-88-0019 "Experimental Investigation of Primary - Secondary System Interaction," by G.D. Manolis, G. Juhn and A.M. Reinhorn, 5/27/88, (PB89-122204/AS).

NCEER-88-0020 "A Response Spectrum Approach For Analysis of Nonclassically Damped Structures," by J.N. Yang, S. Sarkani and F.X. Long, 4/22/88, (PB89-102909/AS).

NCEER-88-0021 "Seismic Interaction of Structures and Soils: Stochastic Approach," by A.S. Veletsos and A.M. Prasad, 7/21/88, (PB89-122196/AS).

NCEER-88-0022 "Identification of the Serviceability Limit State and Detection of Seismic Structural Damage," by E. DiPasquale and A.S. Cakmak, 6/15/88, (PB89-122188/AS).

NCEER-88-0023 "Multi-Hazard Risk Analysis: Case of a Simple Offshore Structure," by B.K. Bhartia and E.H. Vanmarcke, 7/21/88, (PB89-145213/AS).

NCEER-88-0024 "Automated Seismic Design of Reinforced Concrete Buildings," by Y.S. Chung, C. Meyer and M. Shinozuka, 7/5/88, (PB89-122170/AS).

NCEER-88-0025 "Experimental Study of Active Control of MDOF Structures Under Seismic Excitations," by L.L. Chung, R.C. Lin, T.T. Soong and A.M. Reinhorn, 7/10/88, (PB89-122600/AS).

NCEER-88-0026 "Earthquake Simulation Tests of a Low-Rise Metal Structure," by J.S. Hwang, K.C. Chang, G.C. Lee and R.L. Ketter, 8/1/88, (PB89-102917/AS).

NCEER-88-0027 "Systems Study of Urban Response and Reconstruction Due to Catastrophic Earthquakes," by F. Kozin and H.K. Zhou, 9/22/88, (PB90-162348/AS).

NCEER-88-0028 "Seismic Fragility Analysis of Plane Frame Structures," by H.H-M. Hwang and Y.K. Low, 7/31/88, (PB89-131445/AS).

NCEER-88-0029 "Response Analysis of Stochastic Structures," by A. Kardara, C. Bucher and M. Shinozuka, 9/22/88, (PB89-174429/AS).

NCEER-88-0030 "Nonnormal Accelerations Due to Yielding in a Primary Structure," by D.C.K. Chen and L.D. Lutes, 9/19/88, (PB89-131437/AS).

NCEER-88-0031 "Design Approaches for Soil-Structure Interaction," by A.S. Veletsos, A.M. Prasad and Y. Tang, 12/30/88, (PB89-174437/AS).

NCEER-88-0032 "A Re-evaluation of Design Spectra for Seismic Damage Control," by C.J. Turkstra and A.G. Tallin, 11/7/88, (PB89-145221/AS).

NCEER-88-0033 "The Behavior and Design of Noncontact Lap Splices Subjected to Repeated Inelastic Tensile Loading," by V.E. Sagan, P. Gergely and R.N. White, 12/8/88, (PB89-163737/AS).

NCEER-88-0034 "Seismic Response of Pile Foundations," by S.M. Mamoon, P.K. Banerjee and S. Ahmad, 11/1/88, (PB89-145239/AS).

NCEER-88-0035 "Modeling of R/C Building Structures With Flexible Floor Diaphragms (IDARC2)," by A.M. Reinhorn, S.K. Kunnath and N. Panahshahi, 9/7/88, (PB89-207153/AS).

NCEER-88-0036 "Solution of the Dam-Reservoir Interaction Problem Using a Combination of FEM, BEM with Particular Integrals, Modal Analysis, and Substructuring," by C-S. Tsai, G.C. Lee and R.L. Ketter, 12/31/88, (PB89-207146/AS).

NCEER-88-0037 "Optimal Placement of Actuators for Structural Control," by F.Y. Cheng and C.P. Pantelides, 8/15/88, (PB89-162846/AS).

NCEER-88-0038 "Teflon Bearings in Aseismic Base Isolation: Experimental Studies and Mathematical Modeling," by A. Mokha, M.C. Constantinou and A.M. Reinhorn, 12/5/88, (PB89-218457/AS).

NCEER-88-0039 "Seismic Behavior of Flat Slab High-Rise Buildings in the New York City Area," by P. Weidlinger and M. Ettouney, 10/15/88, (PB90-145681/AS).

NCEER-88-0040 "Evaluation of the Earthquake Resistance of Existing Buildings in New York City," by P. Weidlinger and M. Ettouney, 10/15/88, to be published.

NCEER-88-0041 "Small-Scale Modeling Techniques for Reinforced Concrete Structures Subjected to Seismic Loads," by W. Kim, A. El-Attar and R.N. White, 11/22/88, (PB89-189625/AS).

NCEER-88-0042 "Modeling Strong Ground Motion from Multiple Event Earthquakes," by G.W. Ellis and A.S. Cakmak, 10/15/88, (PB89-174445/AS).

NCEER-88-0043 "Nonstationary Models of Seismic Ground Acceleration," by M. Grigoriu, S.E. Ruiz and E. Rosenblueth, 7/15/88, (PB89-189617/AS).

NCEER-88-0044 "SARCF User's Guide: Seismic Analysis of Reinforced Concrete Frames," by Y.S. Chung, C. Meyer and M. Shinozuka, 11/9/88, (PB89-174452/AS).

NCEER-88-0045 "First Expert Panel Meeting on Disaster Research and Planning," edited by J. Pantelic and J. Stoyle, 9/15/88, (PB89-174460/AS).

NCEER-88-0046 "Preliminary Studies of the Effect of Degrading Infill Walls on the Nonlinear Seismic Response of Steel Frames," by C.Z. Chrysostomou, P. Gergely and J.F. Abel, 12/19/88, (PB89-208383/AS).

NCEER-88-0047 "Reinforced Concrete Frame Component Testing Facility - Design, Construction, Instrumentation and Operation," by S.P. Pessiki, C. Conley, T. Bond, P. Gergely and R.N. White, 12/16/88, (PB89-174478/AS).

NCEER-89-0001 "Effects of Protective Cushion and Soil Compliancy on the Response of Equipment Within a Seismically Excited Building," by J.A. HoLung, 2/16/89, (PB89-207179/AS).

NCEER-89-0002 "Statistical Evaluation of Response Modification Factors for Reinforced Concrete Structures," by H.H-M. Hwang and J-W. Jaw, 2/17/89, (PB89-207187/AS).

NCEER-89-0003 "Hysteretic Columns Under Random Excitation," by G-Q. Cai and Y.K. Lin, 1/9/89, (PB89-196513/AS).

NCEER-89-0004 "Experimental Study of 'Elephant Foot Bulge' Instability of Thin-Walled Metal Tanks," by Z-H. Jia and R.L. Ketter, 2/22/89, (PB89-207195/AS).

NCEER-89-0005 "Experiment on Performance of Buried Pipelines Across San Andreas Fault," by J. Isenberg, E. Richardson and T.D. O'Rourke, 3/10/89, (PB89-218440/AS).

NCEER-89-0006 "A Knowledge-Based Approach to Structural Design of Earthquake-Resistant Buildings," by M. Subramani, P. Gergely, C.H. Conley, J.F. Abel and A.H. Zaghw, 1/15/89, (PB89-218465/AS).

NCEER-89-0007 "Liquefaction Hazards and Their Effects on Buried Pipelines," by T.D. O'Rourke and P.A. Lane, 2/1/89, (PB89-218481).

NCEER-89-0008 "Fundamentals of System Identification in Structural Dynamics," by H. Imai, C-B. Yun, O. Maruyama and M. Shinozuka, 1/26/89, (PB89-207211/AS).

NCEER-89-0009 "Effects of the 1985 Michoacan Earthquake on Water Systems and Other Buried Lifelines in Mexico," by A.G. Ayala and M.J. O'Rourke, 3/8/89, (PB89-207229/AS).

NCEER-89-R010 "NCEER Bibliography of Earthquake Education Materials," by K.E.K. Ross, Second Revision, 9/1/89, (PB90-125352/AS).

NCEER-89-0011 "Inelastic Three-Dimensional Response Analysis of Reinforced Concrete Building Structures (IDARC-3D), Part I - Modeling," by S.K. Kunnath and A.M. Reinhorn, 4/17/89, (PB90-114612/AS).

NCEER-89-0012 "Recommended Modifications to ATC-14," by C.D. Poland and J.O. Malley, 4/12/89, (PB90-108648/AS).

NCEER-89-0013 "Repair and Strengthening of Beam-to-Column Connections Subjected to Earthquake Loading," by M. Corazao and A.J. Durrani, 2/28/89, (PB90-109885/AS).

NCEER-89-0014 "Program EXKAL2 for Identification of Structural Dynamic Systems," by O. Maruyama, C-B. Yun, M. Hoshiya and M. Shinozuka, 5/19/89, (PB90-109877/AS).

NCEER-89-0015 "Response of Frames With Bolted Semi-Rigid Connections, Part I - Experimental Study and Analytical Predictions," by P.J. DiCorso, A.M. Reinhorn, J.R. Dickerson, J.B. Radziminski and W.L. Harper, 6/1/89, to be published.

NCEER-89-0016 "ARMA Monte Carlo Simulation in Probabilistic Structural Analysis," by P.D. Spanos and M.P. Mignolet, 7/10/89, (PB90-109893/AS).

NCEER-89-0017 "Proceedings from the Conference on Disaster Preparedness - The Place of Earthquake Education in Our Schools," Edited by K.E.K. Ross, 12/31/89.

NCEER-89-0018 "Multidimensional Models of Hysteretic Material Behavior for Vibration Analysis of Shape Memory Energy Absorbing Devices, by E.J. Graesser and F.A. Cozzarelli, 6/7/89, (PB90-164146/AS).

NCEER-89-0019 "Nonlinear Dynamic Analysis of Three-Dimensional Base Isolated Structures (3D-BASIS)," by S. Nagarajaiah, A.M. Reinhorn and M.C. Constantinou, 8/3/89, (PB90-161936/AS).

NCEER-89-0020 "Structural Control Considering Time-Rate of Control Forces and Control Rate Constraints," by F.Y. Cheng and C.P. Pantelides, 8/3/89, (PB90-120445/AS).

NCEER-89-0021 "Subsurface Conditions of Memphis and Shelby County," by K.W. Ng, T-S. Chang and H-H.M. Hwang, 7/26/89, (PB90-120437/AS).

NCEER-89-0022 "Seismic Wave Propagation Effects on Straight Jointed Buried Pipelines," by K. Elhmadi and M.J. O'Rourke, 8/24/89, (PB90-162322/AS).

NCEER-89-0023 "Workshop on Serviceability Analysis of Water Delivery Systems," edited by M. Grigoriu, 3/6/89, (PB90-127424/AS).

NCEER-89-0024 "Shaking Table Study of a 1/5 Scale Steel Frame Composed of Tapered Members," by K.C. Chang, J.S. Hwang and G.C. Lee, 9/18/89, (PB90-160169/AS).

NCEER-89-0025 "DYNA1D: A Computer Program for Nonlinear Seismic Site Response Analysis - Technical Documentation," by Jean H. Prevost, 9/14/89, (PB90-161944/AS).

NCEER-89-0026 "1:4 Scale Model Studies of Active Tendon Systems and Active Mass Dampers for Aseismic Protection," by A.M. Reinhorn, T.T. Soong, R.C. Lin, Y.P. Yang, Y. Fukao, H. Abe and M. Nakai, 9/15/89, (PB90-173246/AS).

NCEER-89-0027 "Scattering of Waves by Inclusions in a Nonhomogeneous Elastic Half Space Solved by Boundary Element Methods," by P.K. Hadley, A. Askar and A.S. Cakmak, 6/15/89, (PB90-145699/AS).

NCEER-89-0028 "Statistical Evaluation of Deflection Amplification Factors for Reinforced Concrete Structures," by H.H.M. Hwang, J-W. Jaw and A.L. Ch'ng, 8/31/89, (PB90-164633/AS).

NCEER-89-0029 "Bedrock Accelerations in Memphis Area Due to Large New Madrid Earthquakes," by H.H.M. Hwang, C.H.S. Chen and G. Yu, 11/7/89, (PB90-162330/AS).

NCEER-89-0030 "Seismic Behavior and Response Sensitivity of Secondary Structural Systems," by Y.Q. Chen and T.T. Soong, 10/23/89, (PB90-164658/AS).

NCEER-89-0031 "Random Vibration and Reliability Analysis of Primary-Secondary Structural Systems," by Y. Ibrahim, M. Grigoriu and T.T. Soong, 11/10/89, (PB90-161951/AS).

NCEER-89-0032 "Proceedings from the Second U.S. - Japan Workshop on Liquefaction, Large Ground Deformation and Their Effects on Lifelines, September 26-29, 1989," Edited by T.D. O'Rourke and M. Hamada, 12/1/89.

NCEER-89-0033 "Deterministic Model for Seismic Damage Evaluation of Reinforced Concrete Structures," by J.M. Bracci, A.M. Reinhorn, J.B. Mander and S.K. Kunnath, 9/27/89, to be published.

NCEER-89-0034 "On the Relation Between Local and Global Damage Indices," by E. DiPasquale and A.S. Cakmak, 8/15/89, (PB90-173865).

NCEER-89-0035 "Cyclic Undrained Behavior of Nonplastic and Low Plasticity Silts," by A.J. Walker and H.E. Stewart, 7/26/89, (PB90-183518/AS).

NCEER-89-0036 "Liquefaction Potential of Surficial Deposits in the City of Buffalo, New York," by M. Budhu, R. Giese and L. Baumgrass, 1/17/89.

NCEER-89-0037 "A Determinstic Assessment of Effects of Ground Motion Incoherence," by A.S. Veletsos and Y. Tang, 7/15/89, (PB90-164294/AS).

NCEER-89-0038 "Workshop on Ground Motion Parameters for Seismic Hazard Mapping," July 17-18, 1989, edited by R.V. Whitman, 12/1/89, (PB90-173923/AS).

NCEER-89-0039 "Seismic Effects on Elevated Transit Lines of the New York City Transit Authority," by C.J. Costantino, C.A. Miller and E. Heymsfield, 12/26/89.

NCEER-89-0040 "Centrifugal Modeling of Dynamic Soil-Structure Interaction," by K. Weissman, Supervised by J.H. Prevost, 5/10/89.

NCEER-89-0041 "Linearized Identification of Buildings With Cores for Seismic Vulnerability Assessment," by I-K. Ho and A.E. Aktan, 11/1/89.